https://doi.org/10.59761/RCR5182

Acetylene semi-hydrogenation: recent advances

Yulia V. Gyrdymova, Konstantin S. Rodygin*

Saint Petersburg State University, 199034 Saint Petersburg, Russian Federation

The development of new catalysts with improved properties for organic reactions is relevant both for solving fundamental chemical challenges and for their implementation into production. In industry, acetylene hydrogenation is a catalytic process. The role of a catalyst is to increase the selectivity of hydrogenation to ethylene and prevent over-hydrogenation to ethane. Research in the field of selective hydrogenation of acetylene, in addition to the applied relevance, is also of academic interest, since it discovers the nature of catalysis in details. Amazingly, acetylene hydrogenation has become, in a sense, a criterion for assessing the properties of synthesized catalysts, demonstrating the 'structure-properties' relationship. Changes in the structure of a catalyst immediately result in changes in its catalytic characteristics, which, in turn, led to a more complete understanding of the processes occurring on the catalyst surface. A sharp increase in the number of researches on this subject that occurred in the period from 2021 to 2024 was due to the possibilities of obtaining and describing single-atom catalysts with the identification of the key dependence 'particle size–activity'. This review not only complements previous summarizing works on selective hydrogenation of acetylene, but also differs significantly in the arrangement of the material. Various approaches to the design of catalysts for this reaction are discussed based on the insight into its pathway. Mono- and bimetallic catalysts based on active metals such as palladium, nickel, copper, *etc*. are considered. Particular attention is paid to the application of single-atom catalysts. At the conclusion of this review, we summarized the catalytic characteristics of various systems in a table.

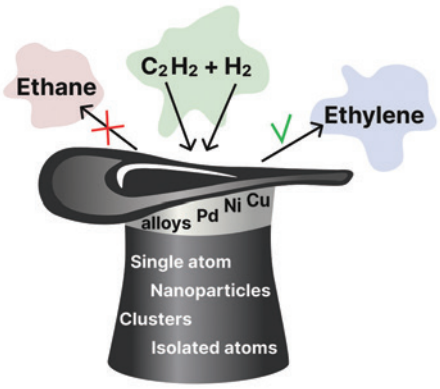

The bibliography includes 267 references.

Keywords: selective hydrogenation, acetylene, single-atom catalysts, catalyst cocktail.

Contents

1. Introduction

Catalytic processes have been the subject of research throughout their creation, both from the academic and industrial perspective. The first industrial catalytic processes of nitrogen fixation to ammonia and the development of catalysts for ethylene polymerization marked a new era in the development of chemistry. Many important chemical transformations are catalytic today, *e.g.*, cross-coupling,[1–4] hydrogenation,[5–9] alkylation, and many others.[10–16] The use of transition metal compounds were for these purposes a common case. The variable oxidation state and d-orbital in the atomic structure of these metals provide many opportunities for tuning the electronic structure of the metal centre and increase the number of possible compounds that it can form.

Pd, Pt, Ru, Ni, and Cu-based catalysts are extremely active even in small amounts. Typically, catalytic systems including noble metals are characterized by low selectivity and promote the reaction in all possible directions. At the same time, they are prone to poisoning by impurities that can block their active centres. Yet another issue is sintering (coking) due to high temperatures. All these factors adversely affect the selectivity and performance of catalysts, reducing their durability. The said drawbacks stimulate research to improve the properties of available catalysts and develop new more efficient catalytic systems.

The study of the properties of catalysts is usually carried out on model reactions. Ideally, the most appropriate reactions should proceed completely and selectively, and the product should be clearly identified in the mixture. Hydrogenation is one of the key catalytic reactions in chemical synthesis,[17–27] that meets the listed requirements. In particular, acetylene hydrogenation can be considered as a convenient model for studying the properties of metal catalysts.

Yu.V.Gyrdymova. PhD in Chemistry, Researcher at the Department of Organic Chemistry, Saint Petersburg State University.
E-mail: y.gyrdymova@spbu.ru
Current research interests: hydrogenation of unsaturated compounds, acetylene.
K.S.Rodygin. Doctor of Chemical Sciences, Associate Professor at the Department of Organic Chemistry, Saint Petersburg State University.
E-mail: k.rodygin@spbu.ru
Current research interests: catalysts preparation, unsaturated compounds, biodiesel.

Received 20 May 2025

Why acetylene hydrogenation? Acetylene is the simplest alkyne consisting of triple-bonded two carbon atoms. Unsaturated character of acetylene is widely used in the synthesis of vinyl monomers, heterocycles, and a wide range of valuable chemicals.[28–33] Hydrogenation of acetylene can proceed with the formation of ethylene or ethane. Semi-hydrogenation of acetylene is a critical process providing selective conversion of acetylene to ethylene, while preventing further hydrogenation to ethane. Ethylene is one of the key raw materials of the chemical industry, representing the main supplier of the C_2 monomer unit. In 2023, global polyethylene production amounted to 141 million tons.[34] Ethylene obtained by high-temperature cracking contains up to 2% of acetylene as an impurity.[35–39] Since acetylene is a catalytic poison in further ethylene polymerization, ethylene must be carefully purified from acetylene, and the residual amount of acetylene should not exceed 5 ppm.[40] Separating ethylene and acetylene is a complicated, labour-intensive task, that requires special approaches.[41–44] Currently, the removal of acetylene from ethylene prior to polymerization is usually realized *via* selective hydrogenation of acetylene to ethylene.

Acetylene hydrogenation is a tandem reaction including two competing parallel reaction pathways:[†] sequential hydrogenation of acetylene to produce ethylene (reaction (1)) and its further hydrogenation to ethane (reactions (2) and (3)).[45]

$$C_2H_2 + H_2 \longrightarrow C_2H_4,\ \Delta H° = -172\ \text{kJ mol}^{-1} \quad (1)$$

$$C_2H_4 + H_2 \longrightarrow C_2H_6,\ \Delta H° = -136\ \text{kJ mol}^{-1} \quad (2)$$

$$C_2H_2 + 2\,H_2 \longrightarrow C_2H_6,\ \Delta H° = -308\ \text{kJ mol}^{-1} \quad (3)$$

$$C_2H_2 + H_2 \longrightarrow C_{4+}\ (\text{‘green oil’}) \quad (4)$$

Prolonged hydrogenation of acetylene in the reducing medium in presence of a catalyst results in the formation of oligomerization products of a linear structure with an even number of carbon atoms (C_{4+}, reaction (4)). The liquid fraction of the hydrocarbons is called ‘green oil’.[46] The oil is formed on the surface of catalysts only in the combined presence of acetylene and hydrogen,[47,48] and blocks active centres, deactivating a catalyst.[49, 50] Most traditionally employed noble metal-based hydrogenation catalysts[51–60] promote all possible reactions, including the formation of the ‘green oil’. Therefore, the best or ideal catalyst, in addition to high selectivity to acetylene semi-hydrogenation and anti-coking properties, should inhibit the formation of oligomerization products and be resistant to their effects (if green oil is formed). The research of many scientific groups is focused on solving precisely these problems.

According to the SciFinder database, the next trend in publication activity in the field of selective catalysts development and their application in hydrogenation of acetylene occurred over the period 2021–2024 (Fig. 1). This increase in the number of works was largely determined by the wide access to the synthesis and study of single-atom catalysts, which significantly changed the ideas about the nature of catalysis *per se* in general.

The previous reviews have contributed greatly to the summarization of methods for the selective hydrogenation of acetylene,[61] the systematization of approaches to bimetallic[62, 63] and single-atom catalysts,[64] and also revealed the role of solid solutions of insertion in the palladium-catalyzed hydrogenation of acetylene to ethylene.[65, 66]

[†]After the reaction equation, the values of their standard enthalpies ($\Delta H°$) are given.

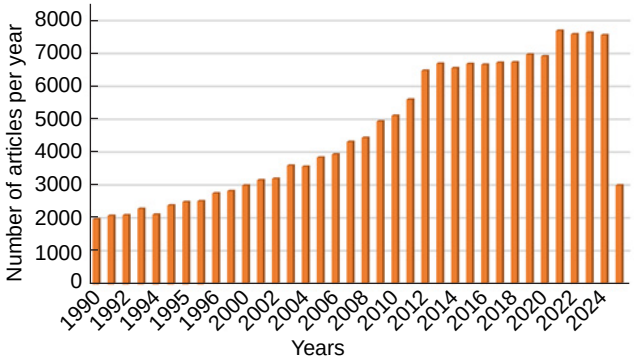

Figure 1. Analysis of publication activity on selective hydrogenation of acetylene in the period 1990–2025, carried out using the CAS SciFinder search system.

In this review, we summarized information on the achievements in the field of metal-catalyzed selective hydrogenation of acetylene over the last five years. The available data on the nature of the element used as a catalytically active component of the reaction have been systematized. The work is not limited to palladium and its compounds, but includes studies on the activity of nickel, copper, and bimetallic systems. The authors do not limit themselves to considering only heterophase processes, but also jointly consider the hydrogenation of an ethylene mixture with an admixture of acetylene and pure acetylene into ethylene.

2. Study of the mechanisms of catalytic processes and development of new approaches to design of hydrogenation catalysts

An effective catalytic system involves obtaining the desired compounds by the chemical reaction in high yields in the absence of by-products. The challenge of catalytic transformations in chemistry is significantly complicated by additional needs, *viz*., the possibility of catalyst regeneration,[67] the use of minimal catalyst loadings, the absence of stabilizers and expensive ligands,[68] the use of cheap metals.[69] Homogeneous and heterogeneous catalysts are successfully used to solve many problems in organic synthesis.[70–75] Homogeneous catalysts are effective and selective, mainly due to the fact that they generate certain rather stable molecular species in the reaction medium. However, it is usually not possible to reuse such catalysts. Heterogeneous catalysts may be used several times. However, with an increase in the number of cycles, their activity and selectivity may significantly decrease, and the detection of metal-containing species in the solution indicates the transition of part of the catalyst into the solution. This calls into question the heterogeneous nature of the processes and also leads to a decrease in the amount of catalyst and the impossibility of its reuse.

In recent years, there has been a significant accumulation of new knowledge and an evolution of our understanding of catalysis and catalysts. An important conceptual achievement is the development of ideas that expand our understanding of homogeneous and heterogeneous systems and the discovery of dynamic catalyst cocktail systems.[76, 77] Catalyst cocktail systems were first described by Ananikov and co-workers.[78] In this Section, mechanistic studies of the dynamic nature of catalysis using various reactions as examples are described, which is

necessary for forming ideas about the methods for studying dynamic phenomena in catalysis. At the end of this Section, the effects of 'cocktail' systems on the mechanisms of hydrogenation reactions are considered. In the following Sections, specific examples of hydrogenation reactions are given, many of which highlight various aspects of the dynamic behaviour of catalytic systems.

The type (or nature) of catalysis is largely determined by the particle size.[79,80] Nanoparticles and their assemblies[81,82] have fundamentally different properties compared to microparticles. Further reduction in particle size leads to the formation of clusters consisting of several atoms, as well as individual atoms.[83–86] An even greater reduction in the concentration of active sites on the surface of a heterogeneous catalyst is achieved by isolating the active metal with another metal, which can lead to the formation of alloys or intermetallides. All of these particles exhibit different behaviour patterns, and the variability of the processes is astounding. Catalytically active species can stick together, pass into solution as complexes and precipitate back as particles, migrate along the surface of the substrate, be immersed in the substrate, and become coated with a layer of other compounds. All this significantly changes the catalytic activity and selectivity[87,88] and makes the nature of catalysis dynamic.[89,90]

Thus, it was shown that in a model cross-coupling reaction[91,92] the used Pd/NHC (NHC is N-heterocyclic carbene) complex catalysts are transformed in the course of the reaction into metal nanoparticles and clusters due to the rupture of Pd-NHC coordination bonds and the transformation of the ligand, as evidenced by electrospray ionization high resolution mass-spectrometry (ESI-HRMS).[93] It is important to note that the catalyst transformations did not reduce the catalytic activity of the system. This was probably due to the formation of new catalytically active species *via* the leaching of Pd particles from the surface of the metal catalyst. The reversibility of the transition of species into solution (leaching) and back was calculated using density functional theory (DFT) modelling methods on model reactions of C–H-arylation, Heck, and amination.[94] As was found out, Pd leached into solution from the catalyst was the progenitor of a 'cocktail' of compounds that were classified into three main groups (Fig. 2):

1) catalytically active Pd nanoparticles with a high concentration of surface defects,

2) monomeric and oligomeric L[ArPdX]$_n$L (L is a ligand) particles,

3) irreversibly deactivated Pd species.

The study of complex systems requires a special approach. The traditionally used mercury test, despite its rapidity and versatility for identifying homogeneous and heterogeneous catalysis, demonstrated low analytical accuracy and low reproducibility for Pd and Pt complexes.[95] A low-temperature solid-state NMR spectroscopy technique was proposed to monitor hybrid catalytically active species and study the mechanisms of their reactions.[96] It was shown that for certain nanoparticle sizes, only six NHC ligands are sufficient to cover 80% of the surface of Pd particles measuring ~1 nm. Later, the concept of 4D catalysis was proposed, combining the achievements of instrumental analysis methods and the potential of machine learning for studying the mechanisms of dynamic catalysis.[97]

Leaching of a metal catalyst is uneven and depends on the type of facet of the metal catalyst surface. In bimetallic nanocatalysts, predominantly one metal is etched. Surface particles can migrate to the surface, stick together or separate from the surface and settle on it again. The presence of oxygen in the system can contribute to the formation of defects in the crystal lattice of metal particles and clusters, which sometimes plays a decisive role in some catalytic processes. All possible processes are characteristic of the formed catalyst particles: growth and dissolution of particles, movement along the surface and changes in the internal structure at the level of individual atoms, clusters and nanoparticles (NPs). Atoms are also detached from the edges and corners of NPs. Atoms can precipitate from the solution on the catalyst surface both on free surface areas and on NPs. In the first case, atoms can re-enter the catalytic cycle, in the second, they are poisoned by nanoparticles, changing the morphology of the particles and causing their growth.

Not only palladium but also nickel form catalytic systems of the 'cocktail' type. In a study,[98] a comparative characteristics and properties of two widely used nickel and palladium catalysts are given. Due to several oxidation states, nickel provides higher activity and larger variety of chemical transformations than palladium. This becomes possible despite the higher activation barrier of nickel catalysts than palladium ones. The authors note that Pd catalytic systems can easily form a 'cocktail of species' from various palladium compounds, but with similar oxidation states (Pd_1, Pd_n, Pd NPs), while nickel can behave as a 'cocktail of species' in different oxidation states with a smaller number of compounds.

Dynamic transformations of the catalyst in chemical processes significantly complicate the study of reaction mechanisms and catalytic cycles. Nevertheless, these data are necessary for understanding not only the course of reactions, but also the essence and nature of catalysis *per se*. Hydrogenation of alkynes can be considered as one of the representative examples for studying the nature of catalysis.[99,100]

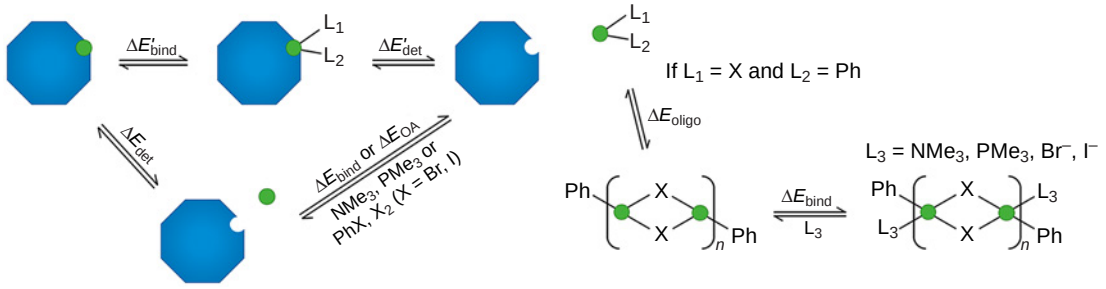

Figure 2. Possible processes of leaching, trapping and oligomerization in Pd catalytic systems. Pd nanoparticles are shown in blue, Pd species that have passed into solution are shown in green. Reproduced from Ref. 94 under a CC-BY-NC-ND license.

Metal-catalyzed hydrogenation with hydrogen is carried out in a homogeneous or heterogeneous mode using catalysts based on palladium, nickel and some other transition metals. According to the Horiuti–Polanyi principle (dissociative mechanism), the heterogeneous hydrogenation pathway involves the sorption of the substrate and hydrogen on the catalyst surface. In this case, two variants of the reaction are possible: hydrogenation on the surface of metal particles occurs selectively to an alkene. Sorption of reagents in the entire volume of the catalyst promotes the hydrogenation of an alkyne to an alkane. Adsorption and activation of hydrogen are important steps in the hydrogenation process.

On metal catalysts, the bond in the hydrogen molecule can undergo both homolytic and heterolytic cleavage. This is because transition metals have unoccupied d-orbitals to accommodate hydrogen electrons. At the same time, the heterolytic cleavage of the H–H bond creates a vacant s-orbital for the transfer of electrons from the metal.

In the Langmuir–Hinshelwood mechanism, which remains the most common for heterogeneous catalytic systems, two pathways can be distinguished (Fig. 3). The Horiuti–Polanyi mechanism, or the so-called dissociative mechanism, proposed in 1934, involves the homolytic dissociation of hydrogen on the metal surface, followed by the sequential addition of H atoms to the adsorbed alkynes.[100] Hydrogenation of an alkyne with molecular hydrogen begins with the sorption of the alkyne and hydrogen on the catalyst by bonding the Pd atom with the electrons of the π-bond and forming the [alkyne–Pd] complex (Fig. 3, route **A**–**B**).[101] The heat of adsorption of ethyne on palladium through the coordination of both π-bonds of the alkyne molecule with the metal is 112 kJ mol^{-1}. The next step (route **B**–**C**) comprises the migration and addition of the adsorbed H_2 molecule to the [alkyne–Pd] complex. In this case, a σ-bond is formed between the adjacent carbon and Pd, yielding an intermediate (Z)-vinylalkyl compound **C** or σ-vinyl[Pd]. Upon addition of an additional H atom, σ-vinyl[Pd] is converted to π-alkene[Pd]. This process is thermodynamically favourable ($\Delta H = -136$ kJ mol^{-1}).

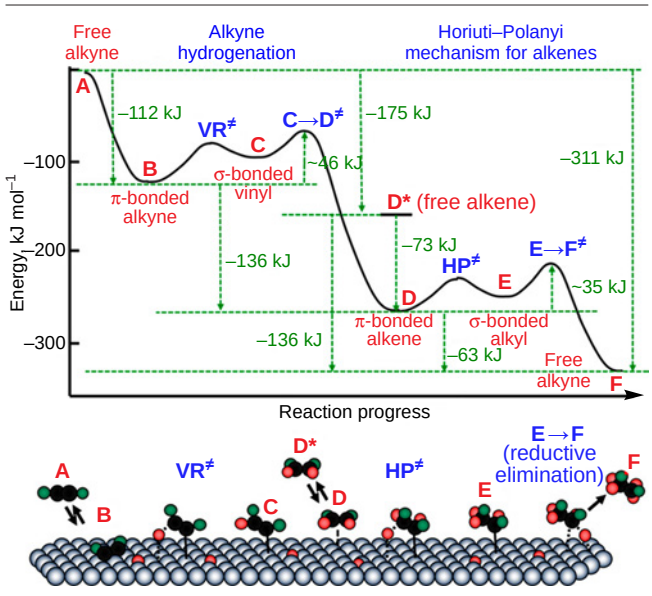

Figure 3. Mechanisms of hydrogenation of alkynes and alkenes. Red balls are H atoms in molecular hydrogen, green balls are H or D atoms attached to the unsaturated substrate. Reproduced from Ref. 101 with permission from the American Chemical Society.

Further, the hydrogenation process can proceed in two directions. The first consists of the decomposition of the π-alkene[Pd] complex to give free alkene **D*** (semi-hydrogenation). The second direction is further hydrogenation of the resulting alkene. π-Alkene[Pd] can add adsorbed hydrogen to form a σ-bonded alkyl complex **E**. This process is energetically less favourable than the formation of a free alkene (route **D**–**E**, $\Delta H = -35$ kJ mol^{-1}). At the final stage **E**–**F**, the σ-bond Pd–C is broken with the complete hydrogenation product **F**.

The mechanism of alkyne hydrogenation over alloy catalysts is somewhat more complex, since it is necessary to study and take into account the effect of each metal in the alloy separately. The mechanism of acetylene hydrogenation on the Pd–Mn/Al_2O_3 alloy catalyst is similar to that on the monometallic Pd catalyst.[102] The authors noted that the initial stage of formation of the π-complex of acetylene with the active centre of the catalyst is fast. The subsequent stages of hydrogen addition there to give ethylene and the formation of the [alkene-metal] complex occur much more slowly. In a study,[103] the mechanism of acetylene hydrogenation over the Pd–Ag/α-Al_2O_3 alloy catalyst was studied using the theory of quantum mechanics and the Monte Carlo method. The doping of the Pd catalyst with Ag reduced the adsorption energies of C_2H_2 and C_2H_4 on the catalyst surface (Fig. 4) and facilitated the desorption of ethylene from the catalyst surface, thereby improving the selectivity of hydrogenation. It is noted that the adsorption energy of acetylene and ethylene decreased with a decrease in the number of Pd atoms or an increase in the number of Ag atoms. Therefore, the activity of the catalysts was proportional to the number of Pd atoms and inversely proportional to the number of Ag atoms, which was consistent with the experimental results.

During the hydrogenation, the dispersed Pd–Ag/α-Al_2O_3 catalytic particles undergo agglomeration, and their average size increases almost 2-fold.[104] Analysis of images obtained by scanning electron microscopy (SEM) (Fig. 5) showed that in the course of hydrogenation, polymeric compounds and coke accumulate on the catalyst surface, which in turn leads to its deactivation.

Homogeneous hydrogenation can involve activation of the alkyne within the metal complex. Pd/NHC complexes are widely used as catalysts in homogeneous hydrogenation reactions. Denisova *et al.*[105] described the experience of successful use of Pd/NHC complexes in homogeneous-heterogeneous (transfer) catalytic hydrogenation. It was found that using a ^{13}C-labeled

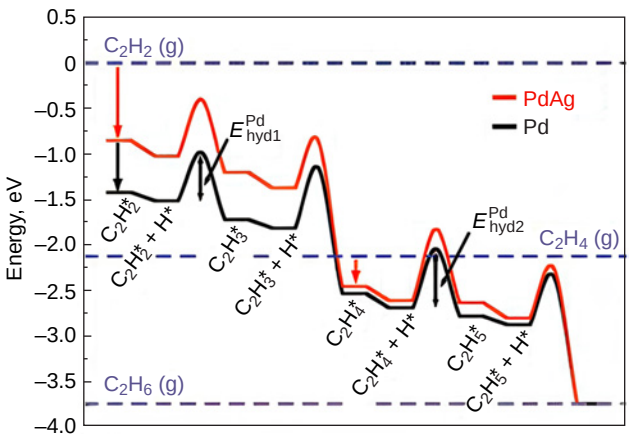

Figure 4. Effect of Ag doping on the activation energy of acetylene hydrogenation. Reproduced from Ref. 103 with permission from Taylor & Francis.

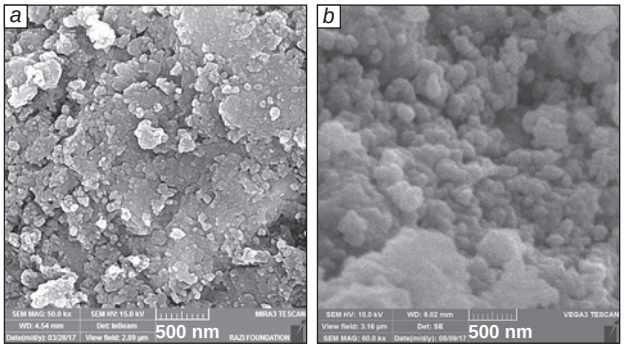

Figure 5. SEM images of fresh (*a*) and spent (*b*) catalysts. Darker areas correspond to polymer formations on the catalyst surface. Reproduced from Ref. 104 under a Creative Commons Attribution (CC BY) license.

NHC ligand, the Pd/NHC catalysts are converted to Pd NPs (1–9 nm) in the first minutes of the diphenylacetylene transfer hydrogenation, indicating a mixed type of catalysis. The authors proposed a mechanism of mixed hydrogenation, in which oxidative addition occurs on the surface of Pd particles, and the stages of *syn*-addition of alkynes and reductive elimination occur in the zone of Pd nanoparticles modified with NHC ligands. Using DFT calculations on the Pd_3 catalyst model, a mechanism of three-stage hydrogenation was proposed that includes the reaction of oxidative addition of molecular hydrogen to the Pd cluster, *syn*-addition of H_2 to the triple C≡C bond of acetylene and reductive elimination to give an ethylene molecule. The presence of a ligand on the metal surface complicates the addition of hydrogen.

Similar studies were carried out for the Pd/NHC-catalyzed semi-hydrogenation of 1,2-diphenylacetylene.[106] Using modern NMR, high resolution mass spectrometry with electrospray ionization (ESI-HRMS) and SEM/TEM methods, it was shown that during the hydrogenation process, the metal complexes are transformed into Pd NPs with the formation of a heterogeneous phase. Modification of the surface of these NPs with organic ligands under the reaction conditions significantly affected their catalytic activity.

It is worth noting that studies in the field of homogeneous catalysis confidently demonstrate the presence of dynamic processes. The composition of particles is constantly changing, which means that their properties and the very catalytic activity change. Under conditions of heterogeneous catalysis, the number of possible processes seems more limited. However, even in the solvent-free heterogeneous systems, it has been shown that metal atoms can migrate along the substrate surface and undergo various changes, *e.g.*, combine into larger clusters. This suggests that the heterogeneous process is also an evolutionary system. This raises a question that bridge across the present Section with the following ones: is it possible to discuss the dynamic nature of catalysis in relation to heterogeneous systems? In the authors opinion, the reaction of acetylene hydrogenation is a very convenient tool for proving this fact.

3. Monometallic Pd as catalyst for acetylene semi-hydrogenation

Palladium is a heterogeneous effective hydrogenation catalyst for a wide range of compounds.[107–115] The high activity of Pd catalysts is both an advantage and disadvantage. High-pressure hydrogenation of acetylene in the presence of Pd compounds produces mainly ethane rather than ethylene. Suppression of excess Pd activity to increase selectivity of acetylene semi-hydrogenation reactions is one of the main areas of catalysis. Common tools for varying the properties of a catalyst include reducing the size of catalytic species, the use of bimetallic catalysts, and varying the support (carrier) for the metal particles. Below are the main advances in the field of increasing the selectivity of Pd hydrogenation catalysts.

Single-atom (SA) catalysts have attracted particular attention due to their high reactivity and excellent catalytic efficiency,[116–120] which the small particle size and the resulting weak adsorption of ethylene on its surface. selectivity of acetylene semi-hydrogenation was using the DFT method. The dependence of the increase in selectivity of acetylene semi-hydrogenation on the decrease in the catalyst particle size was calculated using DFT method.[121] Pd/C catalyst obtained by impregnation with subsequent hydrogenation in a hydrogen stream at 500°C was used as a model catalyst. S-containing silane agents served as nanoparticle size regulators. Metal NPs were firmly fixed on the support due to the formation of Pd–S bonds with thiol groups, and were uniformly distributed over the surface. Interestingly, the Pd particle size of 2 nm was crucial, since particles of this size contributed to the formation of C_4 hydrocarbons and 'green oil'.

For example, 26 nm Pd NPs with a close-packed (Pd(111)) surface demonstrated 16 times greater ethylene selectivity than commercially available Pd/C.[122] At 100% acetylene conversion, the selectivity to acetylene was 76.5% and 4.5% for Pd(111) and Pd/C, respectively (Fig. 6, TEM is transmission electron microscopy). The authors suggested that the increase in the selectivity of nanostructured Pd stemmed from lower hydrogen adsorption on the metal catalyst because of the formation of palladium hydride sites Pd_4H_3 in the hydrogen stream.

In fact, the selective hydrogenation of acetylene requires the reaction to occur on the surface of the catalyst, not in its bulk. The same idea on the need to separate the surface and bulk reactions of acetylene hydrogenation to increase selectivity to ethylene was highlighted in the work [123] (Fig. 7). According to *in situ* X-ray photoelectron spectroscopic analysis of solid Pd catalysts, non-selective hydrogenation occurred at a low carbon content in the catalyst, and the process itself occurred on hydrogen-saturated β-hydride in the catalyst bulk.

The high selectivity to ethylene in the semi-hydrogenation of acetylene at high temperatures on the Pd(111) catalyst was in good agreement with the calculated value (82% at 300 K), obtained by *ab initio* molecular dynamics (AIMD) methods. The calculated values of the free energy barriers for ethylene desorption on Pd(111) were 0.51 eV at 300 K and 0.39 eV at 500 K.[124] The surface of the close-packed monoatomic Pd(211) catalyst was more active than that of Pd(111). At the same time, differential chemisorption energy of Pd(211) catalyst was higher with a lower barrier to further hydrogenation of ethylene (Table 1).[125] DFT calculations and coverage-dependent microkinetic simulations showed that ethylene was produced on the close-packed regions of the catalyst, while the defective surface regions were significantly more active in selective ethane formation.

According to DFT calculations, hydrogenation of ethylene to ethane on the SA–Pd catalyst required overcoming two barriers of 0.93 and 1.22 eV.[126] The chemical adsorption energy of ethylene is 0.76 eV, while the hydrogenation barriers are only 0.62 and 0.35 eV, located below the ethylene level.

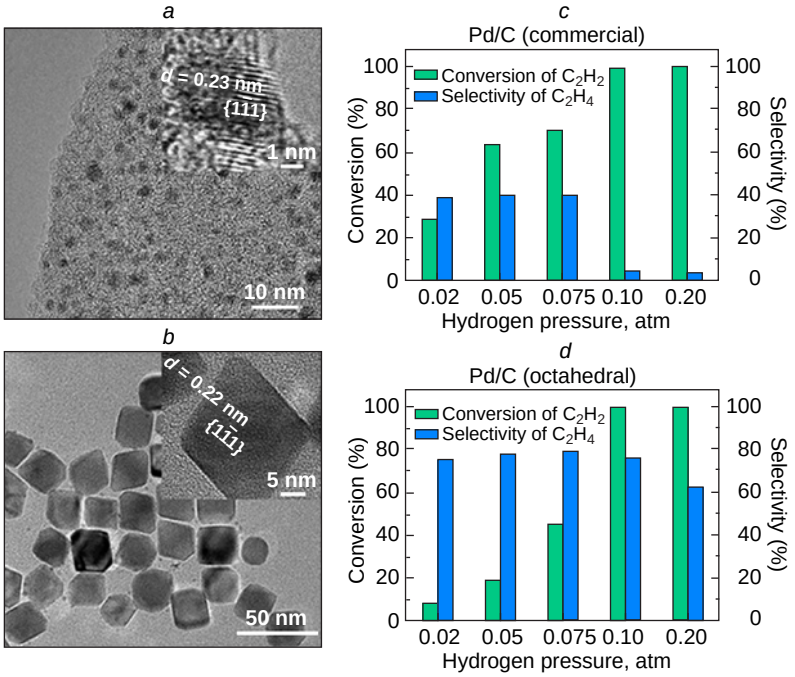

Figure 6. TEM images of a commercially available Pd/C catalyst (*a*) and octahedral Pd/C (*b*). Acetylene conversion and selectivity to ethylene in acetylene hydrogenation over commercial Pd/C (*c*) and octahedral Pd/C (*d*) catalysts at 293 K, $p(C_2H_2) = 0.02$ atm, gas hourly space velocity (GHSV) is 120 000 h^{-1}. The insets in the upper corners show enlarged high resolution TEM images. Reproduced Ref. 122 with permission from the American Chemical Society.

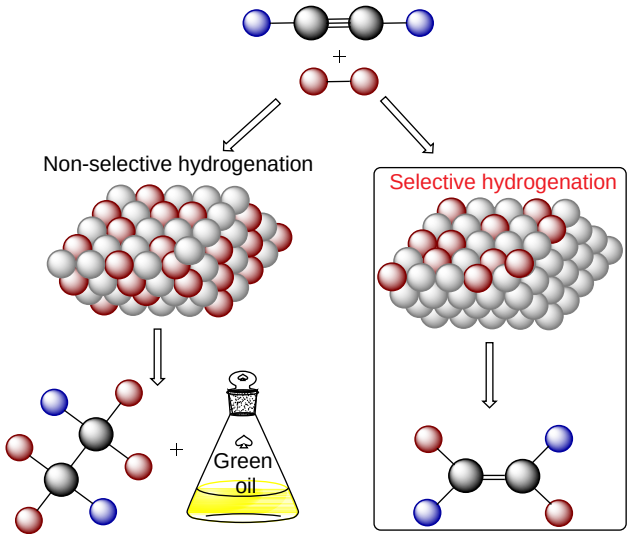

Figure 7. Schematic view of the processes of non-selective and selective hydrogenation of acetylene. Grey balls represent the metal catalyst, red balls represent hydrogen atoms in molecular H_2 as, blue balls represent hydrogen atoms in acetylene, and black balls represent carbon atoms.

Table 1. Adsorption energies (E_{ads}, eV) and free adsorption energies (G_{ads}, eV) of acetylene and ethylene on palladium surfaces.[125]

	Pd(211)		Pd(111)	
	E_{ads}	G_{ads}	E_{ads}	G_{ads}
C_2H_2	–2.33	–1.65	–2.01	–1.49
C_2H_4	–1.21	–0.81	–0.87	–0.34

Template method was used for the Pd catalyst design. Isolated Pd atoms (Pd-ISA) were anchored on the inner walls of mesoporous nitrogen-doped carbon foam nanospheres (MPNC).[127] Such catalyst provided complete conversion of acetylene hydrogenation at only 60°C! However, the selectivity of the catalyst was lower than 20%. Increasing the temperature improved the hydrogenation selectivity. The ISA-Pd/MPNC and ISA-Pd/non-MPNC (non-MPNC is non-mesoporous analogue of MPNC) catalysts were used at 120 and 140°C, respectively, and were more selective at lower loadings (200 *vs*. 300 mg): acetylene conversion was 83% and 32%, respectively, and ethylene selectivity was 82% and 17%, respectively.

Atomically dispersed Pd_1/C_3N_4 catalyst and Pd NP catalyst supported on graphite carbon nitride (gC_3N_4), Al_2O_3 and SiO_2 were synthesized by wet-impregnation of the support with a solution of $Pd(acac)_2$ (acac is acetyl acetonate) followed by calcination in a flow of 10% O_2/He and H_2.[128] Surprisingly, when hydrogenating acetylene in excess ethylene, the Pd NPs/gC_3N_4 catalysts demonstrated higher selectivity to ethylene than the common Pd/Al_2O_3 and Pd/SiO_2 catalysts. The high catalytic performance was, probably, due to the significant charge transfer from Pd NPs to the gC_3N_4 support. A single-atom Pd_1/C_3N_4 catalyst demonstrated superior catalytic performance compared to Pd NPs/gC_3N_4 catalysts with higher selectivity to ethylene and higher coking stability in both reducing and oxidizing media at high temperatures. Atomically dispersed palladium species Pd-ISAS/CN immobilized on N-doped carbon nanospheres obtained from covalent organic frameworks (COFs) (demonstrated 80% selectivity to ethylene and 92% acetylene conversion at 100°C, with the catalyst activity of 712 $mol_{C_2H_2}$ $(mol_{Pd}\ h)^{-1}$.[129]

Ultrasmall Pd NPs prepared using H_2 instead of $NaBH_4$ to reduce $NaBH_4$ and immobilized in the micropores of layered covalent triazine frameworks (CTFs) demonstrated 100% acetylene conversion with 99.9% ethylene selectivity, as well as excellent stability at 250°C and a space velocity of 110 000 h^{-1}.[130] The nanocatalyst demonstrated high recycling potential with full conversion and selectivity maintained for 5 cycles. The authors explained the improved selectivity rates by the layering CTFs into thinner and smaller sheets during the reaction, which provides greater access of reagents to the catalytically active Pd sites and increased mass transfer.

Varying the support for immobilization of metals is a convenient tool for controlling the catalyst properties. MgO-

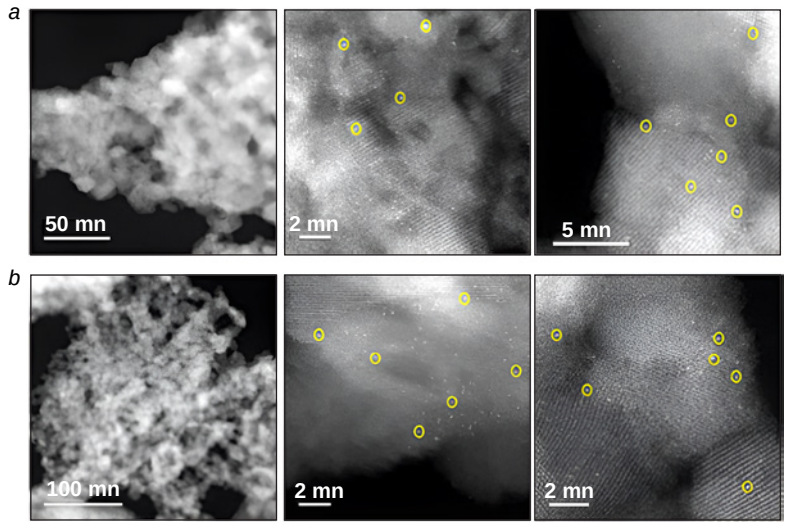

Figure 8. AC-HAADF-STEM images of the surface of Pd_1/MgO (*a*) and (b) Pd_1/MgO-H100, which is parent Pd_1/MgO particles reduced at 100°C with 10 vol.% H_2 (*b*). A part of isolated Pd atoms are designated as yellow circles. Reproduced from Ref. 133 with permission from Wiley.

supported metal Pd particles (Pd/MgO) showed high selectivity (82%) in the hydrogenation of acetylene to ethylene at 200°C with ultra-low catalyst loading (0.05 wt.%).[131] Such catalyst with a nominal Pd loading of 0.001% demonstrated excellent performance, providing high acetylene conversion (97%) and good selectivity to ethylene (89%).[132] Amazingly, but under the same conditions, the ethylene selectivity of 1% Pd/MgO catalyst was lower than 4%. Kinetic isotope effect and IR spectroscopy data suggested heterolytic H_2 dissociation on isolated Pd atoms to form the O–H bond. This probably determines the high selectivity in the selective hydrogenation of acetylene. Moreover, dispersed Pd atoms were inactive for ethylene hydrogenation, which prevented the formation of ethane.

Single-atom Pd_1/MgO acetylene semi-hydrogenation catalyst was obtained mechanochemically in a ball mill by grinding palladium phthalocyanine and magnesium phthalocyanine, followed by calcination at 600°C.[133] The nature of single-atom Pd species after hydrogenation at 100°C was confirmed by aberration-corrected high-angle annular dark-field scanning transmission electron microscopy (AC-HAADF-STEM) (Fig. 8). The strong interaction between Pd atoms and MgO support not only inhibited the aggregation of Pd atoms, but also resulted in high ethylene desorption ability of Pd, thereby providing high selectivity of acetylene semi-hydrogenation: 100% C_2H_2 conversion with 60% selectivity to acetylene at 140°C and TOF = 0.074 s^{-1}.

Pd_1/CeO_2 and Pd_1/α-Fe_2O_3 catalysts were prepared by reducing conventional supported Pd/CeO_2 and Pd/α-Fe_2O_3 obtained by impregnating the supports with $Pd(NO_3)_2$ solution, followed by reduction with 10 vol.% H_2/He at 200, 500, and 600°C and oxidation with 20 vol.% O_2/He at 500°C to selectively encapsulate Pd nanoparticle clusters.[134] Single atoms exhibited strong metal–support interactions only at higher reduction temperatures than for nanoparticles/clusters, thus contributed to increased selectivity and stability in acetylene semi-hydrogenation. Pd/CeO_2 catalyst prepared by impregnation with the initial humidity and calcined at 600°C and 800°C demonstrated excellent ethylene selectivity (~100%) in acetylene hydrogenation in large excess of ethylene at 50–200°C.[135] This was probably due to the formation of $Pd_xCe_{1-x}O_{2-y}$ or Pd–O–Ce phases on the catalyst surface, as confirmed by the results of X-ray diffraction (XRD) and X-ray photoelectron spectroscopy and indicated a strong interaction of Pd and Ce.

SA catalyst coordinated by 1,10-phenanthroline-5,6-dione (PDO) was successfully used for the semi-hydrogenation of acetylene under mild conditions.[136] The hydrogenation selectivity was highly dependent on the metal : ligand molar ratio. Surprisingly, the increase in ligand loading promoted the hydrogenation of acetylene to ethylene. In the absence of an organic ligand, 100% conversion of acetylene to ethane was observed. At a PDO : Pd ratio of 1 : 1, the ethylene selectivity was 30%. The best selectivity (80%) was obtained at a ligand : Pd ratio of 6 : 1, which remained constant after a further increase in the ligand amount (Fig. 9). The authors suggested, that the metal atoms are maximally coordinated and are unable to form bonds with other ligand molecules at a ratio of 6 : 1. According to calculations, the binding of hydrogen to the ligand switches the reaction towards ethylene formation. The measured activation energies for the PDO–$Pd(1:1)/CeO_2$ and PDO–$Pd(6:1)/CeO_2$ catalysts were 36 kJ mol^{-1} in both cases. It was later shown that the organic ligand stabilized the single metal atoms through the strong Pd–O or Pd–N interaction.[137] Ethylene molecules were stronger adsorbed on the Pd_1–$PDO/CeO_2(111)$ catalyst than C_2H_2 molecules, which resulted in higher selectivity in the semi-hydrogenation.

Boron nitride (BN) used as a Pd support acted as a regulator of the electron density of Pd and promoted the desorption of ethylene in acetylene semi-hydrogenation.[138] The Pd/BN catalyst provided 100% acetylene conversion and 93% ethylene selectivity with good stability.

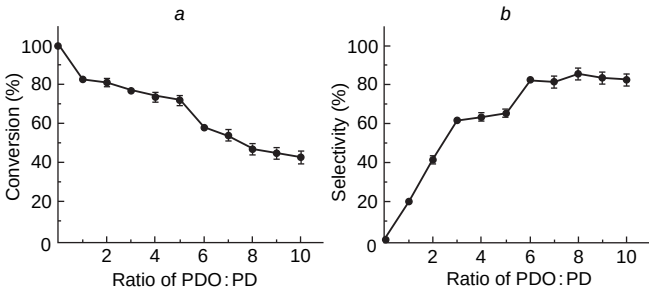

Figure 9. Conversion (*a*) and ethylene selectivity (*b*) of Pd–PDO catalysts as a function of the PDO : Pd ratio in acetylene hydrogenation, T = 120°C. Reproduced from Ref. 136 with permission from Elsevier.

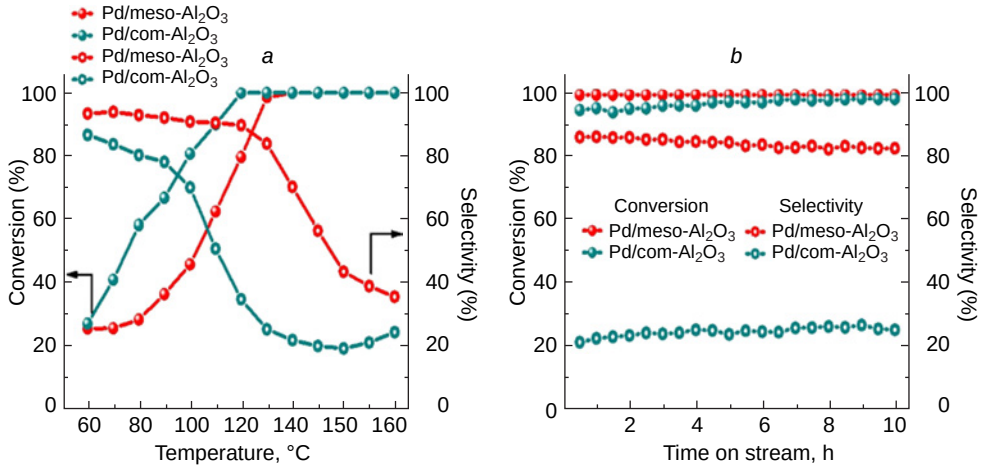

Figure 10. The effect of temperature on acetylene conversion and ethylene selectivity to 0.02% Pd/meso-Al_2O_3 and 0.02% Pd/com-Al_2O_3 catalysts (*a*); and their time dependence under the following reaction conditions: 130°C, gas mixture of 0.33% C_2H_2, 0.66% H_2, 33% C_2H_4, GHSV = 6000 h^{-1}). Reproduced from Ref. 144 with permission from Elsevier.

Single-atom Pd species coordinated by dicyandiamide (N_{dicy}) and supported on hierarchical carbon nanocells (hNCNC) demonstrated an 18-fold increase in activity compared to similar catalysts in the absence of organic ligand (Pd_1/hNCNC) and provided 99% C_2H_2 conversion and 87% selectivity at 160°C due to C_2H_4 desorption on isolated single Pd sites in Pd_1-N_{dicy}/hNCNC.[139] N-doped well-organized carbonaceous cells were prepared *in situ* by the template method at 800°C from MgO and pyridine or benzene as a carbon source. The Pd_1-N_{dicy}/hNCNC catalyst was prepared by pyrolysis of a mixture of the support, $PdCl_2$ and dicyanamide at 700°C.

Single-atom Pd_1/TiO_2 catalyst was prepared by mechanochemical mixing of palladium and titanium phthalocyanines and TiOPc in a ball mill followed by calcination and reduction with hydrogen. For comparison, the same catalyst was obtained by the classical impregnation method. Such catalysts showed low yields in the hydrogenation of acetylene. It should be noted that light irradiation increased the conversion of acetylene hydrogenation from 20 to 80% with a simultaneous decrease in ethylene selectivity. DFT calculations demonstrated, that photoinduced electrons transferred from TiO_2 to adjacent Pd atoms facilitated the activation of acetylene. The selectivity of Pd_1/TiO_2 particles in the form of a small number of encapsulated clusters was significantly higher than that of individual catalytic particles in photothermocatalytic hydrogenation of acetylene at 70°C.[140]

The supported Pd/TiO_2 catalysts containing 0.10 wt.% Pd prepared by precipitation — reduction with $NaBH_4$ at 300–700°C were used in the hydrogenation of acetylene to ethylene.[141] The Pd/TiO_2-HT300‡ sample calcined at 300°C performed best, providing 100% conversion of acetylene and 80% selectivity for ethylene at 55°C (TOF = 0.12 s^{-1}). The authors attributed the catalytic properties to the high content of oxygen vacancies in the sample (71.8%), as confirmed by *in situ* X-ray photoelectron spectroscopy, *in situ* Raman spectroscopy and H_2 desorption.

Pd NPs encapsulated in a thin $SrTiO_3$ shell were synthesized *via* a hydrothermal method from $Sr(OH)_2 \cdot 8H_2O$ and Na_2PdCl_4 followed by calcination in air and H_2/Ar at 200°C for 1 h in a tubular furnace. These catalysts featured lower ethylene adsorption and provided 98% conversion and 92% selectivity to ethylene with a specific activity of 5552 $mol_{C_2H_2}$ $(mol_{Pd}\ h)^{-1}$ at 100°C, significantly exceeding the most catalysts comprising non-encapsulated Pd NPs.[142]

The Pd/Al_2O_3 nanocatalyst with a palladium content of 5% was synthesized by flame spray pyrolysis method and provided 97% conversion of acetylene and 62% selectivity to ethylene, TOF = 5 s^{-1}.[143] In this case, the catalytic properties depended on the type of Al_2O_3 used. The use of Pd supported on pentacoordinated Al_2O_3 (Pd/meso-Al_2O_3) in the hydrogenation of a mixture of 0.33% C_2H_2, 0.66% H_2, 33% C_2H_4 demonstrated higher selectivity than Pd/com-Al_2O_3 (commercially available Al_2O_3) at various reaction temperatures (Fig. 10).[144] At acetylene conversion >99%, the selectivity of Pd/meso-Al_2O_3 catalyst was 83%, whereas with Pd/com-Al_2O_3 it was 25%. According to energy dispersive X-ray spectroscopy (EDS) data, the dispersion of active Pd sites in the Pd/meso-Al_2O_3 catalyst was high and uniform, which contributed to the high catalyst productivity. The dispersion of Pd in the catalyst on the commercial support was low, and the metal formed conglomerates with an average diameter of 5.55 nm according to HR-TEM (HR is high resolution) data.

An important role in the manifestation of the properties of a metal catalyst is played by its precursor. The electronic structure of the metal in the starting compound determines the state of the metal in the catalyst. For example, an increase in the electron density on the metal was reported[145] to reduce the adsorption of ethylene on the negatively charged sites of Pd thereby improving the selectivity of the catalyst. This effect was clearly demonstrated on the example of the catalysts obtained from Na_2PdCl_4, $PdSO_4$ and $Pd(acac)_2$ by the wetness impregnation method followed by calcination in 10% H_2/N_2 at 400°C for 4 h. The Pd/α-Al_2O_3 catalyst synthesized from $Pd(acac)_2$ had a higher electron density of the active Pd sites and demonstrated higher selectivity to ethylene than catalysts obtained from Na_2PdCl_4 and $PdSO_4$ salts (Fig. 11). In addition, Pd/α-Al_2O_3 prepared from $Pd(acac)_2$ was more stable than similar catalysts obtained from Na_2PdCl_4 and $PdSO_4$ due to the formation of PdC phase during the prolonged reaction.

Highly dispersed stable PdC phase supported on α-Al_2O_3 was prepared using N-containing silane coupling agent as a modifier.[146] The resulting catalyst demonstrated ethylene selectivity 15% higher than the conventional PdAg alloy with total acetylene conversion at 240°C and greater time-on-stream stability for 200 h. The excellent ethylene selectivity was mainly due to the special structure of the PdC phase NPs with a distorted lattice, which contributed to weaker ethylene adsorption and led to strong interaction of Pd NPs with the support surface.

‡ The figures in the designation of the support indicate the reduction temperature – 300°C.

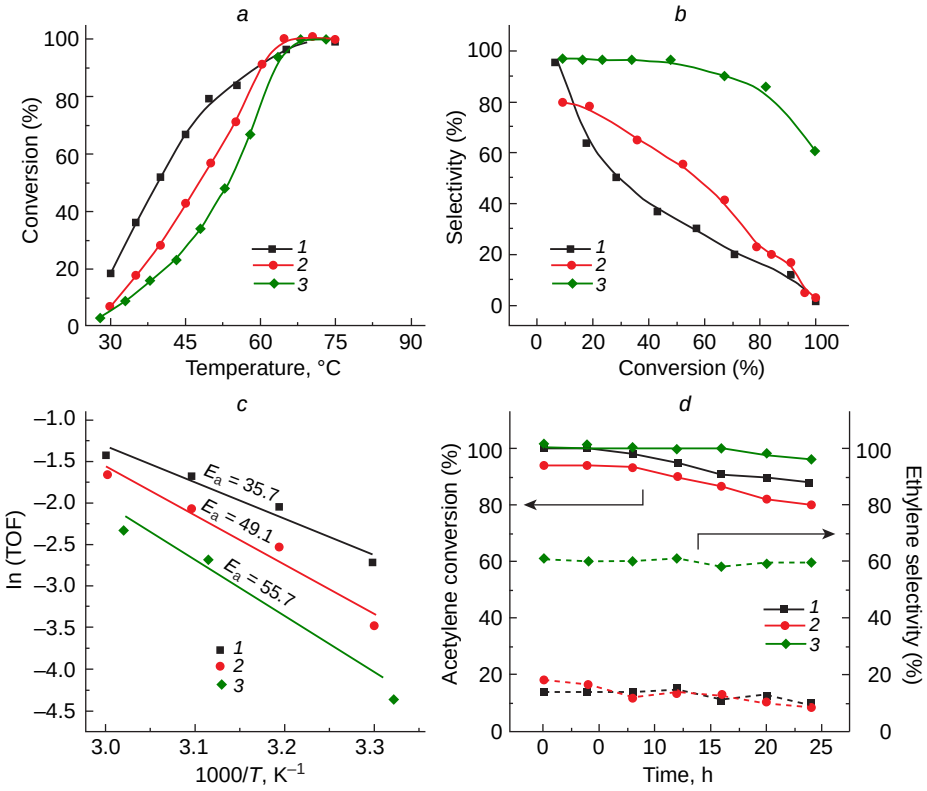

Figure 11. Plots of Acetylene conversion *vs*. temperature (*a*), ethylene selectivity *vs*. acetylene conversion (*b*), ln(TOF) *vs*. corrected temperature (*c*); Arrhenius plots for acetylene conversion and selectivity to ethylene *vs*. time (*d*) for Pd/α-Al_2O_3 catalyst obtained from Na_2PdCl_4 (*1*), $PdSO_4$ (*2*), and $Pd(acac)_2$ (*3*). Fig. 11,*c* shows apparent activation energy values (E_a), kJ mol^{-1}. Reproduced from Ref. 145 with permission from Springer Nature.

The $Pd/MgAl_2O_4$ catalyst, intended for the selective hydrogenation of acetylene, was prepared from Na_2PdCl_4 by impregnation and then supported on mixed oxides followed by calcination at 600°C and reduction with H_2.[147] Partially positively charged Pd atoms effectively reduced the adsorption of intermediates during hydrogenation, providing 96% acetylene conversion with 87% ethylene selectivity and excellent stability for a 50-hours test at 120°C.

Using carbon nanotubes (NTs) as a support for Pd instead of α-Al_2O_3 suppressed the formation of palladium hydrides, thereby increasing the yield of ethylene.[148] X-ray absorption spectroscopy, SEM and temperature programmed desorption (TPD) study of C_2H_4 in combination with DFT calculations demonstrated the presence of a unique local environment of Pd containing subsurface carbon atoms, which increased the acetylene conversion. According to kinetic study of the liquid-phase hydrogenation of acetylene over a commercial 0.5 wt% Pd/Al_2O_3 spherical catalyst in N-methylpyrrolidone (NMP) in a reactor at 60–100°C and 15–250 psi (1–17 bar), the reaction occurs on the surface and is limited by minor diffusion resistances between and within the catalyst species.[149]

$Pd_{0.87}/MoS_2$ catalyst was synthesized by deposition of Pd particles on MoS_2 nanosheets obtained by ultrasonic exfoliation in formamide.[150] The catalyst provided 75% selectivity to ethylene and 100% conversion at a space velocity of acetylene of 40 000 mL h^{-1} g^{-1}. According to SEM, Pd particles were dispersed on the glossy MoS_2 surface with a low nominal Pd loading. Strong Pd–MoS_2 interactions arising from the charge transfer from Pd to MoS_2 were observed by XPS.

The effective interaction between Pd and the support resulted in high selectivity acetylene hydrogenation to ethylene (100% acetylene conversion at 240°C) of the Fe_5C_2-supported Pd/α-Al_2O_3 catalyst.[151] The catalyst was prepared by reduction of $FeCl_3$ with $NaBH_4$ in isopropanol. The resulting Fe NPs reduced Pd^{2+} to Pd^0 when adding $Pd(OAc)_2$ to the solution. The addition of oleylamine and heating under reflux at 350°C afforded the desired catalyst. DFT calculations confirmed that the energy barrier for the conversion of ethylene to ethane on this catalyst was very high, making the complete hydrogenation unlikely.

Natural minerals such as complex silicates and alumosilicates have also found application as supports for hydrogenation catalysts. For example, pre-calcined halloysite nanotubes (HNT-c) were used to support Pd NPs from $PdCl_2$ and $Pd(OAc)_2$ obtained in solutions of ammonia (NH_3), sodium chloride (NaCl), hydrochloride (HCl) and in acetone (Ac).[152] The highest (~65%) ethylene selectivity at acetylene conversion <70% was achieved using Pd-HNT-c-Ac. The other samples demonstrated close selectivity (55–60%), probably due to palladium poisoning with chlorine and amines. Catalysts based on silanized HNTs (HNT-as) provided the selectivity in the range of 45–59% with conversion below 80%. The highest selectivity was demonstrated by Pd-Hal-as-HCl. It should be noted that the performance of Pd-HNT catalysts was comparable to that of palladium catalysts supported on Al_2O_3, SiO_2 and TiO_2. However, their ethylene selectivity is still insufficient for commercial use.

Palygorskite (Pal) is a naturally abundant aluminosilicate mineral that was used as a support for ultralow content Pd (0.8%) hydrogenation catalysts.[153] This mineral was treated ammonia (Pd/N-Pal) or air (A-Pal). The treatment with ammonia to produce Pd/n-Pal ensured easy and strong fixation of metal particles on the support and increased their dispersion due to a decrease in the crystal size and adsorption of H_2 at a temperature of 90–110°C, which ultimately contributed to an increase in the selectivity to C_2H_4. On the contrary, air-treated Pd/A-Pal catalysts demonstrated a weak interaction of Pd particles with the support and low dispersion, therefore, the selectivity to ethylene for these catalysts was lower. The TOF values for Pd/A-Pal and Pd/N-Pal in acetylene hydrogenation at 90°C and the reaction time of 360 min were 0.345 and 0.05 s^{-1}, respectively. It is worth noting that the increase in temperature promoted PdHx hydride phase formation on the Pd/A-Pal

catalyst, providing the complete hydrogenation of acetylene to ethane.

N-Doped carbon-supported Pd/NC catalysts were prepared from H_2PdCl_4, activated carbon and 1,3-diethylimidazole acetate/N-methylpyridinone dihydrogen phosphate ionic liquids by wetness impregnation technique followed by calcination at 650°C and hydrogenation at 400°C for 4 h in a tube furnace.[154] Nitrogen doping altered the electronic structure of Pd NPs, allowing rapid desorption of ethylene and preventing ethane formation during overhydrogenation. The ethylene selectivity to this catalyst was 91.3% over 40 h with 94.6% acetylene conversion.

The single-atom Pd_1-N_8/CNT catalyst on multi-walled carbon nanotubes (CNT) was studied by cyclic voltammetry (CVA).[155] Using voltammograms, the azide ion oxidation into azide radicals with subsequent formation of well-ordered polynitrogen species, as well as the palladium reduction from its oxide were identified. PdO/CNT was used as the working electrode. The N_8 fragment was formed from NaN_3 in a buffer solution under electrolysis and attached to the single-atom Pd, stabilizing it. Calculations using acetylene temperature programmed desorption (C_2H_2–TPD) and DFT confirmed that C_2H_2 favours π-bonding on Pd-SA, and H_2 dissociated on the N atom attached to Pd. This Pd–N synergistic effect favoured the formation of C_2H_4 during acetylene hydrogenation and prevented its complete hydrogenation to C_2H_6.

Modification of the Pd/SiO_2 catalyst with histidine followed by calcination at 240°C provided 1.0 nm Pd NPs compared to the untreated catalyst.[156] According to the XPS data, Pd NPs of the Pd–His/SiO_2 catalyst were highly dispersed and positively charged, which provided a high semi-hydrogenation selectivity of 81.5% (100% acetylene conversion at 160°C) and high stability at 160°C for 50 hours. The desorption temperature of C_2H_2 decreased from 123°C for Pd/SiO_2 to 112°C for Pd–His/SiO_2, while ethylene was easily desorbed from the latter catalyst during the reaction, which prevented the formation of ethane.

Encapsulated palladium nanoparticles or nanoclusters exhibit high selectivity in selective hydrogenation due to the fact that the thin shell of the support or capsule protects the surface of the active metal. Pd nanoclusters coated with a thin $SrTiO_3$ shell demonstrated selectivity to ethylene of 92% with acetylene conversion of 98%.[142] The specific activity of such a catalyst was 5552 $mol_{C_2H_2}$ $(mol_{Pd}\ h)^{-1}$ at 100°C, which significantly exceeds the similar parameter of most palladium-based catalysts. Selectivity was achieved due to the sorption of C_2H_2 on Ti^{3+} capsule sites instead of Pd, and H_2 was sorbed on palladium and transferred to the catalyst shell, where reduction occurred.

An unusual type IL@Pd@NMC palladium catalysts of the core-shell type on N-doped mesoporous carbon (NMC) with a metal content of 20–50% was synthesized by wet impregnation and subsequent treatment with MeCN, ionic liquids (ILs) and drying. These catalysts provided ethylene selectivity >93% with complete acetylene conversion in the temperature range of 100–200°C.[157] Importantly, they demonstrated excellent stability, providing 100 h on stream for the hydrogenation of acetylene to ethylene without any obvious decrease in productivity. The efficiency of IL@Pd@NMC was comparable to Pd@NMC, making it a potential candidate for industrial use.

Similar Pd catalysts Pd@S-1@IL obtained by impregnation of zeolite (S-1) with solutions of tetrapropylammonium hydroxide (TPAOH), tetraethyl orthosilicate (TEOS), hexadecyltrimethoxysilane (HTS) and followed by incapsulation with [Prmim][Cl] ionic liquid (Prmim is 1-methyl-3-n-propylimidazolium) exhibited excellent ethylene selectivity

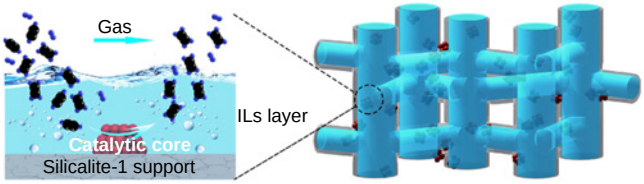

Figure 12. Schematic representation of Pd@S-1@ILs catalysts. Reproduced from Ref. 158 with permission from Elsevier.

(>90%) regardless of the level of substrate conversion and excellent stability over 800 h on stream even under relatively harsh conditions.[158] The high selectivity of the catalyst was due to the structure of the catalyst, which resembled a kind of 'filter' (Fig. 12). Encapsulation of Pd NPs inside the support prevented metal migration, and the IL layer regulated gas sorption-desorption on the catalyst surface, suppressing the process of overhydrogenation to ethane. In addition, the IL layer provided heat removal from the metal catalyst and prevented the formation of hot spots, thereby hampering the formation of polymerization products. The high stability of the atomically dispersed Pd hydrogenation catalysts supported on TiO_2 and coated with 1-*n*-butyl-3-methylimidazolium tetrafluoroborate ([BMIM][BF_4]) was due to the electrostatic interaction of the IL and Pd/TiO_2.[159] Moreover, the synergism of IL and Pd/TiO_2 suppressed coke deposition on the catalyst, ensuring its higher performance and stability. And the ionic liquid shell prevented the formation of 'hot spots', preventing the formation of 'green oil', oligomerization products.

An unusual single-atom catalyst was synthesized by *in situ* confinement of $Pd(acac)_2$ between two-dimensional layers formed by Cu, 4,4′-bipyridine (bipy) ligand and $SiW_{12}O_{40}^{4-}$ (SiW) anions in the outer sphere.[160] The small distance (6.25 Å) between two SiW anions restricted the movement of $Pd(acac)_2$, and the SA-Pd can be directly fixed by oxygen atoms on the SiW surface during the reduction without agglomeration. The resulting Pd_1@Cu–SiW catalyst demonstrated 92.6% ethylene selectivity and complete acetylene conversion at 120°C. Surprisingly, the ethylene selectivity remained >90% with increasing reaction temperature, whereas it usually drops sharply in the presence of common catalysts.

A useful approach to catalytic hydrogenation using parahydrogen (p-H_2) was shown in a series of works by I.V.Koptyug. Parahydrogen is a hydrogen molecule in a singlet state, in which two nuclear spins are antiparallel. The p-H_2 spin order was transferred to product molecules in hydrogenation, provided that the process involved the simultaneous transfer of two hydrogen atoms of the parent p-H_2 molecule to the substrate. This phenomenon of parahydrogen-induced polarization is used in NMR spectroscopy for mechanistic studies of reactions involving molecular hydrogen, *e.g.*, hydrogenation. Strongly enhanced absorption/emission signals were recorded in the NMR spectra of the hydrogenated products. The observed signal enhancement can theoretically reach 105 times and even more than when using ordinary hydrogen.[161] Thus, catalytic hydrogenation with parahydrogen of propyne,[162–166] propene[167,168] and some other compounds[169] was studied.

Selective hydrogenation of acetylene is also of fundamental importance, since it is practically the only way to enrich the nuclear spin isomers of ethylene using p-H_2. For example, in the hydrogenation of acetylene with p-H_2 (C_2H_2 : p-H_2 = 1 : 4) over Pd_{o37}/SiO_2 with octahedral Pd nanoparticles at 150°C (Scheme 1), a strong enhancement of the signals of the

Scheme 1

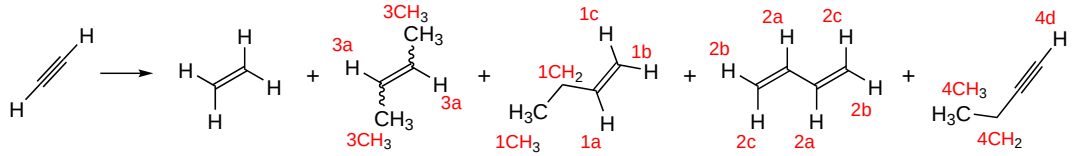

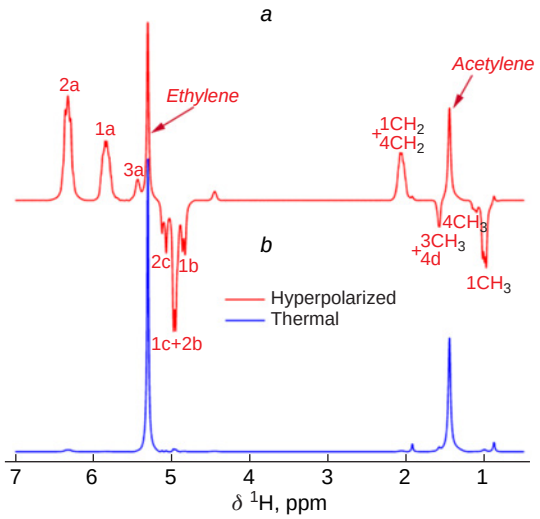

Figure 13. ^{1}H NMR spectra obtained by hyperpolarization of the reaction mixture (*a*) and after thermal equilibrium has been reached in the stopped-flow experiment (*b*). Reproduced from Ref. 170 with permission from the American Chemical Society.

oligomerization products was observed in the NMR spectra against the background of the hydrogenation products of the C≡C triple bond (Fig. 13 *a*).[170] Although ethylene was the predominant reaction product, no enhancement of the signals of the protons at the C=C bond was observed. The reason was in blocking of the nuclear spin polarization by the magnetic equivalence of all protons in the ethylene molecule. The NMR signals of the oligomerization products, on the contrary, were significantly enhanced (nuclear spin polarization >1.7%), despite the low concentration of these compounds in the mixture. For comparison, the spectrum obtained after the nuclear spins returned to thermal equilibrium is shown in Fig. 13 *b*. The authors [170] found, that the signal amplification was higher the larger the catalyst NPs used in hydrogenation. The fact that oligomers accumulated higher polarization than alkenes was additionally confirmed by experiments on propyne hydrogenation.

Hyperpolarized ethylene was obtained by continuously passing a mixture of acetylene and p-H_2 over a Pd/TiO_2 catalyst.[171] A similar experiment was carried out using [D_2] acetylene, which formed DHC=CHD when hydrogenated with p-H_2. This proved that the addition of parahydrogen occurred in pairs and preserved the correlation of individual nuclear spins of the substrate molecule. It was shown that ethylene obtained with p-H_2 exhibited hyperpolarized signals in an anisotropic medium.

Selective hydrogenation of acetylene with parahydrogen over Pd catalysts and iridium complexes was studied.[172] NMR spectroscopy studies showed that isomers of individual nuclear spin complexes of ethylene formed by the addition of p-H_2 to acetylene equilibrated within 3–6 s for spin systems with the same symmetry (*syn*-addition of hydrogen) and within 1700–2200 s for spin systems with different symmetry (*anti*-addition).

Acetylene molecules contain the isotope ^{13}C, the number of which is small and amounts to 2.2% of the total number, according to the natural abundance of the isotope ^{13}C. To achieve specific objectives, the content of the ^{13}C isotope can be artificially increased by ^{13}C-labelling the desired molecule.[173,174] Such molecules, when hydrogenated with parahydrogen, catalyzed by Rh and Ir complexes, would give increased intensity signals of ^{1}H and ^{13}C in the corresponding NMR spectra.[175] The enhancement of the ^{1}H NMR signal of ^{13}C-ethylene protons was 140! And the enhancement of the signals of carbon nuclei was enough to observe ^{13}C-ethylene even at extremely low concentrations due to the polarization caused by parahydrogen. The shape of the line of polarized ^{13}C-ethylene (Fig. 14) unambiguously indicated that the addition of p-H_2 to the acetylene triple bond on immobilized iridium complexes proceeds stereoselectively as *syn*-addition. In fact, this method is an efficient approach for enrichment of nuclear spin isomers of ethylene.[175]

4. Bimetallic palladium catalysts

The introduction of another metal into the catalyst to control the geometry and electronic structure of Pd NPs is widely used strategy to effectively improve its overall catalytic activity.[176,177] The comparison, analysis and summary of the synthetic methods of Pd-based bimetallic compounds can provide useful guidelines for the further development of such catalysts.

A mixed PdAg catalyst supported on the mesoporous carbonaceous material Sibunit was obtained by impregnation

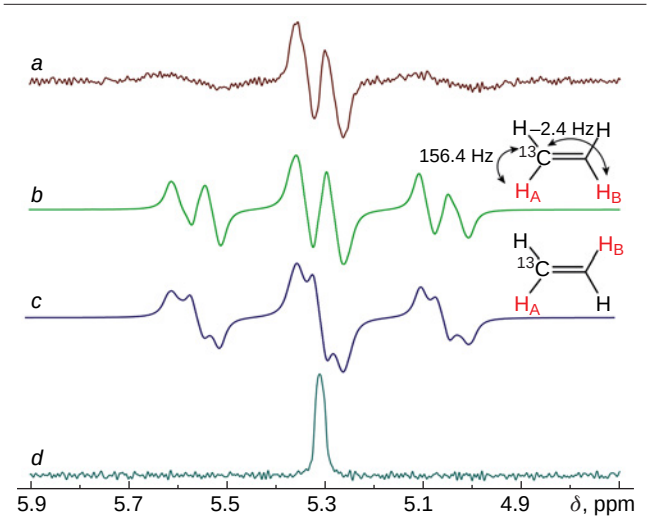

Figure 14. ^{1}H NMR spectra of ethylene formed by hydrogenation of acetylene with the SiO_2-supported catalyst [Ir_2(COD)$_2$(μ-Cl)$_2$] (flow rate of the gas mixture 4.6 mL s^{-1}) before (*a*) and after relaxation of hyperpolarization to thermal equilibrium (*d*); (COD is cycloocts-1,5-diene); simulated spectra of ^{13}C-ethylene formed by *syn*- (*b*) or *anti*- (*c*) addition of p-H_2 (*c*). Reproduced from Ref. 175 with permission from Springer Nature.

followed by reduction. Interestingly, the catalysts synthesized by alternating impregnation of the support with solutions of $Pd(NO_3)_2$ and $AgNO_3$ in a H_2 medium demonstrated lower ethylene selectivity (68–73%) due to the formation of species that were non-uniform in both composition and size (about 4–60 nm). This was probably due to the removal of O-containing functional groups from the carbon surface during the hydrogenation process, which contributed to the formation of larger catalyst particles. Impregnation with a mixture of salts followed by reduction provided the formation of more uniform particles.[178]

A series of bimetallic Pd and Ag catalysts were tested in the selective semihydrogenation of acetylene to identify the leading catalysts.[179] Based on the calculations and a series of experiments, the authors were able to find out that the nature of the catalyst surface directly determined its ability to adsorb acetylene and ethylene. It was also obvious that the nature of the surface can be changed depending on the ratio of metals in an alloy. The screening strategy described in this research, allowed for rational engineering, *i.e.*, theoretical determination of those forms of the catalyst that demonstrated maximum activity and selectivity. Based on this strategy, the catalysts Ag_7@Pd, Pd_1@Ag, and Pd_1Ag_3 were proposed. Further, by means of microkinetic analysis, it was found that the Pd_1Ag_3 alloy demonstrated the superior characteristics of the tested samples. The calculation methods also confirmed that the presence of silver in the alloy catalyst facilitated the desorption of ethylene, thereby increasing the hydrogenation selectivity.[103] Using the calculations and experimental research, interesting patterns were found for alloy binary PdAg catalysts.[180] The formation energy of palladium alloys was 0.06 eV atom^{-1}. The role of silver is to limit the dissolution of hydrogen in palladium. The more silver atoms per palladium atom, the more isolated the palladium active sites are on the surface. Silver atoms are combined on the surface, but this segregation is reversible under the action of hydrogen, so the catalyst surface is constantly changing over time. The nature of the palladium species is also changed: they also tend to aggregate, which led to a deterioration of the catalytic properties of the catalyst as a whole. The highest catalytic activity was found in samples of the Pd_1Ag_3 composition, which is also confirmed by other studies.[179]

An alternative approach to the bimetallic PdAg catalyst was based on mechanochemical action on solid starting compounds.[181] Compared to a similar catalyst obtained by the standard wet impregnation procedure, this catalyst was more resistant to deactivation and withstood 15 h on stream rather that 5–10 h. Therefore, the mechanochemical approach can be considered as an alternative to the synthesis of complex catalytic systems with increased time-on-stream. A number of bimetallic catalysts with different Pd : Ag ratios was obtained by the original procedure from the corresponding nitrates, a stabilizer and sodium cyanide as an auxiliary reagent.[182] The catalysts were then placed on an alumina support and tested in acetylene hydrogenation. Compared to standard hydrogenation catalysts (Pd Nanoselect LF200 and Pd/Al_2O_3), the bimetallic catalyst demonstrated 80% selectivity to ethylene even after 48 h.

As noted above, non-selective hydrogenation of acetylene can produce ethane and C_{4+} oligomeric compounds, the so-called 'green oil', which is a catalyst poison. A study[183] has been conducted to assess the contribution of buta-1,3-diene formed during hydrogenation to the course of the subsequent process. For this purpose, 1,3-butadiene was introduced into the experimental setup for selective hydrogenation of acetylene using $PdAg/Al_2O_3$ as the model catalyst. It was found that C_4H_5 species were intermediates in the formation of C_6 species. It was also proved that butadiene does not react with acetylene to give longer-chain hydrocarbons, but is actively actively hydrogenated to 1-butene, *cis*- and *trans*-2-butenes and butane. The amount of resulting C_4 hydrocarbons directly depends on the reaction time and the catalyst type. Although direct reaction of acetylene and 1,3-butadiene was not observed, two acetylene molecules can react with each other to form C_4H_4 species, which can then react with acetylene to give benzene. In the case of the mixed PdAg catalyst, the treatment of the catalyst with carbon monoxide led to segregation of Pd atoms at room temperature and results in the additional enrichment of the surface with palladium (up to 31%).[184] The IR spectrum of CO on the monometallic Pd catalyst (Fig. 15, the black curve) showed a maximum at 2088 cm^{-1}, which corresponds to linearly adsorbed CO. The maximum at 1990 cm^{-1} and a broad shoulder at 1944 cm^{-1} corresponds to multicoordinated CO. Based on the signal intensities, multicoordination clearly dominated, *i.e.* adsorption on two and three palladium atoms. For the mixed $PdAg_2/Al_2O_3$ catalyst, linearly adsorbed CO dominated (Fig. 15, red curve), which indicated the disappearance of polyatomic Pd centres and the formation of the single-atom Pd catalytic sites, which are separated by Ag atoms. Thus, pre-treatment of the catalyst with CO increases its in activity at 100% selectivity in the acetylene hydrogenation.

A series of core-shell catalysts was prepared using a standard impregnation technique followed by deposition on alumina.[185,186] The resulting catalysts consisted of monoatomic alloys of Pd_1Ag_6 and Pd_1Ag and showed selectivity to ethylene 90% at conversion 80%. However, with an increase in conversion to 100%, the selectivity was less than 60%.

A comparative study of the properties of bimetallic Pd catalysts and their analogues modified with S or Si atoms in acetylene semi-hydrogenation using experimental and computational methods has been reported.[187] According to the calculations, the catalytic efficiency of C_2H_2 semi-hydrogenation largely depends on the spatial extension of the active site and the electronic effect, which consists of a change in the density of the d-zone near the Fermi level and has a significant influence on the sorption characteristics of the catalyst. The electronic effect of the catalyst caused by S atoms was more significant than the

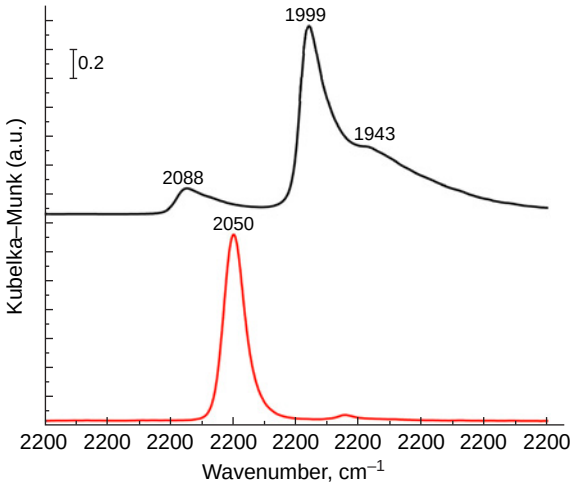

Figure 15. FT-IR diffuse reflectance spectrum of CO adsorbed by Pd/Al_2O_3 (*top*); and by $PdAg_2/Al_2O_3$ (*bottom*). Reproduced from Ref. 184 with permission from Elsevier.

effect of Si atoms. At the same time, the geometry of the active centre for Si-analogues changed more than in S-analogues. Thus, for bimetallic PdAg catalysts, the synergistic geometric and electronic effects caused by S atoms on S/Pd_6Ag, enhanced the activity and selectivity to C_2H_4 formation and significantly prevented the formation of a 'green oil'. Modification of the catalysts with silicon was slightly less effective than with sulfur, and they both increased the selectivity to C_2H_4 and prevented the formation of 'green oil' in the hydrogenation of acetylene on Si/Pd_1Au_1 and Si/Pd_1Ag_1 catalysts.

Bimetallic supported $Ag@Pd/SiO_2$ catalysts coated with Ga_2O_3 demonstrated high selectivity to ethylene (up to 95%) with complete conversion of acetylene in ethylene excess.[188] The Ga_2O_3-coated monometallic Pd/SiO_2 catalyst showed moderate activity. At the same time, the activity and high stability of the Ga_2O_3-coated $Ag@Pd/SiO_2$ catalyst were nearly 50 times higher than those of the reference Pd_1Ag/SiO_2.

Alumina is often used as a support for acetylene hydrogenation catalysts. However, its small surface area limits the dispersion of active metals. To address this issue, alumina was prepared by a special *in situ* growth method (Fig. 16).[189] Then, the alloy bimetallic catalyst PdAg was applied to the obtained support, resulting in 90% acetylene conversion and 89% selectivity. It was due to even greater isolation of the active Pd sites, a more degradation-resistant substrate structure and a decrease in the rate of heat release. Decreased heat release led to a decrease in the number of hot spots on the catalyst surface, and, consequently, to a decrease in the rate of the endothermic coking reaction. As a result, the catalyst pores remained open for a longer time, thereby increasing the catalyst stability.

Liquid-phase hydrogenation of a N_2-stabilized gas mixture consisting of C_2H_2 (8%) CO (20%) and H_2 (50%) was carried out in NMP in the presence of $PdAg/SiO_2$ showed 92% selectivity to ethylene.[190] The similar characteristics for gas-phase hydrogenation of the same mixture was only 71%.

A mixed SiO_2-supported palladium–nickel catalyst was prepared in several steps.[191] First, the Ni/SiO_2 nanocatalyst was synthesized by impregnation with subsequent reduction in a hydrogen stream. Then, single palladium atoms were deposited on the surface. Acetylene hydrogenation over this catalyst at a temperature of 80°C proceeded with a conversion of 92% and a selectivity for ethylene of 88%. The authors were able to prove the presence of SA-Pd on the catalyst surface by scanning transmission electron microscopy–energy dispersive X-ray spectroscopy (STEM-EDS) (Fig. 17).

Metal single-atom alloy (SAA) catalysts based on Pd and Ni were prepared by galvanic replacement (GR) method.[192] For this purpose, nickel nanocrystals were first obtained by the colloidal method. Then, palladium atoms were deposited on nickel *via* galvanic replacement. And the finished nanocrystalline

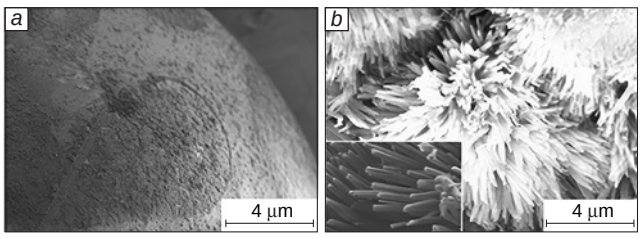

Figure 16. SEM images of the surface of standard spherical aluminum oxide (*a*) and aluminum oxide with a modified flower-shaped array (*b*). Reproduced from Ref. 189 with permission from the American Chemical Society.

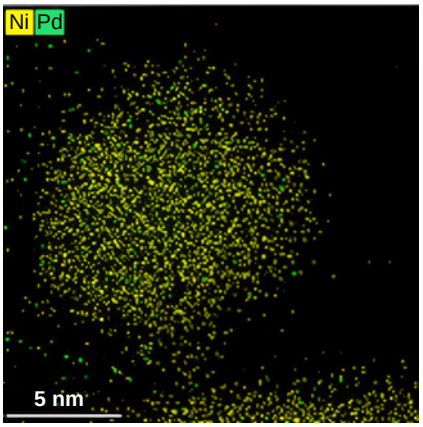

Figure 17. STEM-EDS image of the mixed $PdNi/SiO_2$ catalyst. Yellow dots indicate Ni atoms; green dots indicate Pd atoms. Reproduced from Ref. 191 with permission from Elsevier.

Pd_1Ni alloy was placed on SiO_2 support. The resulting alloy was tested in the selective hydrogenation of acetylene in comparison with a similar catalyst obtained by common impregnation. It was found that the catalyst obtained by the galvanic replacement showed higher selectivity in the range of 30–180°C. According to DFT calculations, electrons were transferred from nickel to palladium atoms in the alloy catalyst.

The efficiency of mixed PdNi catalysts was improved by replacing Pd with monoatomic Pd. Metallic single-atom alloys Pd_1Ni/SiO_2-GR obtained by the galvanic replacement method for selective deposition of colloidal Ni nanocrystals on the SiO_2 support with subsequent deposition of Pd atoms on Ni atoms.[192] The Pd atoms remained atomically dispersed and are located in proximity to Ni atoms (Fig. 18), which improved the ethylene selectivity in the acetylene semi-hydrogenation reaction compared to the reference $PdNi/SiO_2$ catalyst prepared using the impregnation method. The Pd_1Ni/SiO_2-GR catalyst showed higher C_2H_4 selectivity over a wide temperature range (30–180°C), being superior to the Pd_1Ni/SiO_2, Pd/NiO, and Pd/SiO_2 SAA catalysts prepared by the impregnation method. According to DFT calculations, the enhanced selectivity stems from the electron transfer from a Ni nanocrystal to single Pd atoms due to the close proximity of these species.

The performance of palladium catalyst was significantly improved by inserting tin atoms onto the surface.[193] The resulting Pd_2Sn/C catalyst demonstrated ~95% selectivity in hydrogenation of acetylene with almost complete conversion of the substrate. According to experimental studies and DFT calculations, the addition of tin led to a redistribution of Pd atoms over the catalyst surface, which in turn affected the ethylene sorption. Ethylene molecules adsorbed at 300–600°C were weakly bound to the surface and easily left it being non-dissociated. At the same time, ethylene molecules that were adsorbed at 439 and 500°C were bound to the surface more strongly and could further react with dissociated hydrogen to form ethane.

Mixed Al_2O_3-supported PdMn catalyst was prepared in hydrogen reducing medium.[194] According to analytical studies, the surface of thus modified catalyst lacks the weakly bound hydrogen, which was explained by the presence of a uniform distribution of Mn atoms over the surface. In tests for selective hydrogenation of acetylene, the catalyst demonstrated increased activity and a 20% increase in selectivity compared to the unmodified palladium catalyst. The complex $Pd/In_2O_3@SiO_2$

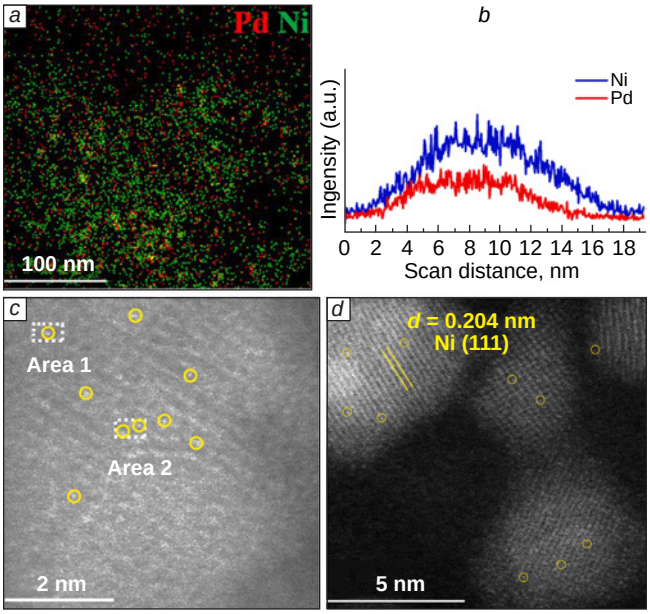

Figure 18. STEM-EDS mapping showing the close contact of Pd and Ni in the Pd_1Ni nanocrystal (*a*); line scan profile of Ni and Pd in $Pd_{0.1}Ni_2/SiO_2$-GR-500R (*b*); AC-HAADF-STEM images of $Pd_{0.1}Ni_2/SiO_2$-GR-500R showing the presence of single Pd and Ni atoms in different scale (*c*, *d*). Reproduced from Ref. 192 with permission from Elsevier.

catalyst was prepared using a standard deposition–precipitation procedure.[195] Doping the catalytic system with indium suppressed palladium activity and also facilitated the adsorption of di-σ-bound ethylene, which significantly improved its desorption. As a result, the selectivity to ethylene was 80% with 100% conversion of acetylene at 140°C for 24 h.

The bimetallic PdZn catalyst demonstrated 85% ethylene selectivity in acetylene hydrogenation even after 70 hours on stream.[196] Comparing to other alloy catalysts, that was not the best result; however, it was very promising because of the room temperature reaction conditions. Based on the calculated data, the authors explained the role of zinc by donating electrons from the occupied zinc d-orbitals to the Pd d-orbitals, which facilitated the interaction of acetylene with the surface. Moderate results were obtained for the bimetallic Sibunit-supported PdZn catalyst.[197] The addition of zinc to Pd : Zn in a ratio of 1 : 1 increased the catalyst selectivity to 67% compared to 42% for monometallic palladium. Further increase in zinc content decreased the selectivity to 62%. According to analytical studies, zinc was incorporated into the palladium crystal lattice during the reduction of metals. With an excess of palladium, the interaction occurred more completely with the formation of an intermetallic phase. With an excess of zinc, lesser incorporation was observed, while zinc was retained in the form of large oxide particles. Further studies demonstrated that an increase in the reduction time of Pd–Zn/C samples in H_2 at 500°C from 1 to 20 h was accompanied by an increase in the number of bimetallic sites and an increase in the coordination number of PdZn from 2.4 to 4.3, as well as a decrease in the Pd_0/PdZn ratio from 0.63 to 0.18.[198] An increase in the number of modified active sites led to higher selectivity to ethylene in the process of liquid-phase hydrogenation of acetylene.

Spinel monolithic Al–LDH catalysts with porous woodpile architecture were fabricated by extrusion three-dimensional (3D) printing of layered aluminate-intercalated double hydroxide (Al-LDH) followed by low-temperature calcination.[199] Porous monolithic catalysts with a high specific surface area facilitated mass and heat transfer and exposed active catalyst sites (Fig. 19). Thus, the 3D-printed spinel-based catalyst loaded with Pd (3D-AI-Pd/MMO (MMO is MgAl-mixed metal oxide) provided 100% conversion in acetylene hydrogenation with selectivity to ethylene more than 84% at 60°C.

$Pd_1–Cu_n/Al_2O_3$ catalysts with single palladium atoms (Pd_1) and copper clusters (Cu_n) were deposited on different supports. The synergistic effect of one palladium atom and a copper cluster provided the isolation effect of catalytic sites and effectively prevented their agglomeration. The activity of the $Pd_1–Cu_n/Al_2O_3$ catalyst increased by 60% compared to the Pd_1/Al_2O_3 catalyst, and its stability increased to more than 100 h with the same conversion values for both catalysts with ethylene selectivity of 83%.[200] The PdCu/siloxene catalyst was prepared by direct reduction in the liquid phase and was characterized by a low loading of Pd distributed in ultrafine Cu species.[201] This catalyst provided 91% acetylene conversion and 93% ethylene selectivity at 200°C in the acetylene semi-hydrogenation reaction. Moreover, PdCu/siloxene also demonstrated high activity and stability under ethylene-rich industrial gas conditions. In addition, the catalyst was resistant to coking at high operating temperatures for 39 hours.

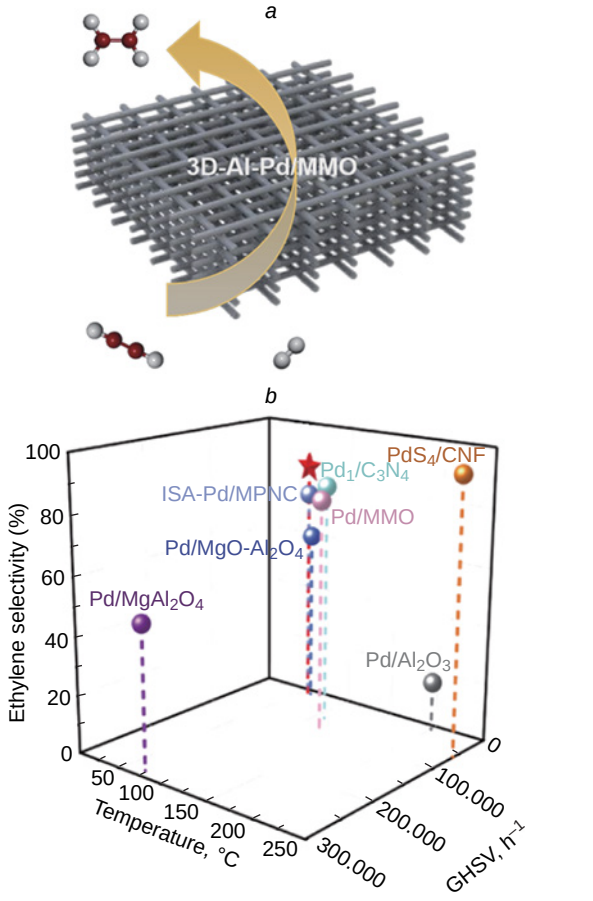

Figure 19. Schematic representation of the selective hydrogenation of acetylene to ethylene over a 3D-printed 3D-AI-Pd/MMO catalyst with a hierarchical porous structure (*a*) and a comparison diagram of different catalysts for this process (*b*). CNF is carbon nanofibers. Reproduced from Ref. 193 with permission from Springer Nature.

The Pd_1Au_1 dimeric catalyst supported on a metal-organic framework demonstrated an outstanding (99.99%) acetylene conversion with a selectivity of over 90% under industrial-scale conditions (1% acetylene, 89% ethylene, 10% H_2 mixture).[202] The catalyst worked efficiently over a wide temperature range (35–150°C), with only ethane as a by-product. The reaction proceeded with an apparent activation energy of ~ 1 kcal mol^{-1} even at 35°C and with operating windows (> 100°C) and mass hourly space velocities (66 000 mL g^{-1} cat h^{-1}) within industrial specifications. Experimental and theoretical studies demonstrated that palladium atoms performed the main catalytic function, while gold atoms and thioether moieties of the metal-organic framework participated in hydrogen dissociation.

An interesting technique for regulating the ratio of metals in a bimetallic catalyst was implemented on the example of a PdCo supported on the carbon material Sibunit.[203] The catalysts were prepared by wet impregnation followed by hydrogenation in the stream of hydrogen at various temperatures. At temperatures below 500°C, palladium was reduced to a metallic state, and cobalt was only partially reduced. As the temperature raised to 700°C, larger amount of cobalt was reduced to metal. In this way, catalysts of compositions from $Pd_{0.6}Co_{0.4}$ to $Pd_{0.45}Co_{0.55}$ were obtained. With an increase in the catalyst treatment temperature, the yield of ethylene in the acetylene hydrogenation also increased from 56% to 68%. For comparison, the yield of ethylene in hydrogenation in the presence of monometallic palladium on carbon was only 52%. According to the data obtained, the improvement in the catalyst characteristics was associated with a change in the electronic state of palladium due to its surrounding by cobalt atoms.

The bimetallic Pd-Ga/γ-Al_2O_3 catalyst obtained by impregnation Al_2O_3 with solutions of the appropriate nitrates demonstrated selectivity to ethylene about 66–70%.[204] Outstanding results were obtained for the calcite-supported PdBi catalyst (PdBi/Calcite) prepared by multistep synthesis that included of metal salt reduction with $NaBH_4$ and deposition on the support.[205] This catalyst showed 99% selectivity to ethylene at 100% conversion over the entire temperature range (50–300°C)! Thus, the working range with acceptable characteristics was 150°C. The authors carried out a series of experiments to clarify the nature of such high activity. An assumption was made about the influence of bismuth oxide on the activity of Pd metal. However, it was found that palladium and bismuth formed intermetallic compounds that significantly contribute to the reaction mechanism, and the key process parameters depend on their formation. At the same time, the contribution of oxides was insignificant. The intermetallic catalysts contained isolated and electron-rich Pd atoms as active catalytic sites and had an extremely weak ability to absorb ethylene and prevent the formation of palladium hydrides (β-PdH_x) on the catalyst surface.

A bimetallic CuPd catalyst was synthesized especially for the selective hydrogenation of acetylene to ethylene.[201] The undoubted novelty of the research was the use of siloxene as a support. Catalytically active sites consisted of isolated palladium species surrounded by ultra-small copper species, and all the species were uniformly distributed in siloxene, which has high porosity and surface area. The catalyst demonstrated high resistance to sintering for 39 h and provided 91% conversion of acetylene with 93% selectivity to ethylene at 200°C.

The synthesis of mixed hydrogenation catalysts obtained by deposition of bismuth on cubic palladium nanoparticles (Pd–NC) was described.[206] Dotted applicated bismuth poisoned palladium atoms, adjusting the catalyst activity. The PdNCs@$Bi_{0.06}/Al_2O_3$ catalyst obtained by applying bismuth to the corners of Pd cubes, provided a selectivity to C_2H_4 of 10.1% with 100% conversion of C_2H_2, which exceeded the catalytic characteristics of the PdNCs/Al_2O_3 catalyst. With an increase in the degree of bismuth inclusion (*i.e.*, with an increase of poisoning), the C_2H_2 conversion gradually decreased, and the C_2H_4 selectivity increased (Fig. 20), which made it possible to vary the conditions depending on the tasks at hand. For example, the Pd-NC@Bi catalyst with bismuth deposited on the corners and faces of Pd nanocubes had C_2H_2 conversion of 99.7% and selectivity to C_2H_4 94.3% at 170°C in acetylene semi-hydrogenation in excess of ethylene.

A mixed Pd–La nanocatalyst was obtained by ultrasonic impregnation using nitrogen-doped biochar derived from *Pennisetum giganteum* as a support (N-pgBC). PdLa/N-pgBC provided 94.2% selectivity to ethylene with full acetylene conversion in the acetylene hydrogenation.[207] The synergistic effect of the inherent high specific surface area of the carbon support together with the separation of the lanthanum-doped catalytic sites promoted adsorption of acetylene and the rapid desorption of ethylene, blocking overhydrogenation of the latter. In addition, the PdLa/N-pgBC catalyst showed a strong dependence on the component composition, which might be due to electronic or geometric modification of metal particles.

5. Pd-Free catalysts for acetylene generation. Ni-based catalysts

Nickel hydrogenation catalysts as completely exposed small metal nanoclusters (Fig. 21), were obtained on a nanodiamond

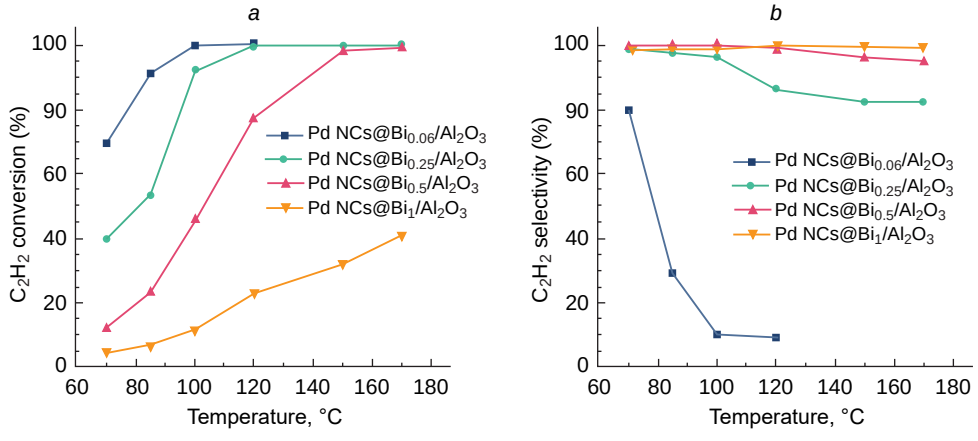

Figure 20. Temperature dependence of conversion (*a*) and selectivity (*b*) of acetylene hydrogenation on Pd-NCs@$Bi_{0.5}/Al_2O_3$ catalyst. Reproduced from Ref. 206 under a Creative Commons Attribution (CC BY) license.

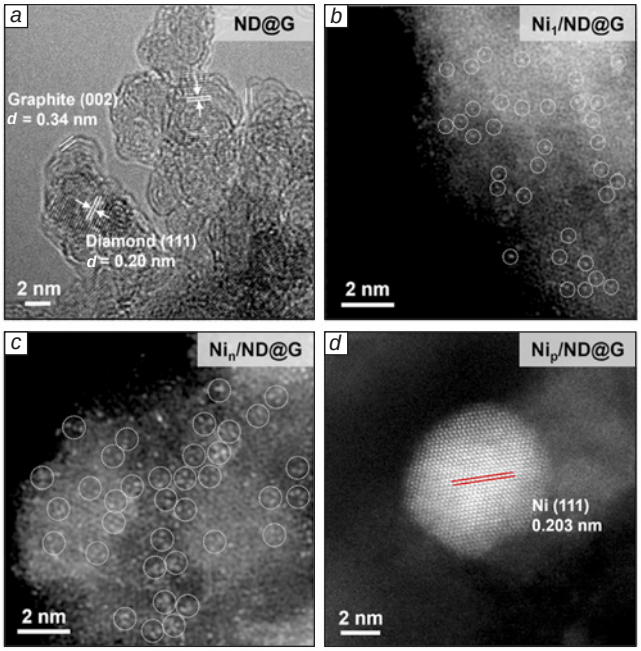

Figure 21. High-resolution transmission electron microscope images of nanodiamond and graphene (*a*), and nickel atoms (Ni_1), nickel NPs (Ni_n) and nickel nanoclusters (Ni_p) supported thereon. Nickel atoms and nickel clusters are circled in white. Reproduced from Ref 208 with permission from the American Chemical Society.

(ND or graphene (G) support.[208] Calculation methods and H_2/D_2 exchange experiments demonstrated that acetylene and hydrogen are completely activated on the catalytic sites. Moreover, the desorption of ethylene on exposed nickel clusters was more energetically favourable than further dissociation of an H_2 molecule. Therefore, exposed nickel clusters were able to completely convert acetylene to ethylene with 85% selectivity at 190°C. When replacing the carbon substrate with a mesoporous material MCM-41 based on silicates and aluminosilicates, the nickel nanocatalyst provided 96% conversion of acetylene and selectivity to ethylene of 87%.[209]

A very interesting idea was realized in the hydrogenation of acetylene to ethylene in the presence of nickel catalysts with a nitrogen-doped carbon support (gC_3N_4).[210] The authors used acetylene obtained by hydrolysis of calcium carbide as a source of ethylene, *i.e.*, ethylene was produced not from the standard cracking of petroleum products. It should be noted, that the use of acetylene from calcium carbide in synthetic transformation is a common practice.[211–218] Nevertheless, the authors managed to obtain impressive results: the catalyst provided 96% conversion of acetylene for 10 hours at 200°C, while the selectivity to ethylene reached 46%.

A similar catalyst was described in a study[219] but it was additionally doped with sulfur. Sulfur-doped nickel supported on gC_3N_4–T (the T and M locants denote the sulfur-doped support and the sulfur-free support, respectively) showed ethylene selectivity >63% with complete acetylene conversion at 175–300°C. XRD, HRTEM, EDS and XPS revealed that the catalyst represents Ni cations enclosed in gC_3N_4-T cavities or a Ni–S solid solution with surface segregation of S different from the Ni species for Ni/gC_3N_4-M. The Ni^{2+} sites above the gC_3N_4-T support promote the acetylene activation *via* electrostatic interaction.

Single-atom nickel-dispersed catalysts were obtained by introducing zinc additive.[220] A nitrogen-doped carbon matrix was used as a support. As a result, the presence of the Ni–N_4 structure in the carbon matrix was detected and confirmed. The conversion of acetylene in a real mixture with ethylene was >97%, which was explained by weak π-adsorption of ethylene on single Ni atoms.

Ni catalysts on various supports (SiO_2, γ-Al_2O_3 and zeolite ZSM-12) were investigated for the hydrogenation of acetylene.[221] The Ni/ZSM-12 catalyst showed low selectivity to ethylene and low stability. However, this catalyst performed better than the Ni/SiO_2 and Ni/γ-Al_2O_3 catalysts. due to the synergistic action of Lewis and Brønsted acid sites. Doping with Sn afforded a more effective Ni_7Sn/ZSM-12 catalyst, which showed 92.51% selectivity to ethylene with complete acetylene conversion at 250°C. These values were 19.4% higher than those in the absence of Sn. According to DFT calculations, the bimetallic catalyst had a rather high energy barrier to the formation of the intermediate compound $C_2H_5^*$ in acetylene hydrogenation, which determined its high selectivity.

Outstanding results necessary to understand the effect of additives on nickel catalysts were demonstrated using Au, Ag and Cu additives as an example.[222] It was found, that the energy of initial adsorption of acetylene changed in the series $AuNi_{0.5}/SiO_2 > AgNi_{0.5}/SiO_2 > CuNi_{0.125}/SiO_2$. Moreover, deactivation of the catalysts was mainly due to coking rather than to a particle size changes. The properties of the NiAg catalyst depended on the depth of penetration of metal species into the matrix, which was definitely a very interesting and unusual marker.[223] Thus, an Al_2O_3-supported complex Ni–Ag@C/Al_2O_3 catalyst on, consisting of carbon-encapsulated Ag NPs and non-encapsulated Ni NPs, was synthesized. Both types of metal NPs were located on the Al_2O_3 support. This was possible due to the catalyst synthesis strategy, which involved the co-precipitation of $AgNO_3$ and $Ni(NO_3)_2 \cdot 6H_2O$ onto Al_2O_3, followed by the transformation of salts into carbonates and calcination in an acetylene atmosphere at 120°C to obtain encapsulated silver NPs (Fig. 22). The last step of reduction of NiO–Ag@C/Al_2O_3 with hydrogen at 500°C provided the formation of Ni NPs on the support. After testing, it was found that the Ni–Ag@C/Al_2O_3 catalyst provided ethylene selectivity of up to 81% with complete acetylene conversion within 30 h (Fig. 23). Interestingly, the use of the monometallic catalyst (Ni/Al_2O_3), gave virtually no target product (yield 6%), and the non-encapsulated Ni–Ag/Al_2O_3 catalyst showed only 54% conversion of acetylene. The improved selectivity of the catalyst was achieved due to the ability of carbon particles to provide hydrogen migration across the surface of the Al support of the

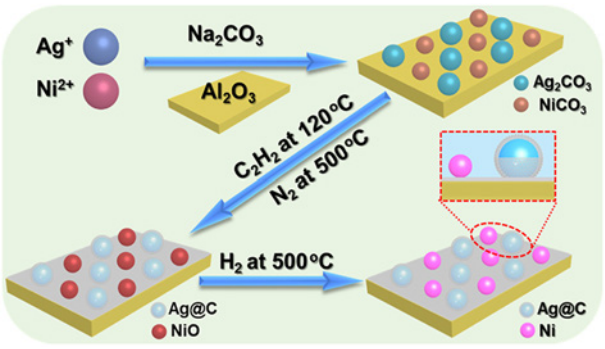

Figure 22. Schematic illustration of the synthesis of Ni–Ag@C/Al_2O_3. Reproduced from Ref. 223 with permission from Elsevier.

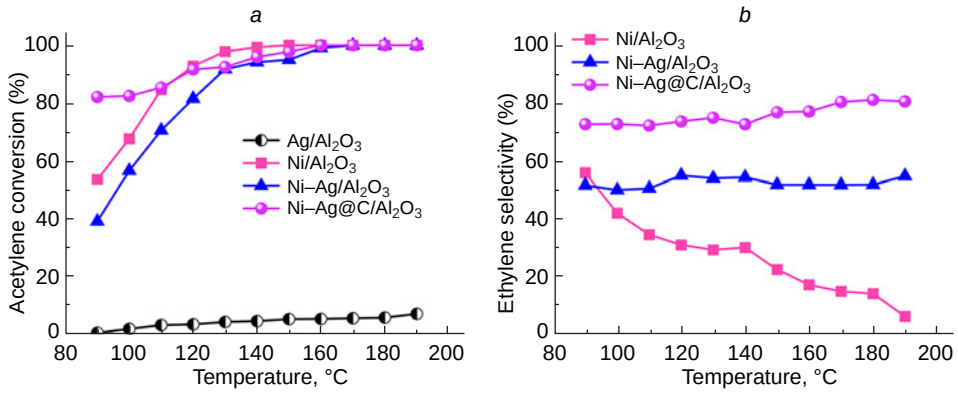

Figure 23. Temperature dependence of acetylene conversion (*a*) and ethylene selectivity (*b*) in acetylene hydrogenation over Ag/Al_2O_3, Ni/Al_2O_3, $Ni-Ag/Al_2O_3$ and $Ni-Ag@C/Al_2O_3$ catalysts. Reproduced from Ref. 223 with permission from Elsevier.

catalyst. At the same time, the carbon shell blocked the formation of oligomers (*i.e.* the chain growth) on Ag NPs.

Intermetallic NiSb catalyst was used for hydrogenation of acetylene in the presence of ethylene.[224] This catalyst was prepared using the strategy of entrapping molten antimony with nickel (Fig. 24). The authors attributed the impressive results (selectivity up to 93.2% with complete acetylene conversion) not only to the weak adsorption of ethylene and strong adsorption of acetylene on the catalyst surface. The electronegative properties of the 'guest' metal (Sb) were used to control the properties of the 'host' metal (Ni), so that Ni_1Sb_2 trimers enclosed in NiSb intermetallic particles were formed on the surface. According to theoretical calculations, these regions provided the selective adsorption of acetylene.

The carbide-type $Ni_3ZnC_{0.7}/C$ catalyst was obtained from the NiZn-ZIF-8/LDH precursor (ZIF is zeolite imidazolate framework) and showed 85% selectivity to ethylene at 100% conversion.[225] The Bader atomic charge distribution analysis demonstrated that the subsurface carbon divided the nickel atoms on the surface into two types: electron-depleted with the subsurface carbon atom and electron-rich with the subsurface zinc atom. According to calculations, the nickel atoms arranged into Ni_3 assemblies promoted ethylene desorption and prevented hydrocarbon chain growth, which ultimately led to an increase in the process selectivity.

The bimetallic NiZn/ZnO catalyst performed better in acetylene semi-hydrogenation in comparison with the intermetallic catalyst Ni_3Zn/ZnO of the ligand type. According to research and DFT calculations, the high selectivity of NiZn/ZnO was due to the non-competitive adsorption of acetylene by the adjacent isolated metal atoms.[226]

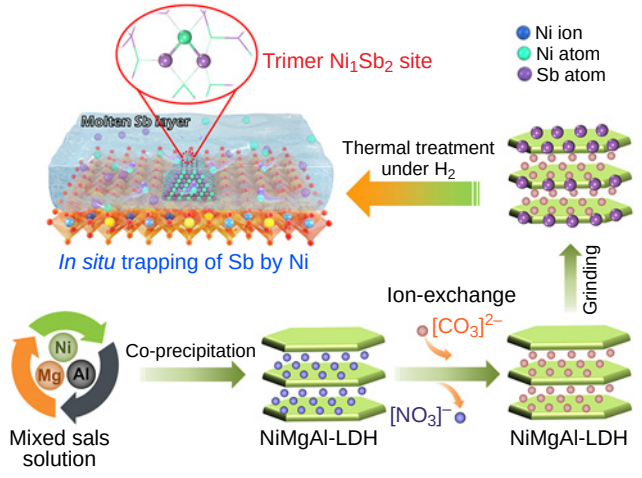

Figure 24. Schematic illustration of the synthesis of a complicated trimeric catalyst Ni_1Sb_2 in the intermetallic compound NiSb. Reproduced from Ref. 224 under a Creative Commons CC BY license.

Features of the influence of the substrate shape on the properties of metal catalyst particles in acetylene hydrogenation were discovered in the Al_2O_3-supported NiCu NPs.[227] It was found that the support atoms govern the arrangement of metal atoms. The spindle-shaped support promoted the formation of NiCu alloys with a predominance of copper on the surface. And the flaky shape led to a switch to monometallic copper and nickel-rich bimetallic systems. The rod-shaped support promoted the appearance of Ni_1Cu_1 alloys, and the coordinatively unsaturated Al^{3+} sites played a key role in the formation of metal NPs, in which nickel atoms were orderly distributed among copper atoms. Uniformly distributed Ni–Cu alloy species with individual nickel sites provided 86% selectivity to ethylene with full conversion at 130°C.

According to calculations, in selective acetylene hydrogenation on intermetallic NiIn catalysts of various compositions, oligomerization products originate exactly from acetylene, not from ethylene.[228] This important conclusion provides deeper insight into the nature of the process and once again emphasizes the need to convert acetylene into ethylene. The calculations also showed that the indium additive to the catalyst improves the selectivity of the process.

NiGa intermetallics were prepared with the aim to elucidate the role of completely isolated nickel sites in the semi-hydrogenation of acetylene.[229,230] It was found out, that isolated nickel sites preferentially π-adsorbed acetylene and promoted ethylene desorption. Three prepared catalysts based on Ni, Ni_5Ga_3 and NiGa had similar particle sizes, but different atomic arrangements, as well as different environment of nickel sites. As can be seen from Fig. 25 *a*, Ni and Ni_5Ga_3 demonstrated higher activity and lower selectivity to ethylene especially at temperatures above 100°C. This suggests that the complete isolation of nickel particles on the surface led to an increase in selectivity. Temperature desorption profiles (Fig. 25 *b*) clearly indicated three peaks for Ni and Ni_5Ga_3 catalysts. The first two peaks might be attributed to weakly adsorbed ethylene, and the third peak at a higher temperature was a signal of strongly adsorbed acetylene. The absence of a high-temperature peak was observed for the NiGa catalyst with completely isolated nickel sites. Therefore, it can be concluded that isolated nickel sites promoted acetylene desorption. Analysis of acetylene conversion shows that in excess ethylene (Fig. 25 *c*), the catalyst with isolated nickel sites provided higher selectivity to ethylene. It is also evident from Fig. 25 *d*, that the addition of gallium not only increased stability of the catalyst, but also inhibited the

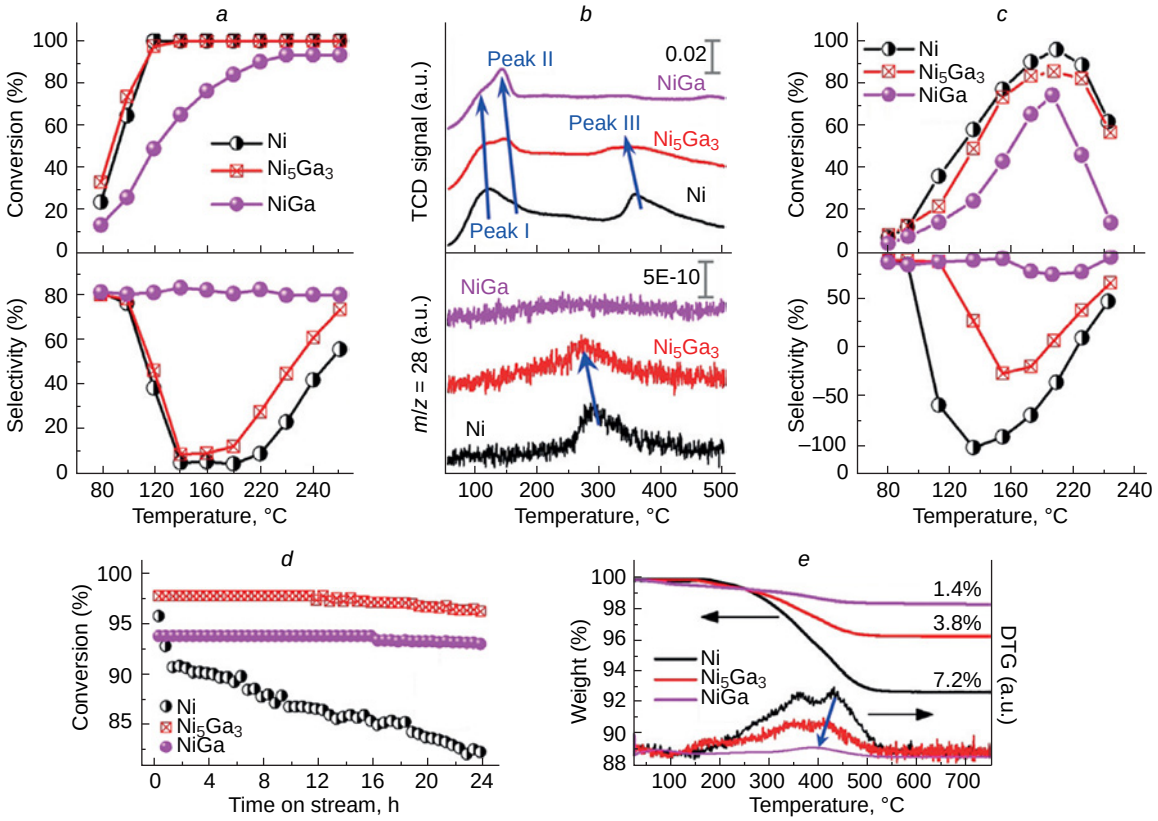

Figure 25. Temperature dependence of acetylene conversion and ethylene selectivity in the absence of ethylene (*a*); TPD-profiles for acetylene (*top*) and ethylene (*bottom*) (*b*); temperature dependence of acetylene conversion and ethylene selectivity in the presence of ethylene (*c*); time dependence of acetylene conversion on stream at 190°C (*d*); thermogravimetric curves of Ni catalysts used: Ni, Ni_5Ga_3 and NiGa (*e*). Reproduced from Ref. 229 with permission from Wiley.

formation of 'green oil', *i.e.* hydrocarbons with longer chains (Fig. 25 *e*). In another study,[231] on the properties of multi-intermetallic NiGa with isolated nickel particles, a whole series of additives (Fe, Cu, Ge) were proposed to stabilize the nickel particles on the surface.

A series of nickel-based catalysts was synthesized to elucidate the effect of various additives on the selective hydrogenation of acetylene.[232] It was found that the introduction of Mg results in a complete hydrogenation of acetylene to ethane, while the addition of tin improves selectivity, making it possible to stop hydrogenation at the step of ethylene formation. The authors associated these patterns with the facilitation of ethylene desorption from the surface of Ni_7Sn/SiO_2, which performed best: 65% yield of ethylene at 250°C. Mg–Al-supported $Ni/MgAl_2O_4$ catalyst provided 99% acetylene conversion with an selectivity to ethylene of more than 80%.[233] The authors attributed such outstanding results to the large surface area (309 $m^2\ g^{-1}$) at the «tuned' acidity.

Thus, the conversion and selectivity to ethylene in the acetylene hydrogenation are directly dependent on the size of the nickel species on the substrate surface. Single-atom catalysts demonstrate higher selectivity compared to nano- or microparticles. The catalytic properties of nickel catalysts are significantly affected by the nature of the support, which can either donate electrons to the metal atom or deplete it of electrons. If the support contains more electronegative atoms relative to nickel, the selectivity of such catalysts is superior to those with a support with less electronegative atoms. Lower electron density on the metal atom leads to easier desorption of ethylene and higher hydrogenation selectivity. The presence of a 'neighbour' element also has a significant effect on the reaction parameters. Firstly, the second component of the nickel alloy allows for a better distribution of particles over the surface due to greater dilution. Secondly, the nickel atom can transfer part of its electron density to 'neighbour' atoms (the number of which may be greater), which prevents the appearance of 'hot spots' and ultimately increases the selectivity of the process as a whole.

6. Cu-based catalysts for selective acetylene hydrogenation

Similar to Pd- and Ni-based catalysts, the catalytic activity of Cu catalysts depends on the particle size. It was found that the copper particle size played a crucial role in many catalytic transformations.[234] In order to find out how the properties of a copper catalyst are changed in the selective hydrogenation of acetylene, the single-atom catalyst and copper NPs of different sizes (3.4, 7.3, 9.3 nm) were obtained with their subsequent deposition onto aluminium oxide surface. It was found, that with a decrease in the particle size, the catalyst activity decreased. At the same time, selectivity and stability are significantly increased. In particular, single-atom copper catalysts showed 91% selectivity to ethylene with complete conversion and stability for at least 40 hours on stream. The difference in the properties of catalysts with varying particle sizes can be explained by different types of sorption — desorption of ethylene/acetylene (Fig. 26). According to the temperature profiles, acetylene desorption is observed at a lower temperature for the catalyst with a smaller particle size (89°C *vs.* 105°C). Therefore, the weak binding of acetylene on catalysts with a

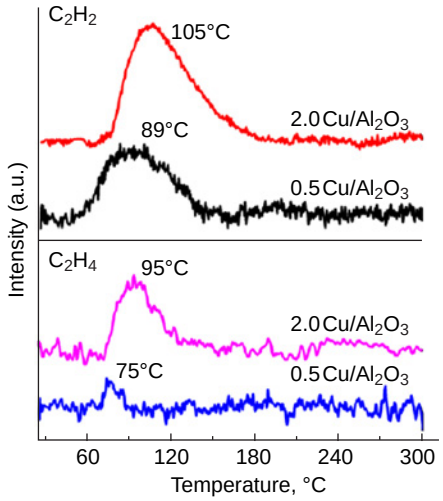

Figure 26. TPD profiles of C_2H_2 (*top*) and C_2H_4 (*bottom*) on 0.5 Cu/Al_2O_3 and 2.0 Cu/Al_2O_3 (The figures indicate the mass weight of metal in the catalysts). Reproduced from Ref. 234 with permission from the American Chemical Society.

smaller particle size leads to lower sorption and lower concentration and hence to lower activity. A similar trend is observed for ethylene. In the case of ethylene, this leads to the less sorption of ethylene by the catalyst and, as a result, to less hydrogenation. Therefore, the selectivity of the process as a whole increases.

The bimetallic catalyst, Zn–Cu_xC was obtained by co-precipitation of the appropriate starting reagents. The addition of Zn contributed to a decrease in the size and an increase in the number of Cu_xC crystals.[235] In turn, it caused an increase in the activity of the catalyst in transformation of acetylene to ethylene, and the catalyst *per se* had excellent stability (> 140 h on stream) at 100°C even in the presence of a large excess of ethylene.

A composite catalyst based on copper and iron was prepared to study the mutual influence of the Fe support atoms on copper atoms.[236] Varying the ratio of elements in the catalyst, the authors managed to achieve 95% selectivity to ethylene with full conversion using the $CuFe_{0.16}MgO_x$ catalyst. Based on the analytical data and calculations, the formation of the $Cu^{\delta-}Fe^{\delta+}_{0.16}MgO_x$ complex was observed, which played a crucial role in the activation of acetylene and hydrogen. This complex of a certain composition was bonded to both other copper and other iron atoms (with those that were not part of the complex). According to the data obtained, the desorption of ethylene on this complex was more preferable than its further hydrogenation. As the amount of iron in the catalyst increased, its catalytic activity expectedly increased, since the number of complexes and, accordingly, the routes for hydrogen dissociation increased. However, at the atomic ratio Cu/Fe > 0.16, *i.e.* increasing the proportion of iron, the activity of the catalyst decreased, since the iron particles covered the copper particles. Thus, the activation of acetylene and hydrogen occurred on the copper sites of the catalyst, while the formation of the C–C bond occurred on the Cu/Fe complex, with one carbon atom being bound to a copper atom and the other to an iron atom (Fig. 27).

Copper atoms were immobilized on a defective nanodiamond–graphene and N-doped nanodiamond graphene to reveal the influence of the coordinated environment (Cu–C or Cu–N bonds) on the catalytic activity in acetylene hydrogenation.[237] It was found, that more oxidized copper atoms with Cu–C bonds showed high selectivity (up to 93%) with quantitative conversion and high stability (> 100 h on stream). According to the DFT calculations and isotope exchange experiments, the presence of a copper atom bound to carbon promoted the binding of hydrogen for subsequent dissociation, which was the rate-limiting step of the reaction. The coordination of three carbon atoms near the copper atom led to rapid charge consumption on the copper atoms, which in turn boosted the catalyst activity and, at the same time, increased its resistance to metal leaching from the surface.

Significant progress has been achieved in reduction of long-chain hydrocarbons during the selective hydrogenation of acetylene.[238] For this purpose, a copper catalyst was modified with a hydrophobic C_{16} chain, which was grafted to the metal surface using hexadecyltrimethoxysilane. The similar polarity of the alkyl chain of the catalyst and acetylene facilitated the sorption of the substrate on the catalyst surface, thus ultimately increasing the activity of the catalyst. In addition, the presence of a long hydrocarbon chain on the surface led to steric hindrance on the surface and challenges in the formation of hydrocarbons with a longer chain (C_{4+} hydrocarbons), which, in turn, significantly increased the catalyst lifetime. This modification provided an access to a catalyst capable of semi-hydrogenating acetylene with a selectivity of up to 84% at 140°C for 120 h.

The selective hydrogenation of acetylene on copper catalysts produces copper carbide CuC_2, as well as a number of the other carbides (including mixed ones).[239] The catalyst was prepared from copper hydroxide with subsequent exposing to acetylene and reduction with hydrogen (Fig. 28). The resulting catalyst demonstrated moderate 15% selectivity and lower; however, the very fact of the formation of copper carbides is very interesting. Since the presence of copper acetylide in the solid phase was unambiguously proved, this compound turned out to be a precursor of the true catalyst or an intermediate in the hydrogenation reaction. On the one hand, the formation of copper carbide is a reversible process, and, probably, it is through the carbide that acetylene is hydrogenated. On the other

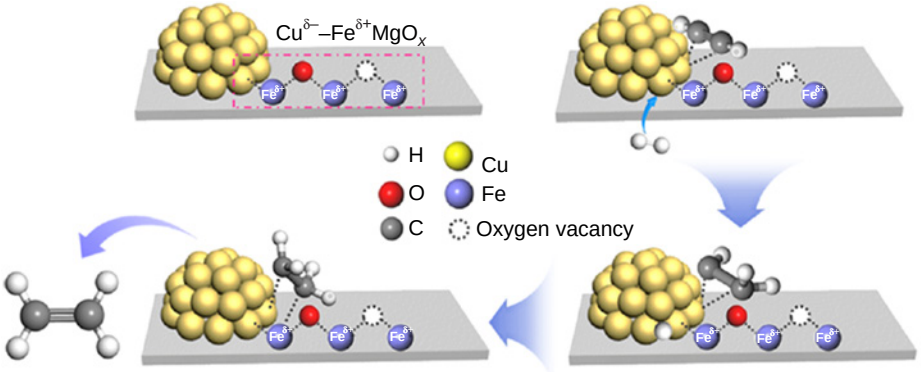

Figure 27. The proposed mechanism of acetylene semi-hydrogenation on the $Cu/Fe_{0.16}MgO_x$ catalyst. Reproduced from Ref. 236 with permission from the American Chemical Society.

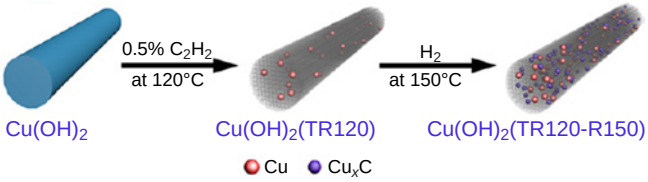

Figure 28. The synthesis of a carbide CuC_x catalyst. Reproduced from Ref. 239 under a CC-BY-NC-ND license.

hand, copper carbide transforms easily into more complicated carbides when heated, which was an irreversible process and could actually be considered as coking of the metal. Copper carbide immersed in a carbon matrix was also found in the catalysts comprising basic copper carbonate.[240] It was found that copper carbides acted as catalytic sites for the dissociation of hydrogen molecules, and the carbon matrix created steric hindrances for further growth of the hydrocarbon chain, which, accordingly, prevented undesirable oligomerization of acetylene. Copper carbides can also be formed by adding the other metals to the catalyst.[235] For example, the addition of zinc promoted the formation of copper carbides, and at the same time the size of the carbide particles was significantly smaller than in the synthesis of copper carbide without the addition of salts of other metals. In the same work, it was established that the addition of zinc does not affect the electronic structure of the carbides.

According to experimental data and DFT calculations, the activation barrier for complete hydrogenation of acetylene on a single-atom copper catalyst was higher than on a copper nanocatalyst.[241] In addition, it was found that ethylene sorption was significantly more complicated on a single-atom catalyst, which led to inhibition of over-hydrogenation.

To prevent the 'hot spot' formation and over-hydrogenation, an electrochemical approach carried out at room temperature was proposed.[242] Hydrogen generated *in situ* during water electrolysis was used as the hydrogenating agent. Copper dendrites, produced electrochemically (electrodeposition from a $Cu(NO_3)_2$ solution provided an extremely high selectivity of 97% with an acetylene content of only 4 ppm in the final mixture, which corresponds to industrial standards for ethylene purity for further polymerization. These results were achieved using a flow electrochemical cell with a large electrode surface area (Fig. 29).

Another approach for the electrochemical hydrogenation of acetylene to ethylene assumed the diffusion of acetylene through a carbon-based gas diffusion layer (GDL) and then through a microporous layer (MPL) directly to the surface of the catalyst.[243] Thus, the reaction interface was a gas/electrolyte/catalyst system

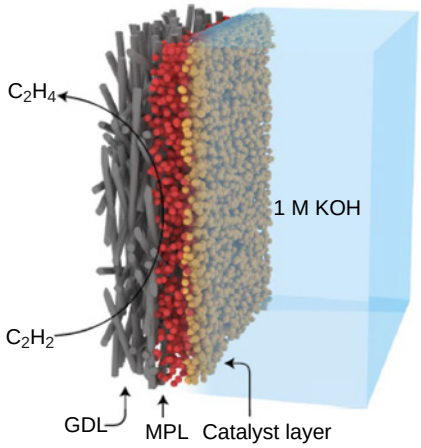

Figure 30. Schematic representation of cathode for acetylene hydrogenation. Reproduced from Ref. 243 with permission from Springer Nature.

(Fig. 30). The process occurred at room temperature and was completed with 99.9% conversion of acetylene with 90.1% ethylene selectivity. These data allow considering electrochemical approach involving the use of hydrogen generated *in situ* by water electrolysis as an alternative to the standard thermal method. Yet another example of electrochemical hydrogenation of acetylene was also demonstrated using a Cu catalyst, which was copper nanodots.[244] In this case, the acetylene content in the final mixture was less than 1 ppm.

A mixed catalyst based on copper and nickel with an aluminosilicate zeolite ZSM-12 support was prepared.[245] During catalytic tests, it was shown that the catalyst can completely convert acetylene with 82.5% selectivity to ethylene. Among the $CuNi_x$/ZSM-12 catalysts ($x = 5$, 7, 9, 11), $CuNi_7$/ZSM-12 performed best. According to the XPS data, the Ni2p peaks of the Ni/ZSM-12 and $CuNi_7$/ZSM-12 catalysts correspond to three components: the satellite peak of Ni, Ni^{2+}, and Ni^0 (Fig. 31 *a*). The signal intensity in the spectra of Ni/ZSM-12 was much higher than that of $CuNi_7$/ZSM-12. All the three peaks have a slight shift towards an increase in the binding energy after the formation of $CuNi_7$ particles, which indicates a strong interaction of copper and nickel particles, expressed in the transfer of electrons. a red shift after the formation of $CuNi_7$ particles, which indicated a strong interaction of copper and nickel particles, expressed in electron transfer. The Cu2p signals in Cu/ZSM-12 and $CuNi_7$/ZSM-12 demonstrated binding energies of 935 and 955 eV, which corresponded to the $Cu2p_{3/2}$ and $Cu2p_{1/2}$ states, respectively (see Fig. 31 *b*). When the support was replaced by ZrO_2, the hydrogenation selectivity increased to 93% also at full conversion of the substrate.[246] The authors have proved the formation of CuNi alloy particles and, using

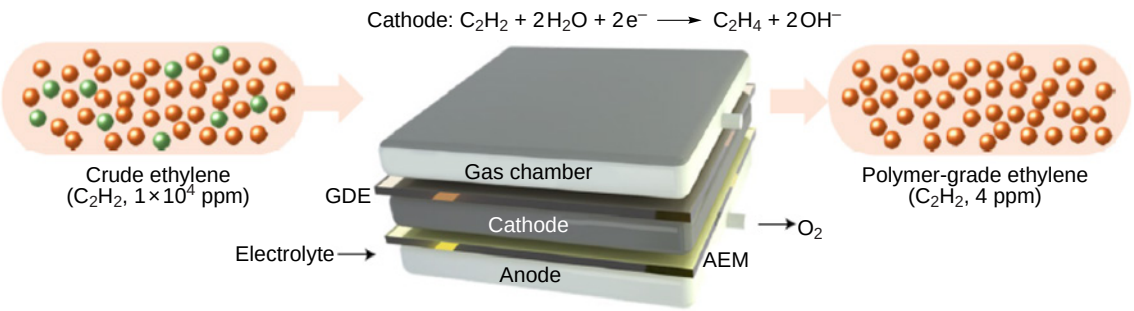

Figure 29. Scheme of electrocatalytic purification of ethylene from acetylene. Reproduced from Ref. 242 with permission from Springer Nature.

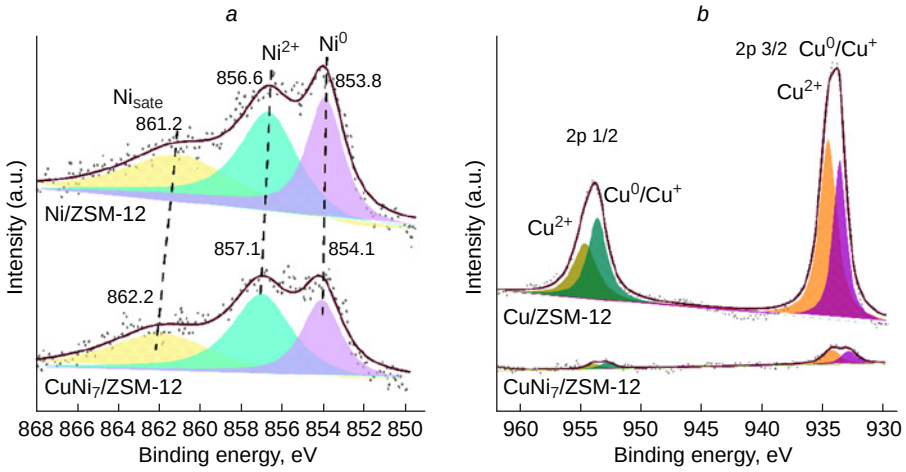

Figure 31. XPS spectra of Ni2p (*a*) and Cu2p (*b*) in Cu/ZSM-12 and $CuNi_7$/ZSM-12 catalysts. Reproduced from Ref. 245 under a Creative Commons Attribution (CC BY) license.

computational methods and analytical studies, explained the improved results by easier adsorption of acetylene and key intermediates.

A series of copper and iron-based kaolin-supported catalysts were synthesized for testing in the semi-hydrogenation of acetylene.[247] The $Cu_3Fe_{0.5}$/kaolin mixture performed best, providing 95% selectivity at 93% conversion. The authors explained this result by the shift of the characteristic Cu peak in the XPS spectra to a lower energy level caused by changes in the electronic structure of the $Cu_3Fe_{0.5}$/kaolin catalyst, as well as the interaction of copper with Fe and support atoms (Al–Si). In addition, electrons from the partially occupied 4s orbital of copper were able to transfer to the partially occupied 3d orbital of iron atoms, which led to hybridization of orbitals in the alloy and a change in the electronic structure of active sites. Under hybridization, the $Cu2p_{3/2}$ signals in the alloy spectra were slightly shifted to lower energies.

Thus, single-atom copper catalysts show increased selectivity in comparison with copper NPs, which was shown by the authors of the original works using particles of different sizes as an example. The interaction of copper with support atoms and adjacent atoms in the case of alloy catalysts can also be noted. Separately, it is worth mentioning the identified phases of copper carbides formed during the immersion of metal atoms into a carbonaceous support Apparently, the formation of carbides is characteristic of most metals. The role of carbides in the hydrogenation of acetylene has not yet been reliably identified, and it remains to be established how the transition of active forms to carbide (or *vice versa*) occurs. Using a copper catalyst as an example, it was shown that grafting a long-chain aliphatic substituent to the metal decreases the amount of acetylene oligomerization products, which can most likely be used in the case of other metals.

7. Other metal catalysts in semi-hydrogenation of acetylene

The common route for removing acetylene from ethylene involves preliminary hydrogen production. An original approach based on the simultaneous production of hydrogen and semi-hydrogenation of acetylene on a Au/α-MoC catalyst was proposed.[55] Hydrogen was obtained by the reaction of carbon monoxide with water. The excess oxygen was removed with CO, which was further oxidized to CO_2, and the released hydrogen was immediately consumed in the hydrogenation reaction. To clarify the mechanism of the process, reagent mixtures with labelled atoms were used: $CO+D_2O$ and $^{13}CO+H_2O$. Analysis of the kinetic isotope effect of the H/D exchange processes and $^{12}C/^{13}C$ in the formation of ethylene revealed the ratios of the formation rates (r):

$$r(H)/r(D) = 2.59,$$

$$r(CO)/r(^{13}CO) = 1.14.$$

In fact, this meant that both the transfer of surface hydrogen to acetylene and the reaction of adsorbed CO with surface oxygen can contribute to the reaction rate. Based on these data, a reaction model was constructed, involving dissociation of water to give hydroxyls, the transfer of hydrogen to acetylene, and the reaction of CO with oxygen with subsequent desorption of CO_2. According to this model, the equilibrium constants of adsorption were determined, which demonstrated a strong competition of acetylene adsorption with the other reagents on the catalyst surface. The authors concluded, that the reaction of the three compounds ($CO+H_2O+C_2H_2$) occurred by removing of boundary oxygen thereby exposing molybdenum sites for acetylene adsorption and water dissociation to hydroxy anions. Then, hydrogen was transferred from hydroxyls to acetylene (formation of ethylene) with the removal of residual oxygen by carbon monoxide. The best results that were achieved in this process were high acetylene conversion (99%) and very promising ethylene selectivity (83%) at low temperature (80°C). The authors indicated, that the proposed path might be an alternative to traditional energy-intensive hydrogenation processes involving molecular hydrogen.

Alumina-supported gold NPs were used as a catalyst in the selective semi-hydrogenation of acetylene to ethylene.[248] The main idea of the work was to decorate the support with carbon atoms (CA) or carbon and nitrogen atoms (CNA), which were obtained by carbonization of the appropriate precursors on the support surface. The catalysts with doped support demonstrated 5 times higher catalytic activity in the catalytic tests (Fig. 32). According to XPS data, the electron transfer between the Au atom and the C and N atoms can play a crucial role in the activity of gold catalytic sites.

Etching the bimetallic AuCu catalyst with acetic acid generates Cu vacancies on the abrupt catalyst surface, which are suitable for alkyne hydrogenation and, in combination with electron-deficient Au atoms, contribute to the increased catalytic properties.[249] The activity of etched Au_3Cu_1/TiO_2 catalysts was 4.6 times higher than that of untreated catalysts, and the ethylene selectivity was 94.0%.

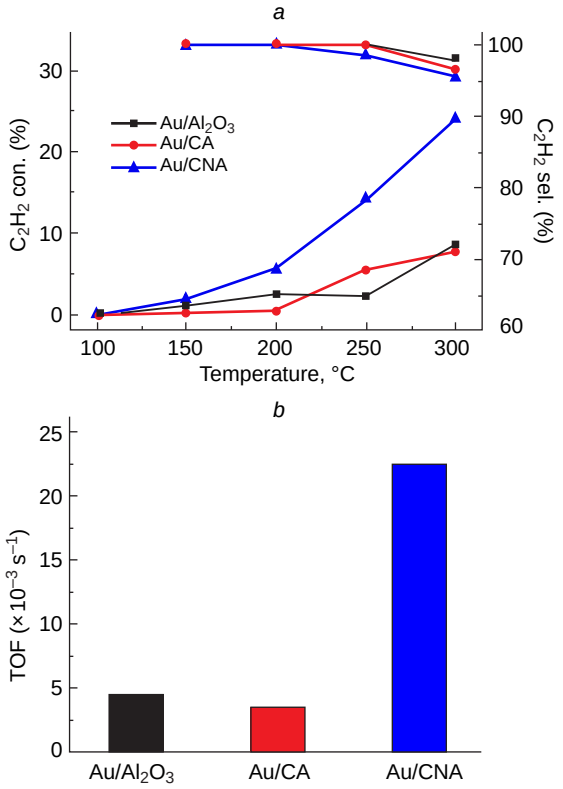

Figure 32. Acetylene conversion and ethylene selectivity as a function of hydrogenation temperature (*a*); TOF values for the Au catalysts on various supports at 250°C (*b*). Reproduced from Ref. 248 with permission from Springer Nature.

ZnO with the disc-like (ZnO–D) and flower-like (ZnO–F) morphology were prepared hydrothermally from $Zn(NO_3)_2 \cdot 6H_2O$ and used as a support for Au/ZnO nanocatalysts.[250] Subsequent treatment of the catalysts with a gas mixture of 10 vol.% O_2/Ar furnished Au/ZnO–F–O, Au/ZnO–D–O and their reduced derivatives, Au/ZnO–F–H and Au/ZnO–D–H, when treating the starting catalysts with a mixture of 10 vol.% H_2/Ar (Fig. 33). The catalytic activity in the semi-hydrogenation of acetylene was directly dependent on the Au^{3+} content in the catalyst and decreased in the series Au/ZnO–F > Au/ZnO–F–H > Au/ZnO–D > Au/ZnO–D–H.

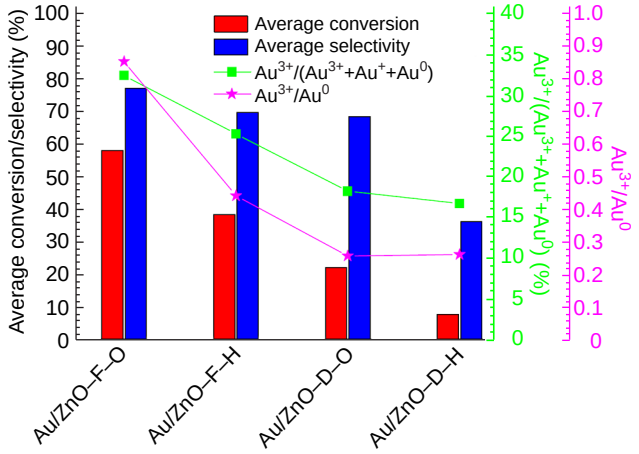

Figure 34. Dependence of conversion/selectivity of acetylene semi-hydrogenation on the chemical state of Au species. Reproduced from Ref. 250 with permission from the American Chemical Society.

The authors explained this effect by the ability of Au^{3+} to take electrons from acetylene into vacant 5d orbitals, providing stronger acetylene adsorption than Au^{+} and Au^{0}. The best acetylene conversion (~58%) and ethylene selectivity (76%) were obtained in the presence of Au/ZnO–F (Fig. 34).

The core-shell type composite Au@Pt NPs were synthesized by impregnation and then investigated as catalysts for selective semi-hydrogenation of acetylene.[251] An imidazole framework was used as a catalyst support. The synthetic procedure involved growing a platinum shell on gold nanorods, followed by oxidative etching of the resulting hollow nanocomposite. At the second step, the resulting composite particles were encapsulated into the substrate. The Au@Pt-NTs@ZIF-67 catalyst was the most active in the process and provided the 49.3% yield of ethylene at the acetylene conversion of 69.1%. Probably, high activity of such catalysts was due to their tubular structure with a high content of active sites on the catalyst surface. The existence of highly active platinum particles around gold particles caused a synergistic effect, which provided conversion of acetylene into ethylene. After the catalytic process, the composite nanotubes retained their hollow tubular structure, *i.e.* the morphology of the particles remained unchanged, opening up abilities for the multiple use of the catalysts.

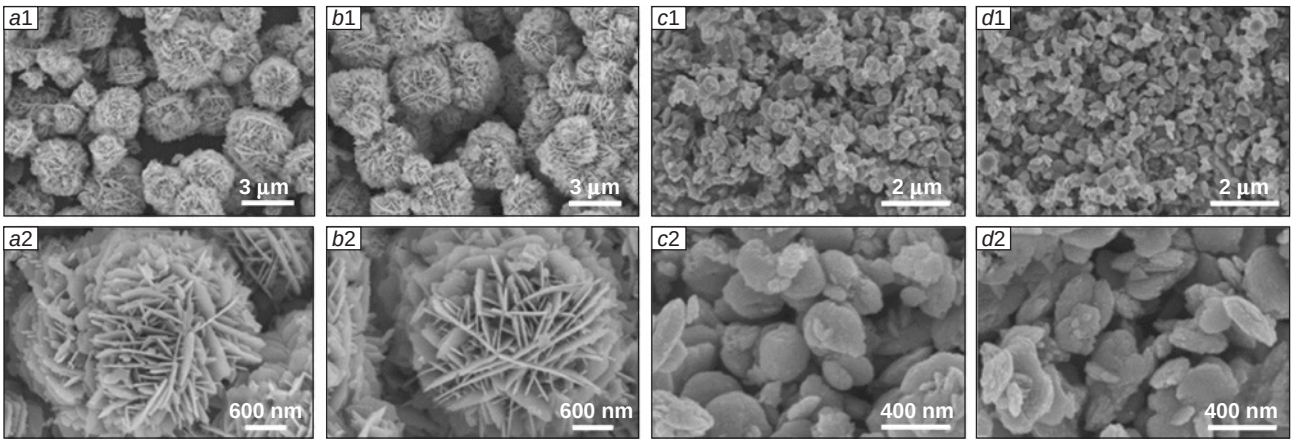

Figure 33. SEM images of Au/ZnO–F–O (*a*1, *a*2), Au/ZnO–F–H (*b*1, *b*2), Au/ZnO–D–O (*c*1, *c*2), Au/ZnO–D–H (*d*1, *d*2). Reproduced from Ref. 250 with permission from the American Chemical Society.

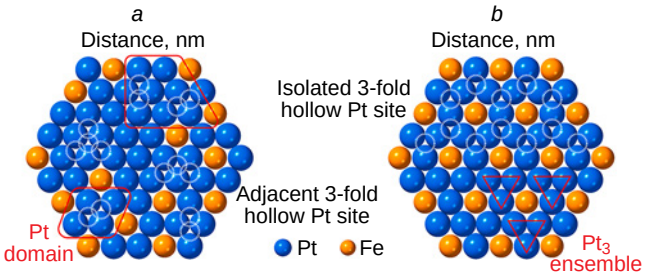

Figure 35. Geometry of the arrangement of Pt and Fe atoms in Pt_3Fe nanoparticles. Configurations of atoms in the dominant planes A1 (*a*) and L12 (*b*). Reproduced from Ref. 252 with permission from Elsevier.

The bimetallic Pt_3Fe nanocatalyst, individual particles of which were encapsulated in a silicon shell, were also studied in the hydrogenation of acetylene to ethylene. High-temperature (773–973 K) hydrogen treatment of the Pt_3Fe surface was carried out, which changed the structure of the catalytic species: disordered Pt species (A1 plane) was formed by ordered Pt_3 assemblies surrounded by Fe atoms (L12 plane) (Fig. 35).[252] The structure of this ensemble structure provided charge transfer from Fe atoms to neighbouring Pt atoms in the catalytic species, facilitating ethylene desorption from it and, accordingly, increasing and maintaining the selectivity of acetylene semi-hydrogenation at 83%.

A systematic and detailed study was carried out for a pair of platinum catalysts PtCu and PtCo.[253] The first important observation concerned the formation of alloy particles. The authors showed that the alloys are formed not only in the course of hydrogenation of metals from their oxides during synthesis of the catalysts, but also in the course of hydrogenation of acetylene. It was also found that larger platinum particles in Co catalysts promoted a higher hydrogenation reaction with increasing temperature thereby improving the yield of ethane. In contrast, in copper catalysts, a decrease in the platinum particle size led to not only to an improved yield of ethylene, but also to losses in the reaction rate. According to the X-ray absorption spectra of the near-threshold fine structure, the threshold energies for PtCu catalysts were 11 566.8 eV, and 11 563.8 eV for PtCo. Accordingly, higher energy implied higher density of unoccupied d-orbitals of Pt, which was a key indicator of improved activity in the semi-hydrogenation of acetylene (87.6% on Cu catalysts *vs*. 62.9% on Co catalysts). DFT calculations also showed that the redistribution of electron density towards platinum in the PtCu catalyst was more pronounced than in the PtCo catalyst. platinum atoms paired with copper atoms contained more electrons than those paired with cobalt atoms. This redistribution results in weaker π-bonding of ethylene on the surface and, accordingly, inhibition of complete hydrogenation. The authors also pointed out, that in addition to obvious Pt–O and Pt–Cu/Co bonds, Pt–O–Cu/Co bonds were formed.[254] In fact, it's about unreduced metal oxides that were used as precursors of metal particles on the catalyst surface. On the one hand, the presence of such particles is obvious. On the other hand, their role and their contribution to the reaction are rarely assessed. It was found that oxygen atoms repel platinum atoms from each other, which furnish Pt–O–Cu and Pt–O–Co atomic structures. Under hydrogenation conditions, the coordination number of the Pt–Co alloy was 4.35, and that of the Pt–Cu alloy was 2.21. At the same time, the coordination numbers of Pt–O–$CuO_{\alpha(\alpha<1)}$ bonds was 7.45, which is 6.48 times greater than that of the Pt–CoO bond (1.15). Another issue was in the absence of the Cu–Cu bond in the Cu catalyst. All these issues provided weak binding of ethylene to the catalyst surface, which in turn decreases the rate of complete hydrogenation.

A series of complicated catalysts containing copper, platinum and cerium simultaneously were prepared for the selective hydrogenation of acetylene.[59] The initially prepared, PtCe alloy was deposited on a support consisting of various zeolites (Y, ZY), as well as on a copper-modified zeolite support to obtain PtCe/Cu–ZY. In addition, the PtCe alloy was deposited on a support of copper-modified oxalate and borohydride ligands (PtCe/CuX–ZY and PtCe/CuB–ZY, respectively). According to experimental data, the ethylene yield was 55.3% using PtCe/ZY catalysts at 120°C; and 71.4% in the presence of PtCe/Cu–ZY at 180°C. At the same time, in the presence of PtCe/CuX–ZY and PtCe/CuB–ZY catalysts, the yields were increased to 81.9 and 92.1% at 180 and 160°C, respectively. Both results demonstrated the positive effect of copper on the catalyst properties.

A silver carbide-like (Ag_xC) catalyst was synthesized by reduction of silver acetylide to Ag_xC under H_2 atmosphere.[255] This catalyst demonstrated promising catalytic activity in the conversion of acetylene to ethylene. The acetylene conversion was 100%, the ethylene selectivity was 88.7%, and the catalyst demonstrated good stability under continuous operation for at least 30 h. High performance was due to the ability of the Ag_xC phase to significantly reduce the activation barrier of H_2 dissociation and easy desorption of ethylene, which prevented overhydrogenation.

It is known, that supported rhodium catalysts are inefficient in semi-hydrogenation reactions. The addition of electron-donating acetylene ligands to atomically dispersed rhodium supported on zeolite provided high selectivity to ethylene (>90%) in the acetylene semi-hydrogenation at 373 K in the presence of a large excess of ethylene.[256]

8. Conclusion

Selective hydrogenation of acetylene continues to be a relevant scientific issue. Obviously, the industrial process of ethylene purification from acetylene impurities stimulates research in this area, but it can be noted that the fundamental interest in this reaction is also extremely high. This is largely due to the need to gain deeper insight into the nature of catalysis, and the reaction of selective hydrogenation of acetylene is a kind of 'textbook' illustrating the selectivity patterns. Another boost for further research in this area was the development of complex catalysts and the discovery of new possibilities for their synthesis. The state-of-the-art experimental methods allow not only to reduce the size of metal particles to the nanoscale, but also provide uniform distribution of particles over the surface with atomic precision. Tuning the structure of complex species opens an access to single-atom catalysts, as well as ensembles of two or more elements of a certain composition and structure. For example, single atoms of one element can be placed in the corners of nanocubic particles of a second. Much of this precision is due not to the procedures *per se*, but rather to improvements in analytical techniques and the associated ability to detect the smallest details of the atomic world.

The highest efficiency in semi-hydrogenation of acetylene is demonstrated by catalysts based on palladium, copper, nickel, silver and their alloys. The general patterns of their action consist of an increase in the selectivity index for ethylene and a simultaneous decrease in the degree of acetylene conversion as the size of the metal particles decreases. Due to the small size of

the metal particles and their distance from each other, the addition of hydrogen to acetylene occurs on the surface of the catalyst, and not in its bulk. 'Dilution' of the active metal with a 'guest' element also improves selectivity by transferring excess heat from the catalytic centre to the 'satellite' element. Another method for increasing selectivity is to reduce the electron density on the active metal. This is achieved by introducing one (or more) components to form alloy particles, or by appropriately designing the support, the atoms of which can deplete the active metal with electron density. A decrease in the electron density at the catalytic centre leads to easier desorption of ethylene formed during hydrogenation, a shorter time of its coordination with the catalyst surface and, accordingly, complicates further conversion into ethane.

As the types and numbers of active species on the catalyst surface continue to increase, and due to the difficulties in interpreting the catalytic pathway, it is likely that new barriers in the analysis of big catalytic data sets will emerge in the future. From this point of view, research in the field of machine learning and the use of artificial intelligence, which allows for the automatic analysis of hundreds and thousands of spectra with automatic processing of the results obtained, seem promising. Today, machine learning is already actively used in the development of approaches to the selective hydrogenation of acetylene[257] and in the design of catalysts for this process,[179,180] in the development of nanocluster[258] and single-atom[259] catalysts, in the search for active catalytic centres,[260] as well as for the identifying of intermediate structures on the surface of catalysts.[261]

In conclusion of the review, the comparison of the catalytic characteristics of the above-discussed single-atom catalysts with other types of catalytic systems used in the selective hydrogenation reaction of acetylene is given in Table 2.

Table 2. Comparison of single-atom catalysts with other types of catalytic systems used in semi-hydrogenation of acetylene.

Catalyst, particle size	Support	Gas mixture $C_2H_2/H_2/C_2H_4$ (vol.%)[a]	*T*, °C	Conversion (%)	Selectivity to C_4H_4	Ref.
		Pd-Catalysts				
Pd-ISA	MPNC	0.5/5/50 + He	110	76	82	127
Pd-ISA	See[b]	0.5/5/50 + He	110	17	84	127
Pd-NP	MPNC	0.5/5/50 + He	110	100	21	127
PdBi-ISA	Calcite	1/20/20 + He	50–300	100	99	205
Pd	Calcite	1/20/20 + He	20	100	–386 (see[c])	205
Pd-ISA	CN	0.65/5/50 + He	100	92	80	129
Pd-NP	CN	0.65/5/50 + He	100	<20	82	129
PdCu-SAA (see[d])	CuMgAl	0.45/0.9/45 + He	82	80	97	262
PdCu-1 (see[e])	CuMgAl	0.45/0.9/45 + He	82	80	61	262
PdCu-2 (see[f])	CuMgAl	0.45/0.9/45 + He	82	80	79	262
Pd_1Ni-SAA	SiO_2	1/10/20 + 5% C_3H_8 + He	80	90	88	191
Pd (see[g])	SiO_2	1/10/20 + 5% C_3H_8 + He	100	90	90	191
Pd_1Ni (see[g])	SiO_2	1/10/20 + 5% C_3H_8 + He	140	90	90	191
$Pd_{0.1}Ni_2$-SAA	SiO_2	1/20/20 + 5% C_3H_8 + He	140	95	91	192
$Pd_{0.1}$	SiO_2	1/20/20 + 5% C_3H_8 + He	140	95	5	192
Pd_1	MgO	1/10/20 + He	60–200	100	60	133
Pd-NP	MgO	1/10/20 + He	100	100	–825	133
Pd_1Ag_6	γ-Al_2O_3	1/93.7/5.3 + He	70	100	57	185
Pd	γ-Al_2O_3	1/93.7/5.3 + He	70	100	30	185
Pd_1	ND@G (see[h])	1/10/20 + He	180	100	90	263
Pd_n	ND@G (see[h])	1/10/20 + He	180	100	–450	263
PdCu-SAA	γ-Al_2O_3	0.5/3 + He	90	100	95	264
Pd-NP	γ-Al_2O_3	0.5/3 + He	90	100	37	264
Pd_1	CNT	2/4/50 + He	40	83	98	155
PdO	CNT	2/4/50 + He	40	92	–36	155
Pd_1-PDO	CeO_2	8/0.4/31.6 (see[i]) + He	120	59	80	136
Pd-PDO	CeO_2	8/0.4/31.6 (see[i]) + He	120	82	20	136
Pd_1Ag	γ-Al_2O_3	1/5/94 + He	76	100	62	186
Pd	γ-Al_2O_3	1/5/94 + He	76	100	37	186
Pd-SA	BN	0.33/6.6/32.9 + N_2	170	100	93	138
Pd-NP	Activated carbon	0.33/6.6/32.9 + N_2	170	100	89	138
Pd-SA	Graphitic C_3N_4	0.5/1/25 + Ar	115	100	82	128
Pd	Al_2O_3	0.5/1/25 + Ar	130	100	31	128
Pd	SiO_2	0.5/1/25 + Ar	70	100	25	128
$Pd_{0.2}Bi_2O_3$	TiO_2	1/20/20 + He	90	90	90	265

Table 2 (continued).

Catalyst, particle size	Support	Gas mixture $C_2H_2/H_2/C_2H_4$ (vol.%)[a]	*T*, °C	Conversion (%)	Selectivity to C_4H_4	Ref.
		Pd-Catalysts				
$Pd_3Bi_2O_3$	TiO_2	1/20/20 + He	90	90	–2000	265
Pd-SA	Modified ZIF-8	0.5/5/50 + He	120	96	93	126
Pd-NP	N-Doped carbon	0.5/5/50 + He	120	70	72	126
$Pd_{0.25}La_{0.25}$-SA	N-Doped pgBC	H_2/C_2H_2 (2 : 1 ratio) + He	100	97	62	207
$Pd_{0.25}$ NPs	N-Doped pgBC	H_2/C_2H_2 (2 : 1 ratio) + He	100	97	42	207
		Cu-Catalysts				
Cu-SA	Al_2O_3	1/10/50 + Ar	188	100	91	234
Cu-NP, 3.4 nm	Al_2O_3	1/10/50 + Ar	184	100	89	234
Cu-NP, 7.3 nm	Al_2O_3	1/10/50 + Ar	180	100	87	234
Cu-NP, 9.3 nm	Al_2O_3	1/10/50 + Ar	179	100	84	234
Cu_1	ND@G	1/10/20 + He	200	95	98	266
Cu_n	ND@G	1/10/20 + He	200	20	92	266
		Ni-Catalysts				
NiGa (isolated)	Unsupported	1/10/20 + N_2	240	94	80	229
Ni ensembles	Unsupported	1/10/20 + N_2	240	98	45	229
Ni_5Ga_3 ensembles	Unsupported	1/10/20 + N_2	240	98	60	229
Ni_1	ND@G	1/10/20 + He	200	0.5	–	208
Ni_n	ND@G	1/10/20 + He	190	100	85	208
Ni_p	ND@G	1/10/20 + He	150	100	–40	208
Cu_1 (see[j])	gC_3N_4	0.5/5/25 + Ar	260	10	60	267
Ni_1-SA	gC_3N_4	0.5/5/25 + Ar	261	33	85	267
Ni_1Cu_2 (see[k])	gC_3N_4	0.5/5/25 + Ar	170	100	90	267

[a] The composition of the gas mixture is given in %, the balance up to 100% is achieved by adding an inert gas, which is indicated after the '+' sign; [b] supported on non-mesoporous N-doped carbon; [c] hereinafter, negative conversion means hydrogenation of ethylene in the mixture to ethane; [d] SAA is a monoatomic alloy; [e] the Cu content in the catalyst is 0.35 wt.%; [g] non-monatomic particles (alloy); [h] graphene with nanodiamond-like structure with facet defects; [i] values are in sccm (standard cubic centimeter per minute, st. cm^3 min^{-1}); [j] mixture of 68% SA, 20% linear trimers, 12% triangular trimers; [k] mixture of 71% linear trimers.

9. List of abbreviations and designations

E_{ads} — adsorption energy,
G_{ads} — adsorption free energy,
$\Delta H°$ — standard enthalpy (of reaction),
r — rate of formation,
Ac — acetone,
acac — acetylacetonate,
AC-HAADF-STEM — aberration-corrected high high-angle annular dark-field scanning transmission electron microscopy,
AIMD — *initio ab initio* molecular dynamics (method),
CN — nitrogen-doped carbon nanospheres obtained from covalent organic frameworks,
CNT — multi-walled carbon nanotubes,
COD — cycloocta-1,5-diene,
COF — covalent organic frameworks,
CTF — layered covalent triazine frameworks,
ESI-HRMS — high resolution mass spectrometry with electrospray ionization,
EDS — energy dispersive X-ray spectroscopy,
G — graphene,
GHSV — gas hourly space velocity,
GR — galvanic replacement (method),
gC_3N_4 — graphene-like carbon nitride,
GDL — carbon-based gas diffusion layer,
hNCNC — hierarchical carbon nanocells,
HR — high resolution,
HTS — hexadecyltrimethoxysilane,
HNT — halloysite nanotubes,
IL — ionic liquid,
ISA — isolated single-atom centres,
L — ligand,
LDH — layered double hydroxides,
MPL — microporous layer,
MPNC — mesoroporous N-doped carbon foam nanospheres,
NC — nanocubes,
ND — nanodiamonds,
NHC — N-heterocyclic carbene,
NMC — N-doped mesoroporous carbon,
NMP — *N*-methyl-2-pyrrolidon,
NP — nanoparticles,
NT — nanotubes,
Ndicy — dicyandiamide,
Pal — palygorskite,
PDO — 1,10-phenanthroline-5,6-dione,
Prmim — 1-methyl-3-*n*-propylimidazolium,
SA — single-atom (catalyst),
SAA — single-atom alloy,
SEM — scanning electron microscopy,
TEM — transmission electron microscopy,
TEOS — tetraethyl orthosilicate,
TOF — catalyst turnover frequency, which is a measure of catalytic activity and shows the number of substrate molecules

transformed into product on one active centre of the catalyst per unit of time,

TPAOH — tetrapropylammonium hydrozide,
TPD — temperature programmed desorption,
XPS — X-ray photoelectron spectroscopy,
XRD — X-ray (powder) diffraction,
ZIF — zeolite imidazolate framework.

10. References

1. C.Liu, H.Zhang, W.Shi, A.Lei. *Chem. Rev.*, **111**, 1780 (2011); https://doi.org/10.1021/cr100379j
2. J.B.Johnson, T.Rovis. *Angew. Chem., Int. Ed.*, **47**, 840 (2008); https://doi.org/10.1002/anie.200700278
3. E.C.Swift, E.R.Jarvo. *Tetrahedron*, **69**, 5799 (2013); https://doi.org/10.1016/j.tet.2013.05.001
4. I.Pérez, J.P.Sestelo, L.A.Sarandeses. *J. Am. Chem. Soc.*, **123**, 4155 (2001); https://doi.org/10.1021/ja004195m
5. H.Wang, J.Wen, X.Zhang. *Chem. Rev.*, **121**, 7530 (2021); https://doi.org/10.1021/acs.chemrev.1c00075
6. J.-H.Xie, S.-F.Zhu, Q.-L.Zhou. *Chem. Rev.*, **111**, 1713 (2011); https://doi.org/10.1021/cr100218m
7. N.Fleury-Brégeot, V.de la Fuente, S.Castillón, C.Claver. *ChemCatChem*, **2**, 1346 (2010); https://doi.org/10.1002/cctc.201000078
8. A.Cabré, X.Verdaguer, A.Riera. *Chem. Rev.*, **122**, 269 (2022); https://doi.org/10.1021/acs.chemrev.1c00496
9. L.Wang, E.Guan, J.Zhang, J.Yang, Y.Zhu, Y.Han, M.Yang, C.Cen, G.Fu, B.C.Gates, F.-S.Xiao. *Nat. Commun.*, **9**, 1362 (2018); https://doi.org/10.1038/s41467-018-03810-y
10. A.Biffis, P.Centomo, A.Del Zotto, M.Zecca. *Chem. Rev.*, **118**, 2249 (2018); https://doi.org/10.1021/acs.chemrev.7b00443
11. B.A.D.Neto, R.O.Rocha, M.O.Rodrigues. *Molecules*, **27**, 132 (2022); https://doi.org/10.3390/molecules27010132
12. A.J.McCue, J.A.Anderson. *Front. Chem. Sci. Eng.*, **9**, 142 (2015); https://doi.org/10.1007/s11705-015-1516-4
13. T.Irrgang, R.Kempe. *Chem. Rev.*, **119**, 2524 (2019); https://doi.org/10.1021/acs.chemrev.8b00306
14. A.Cook, S.G.Newman. *Chem. Rev.*, **124**, 6078 (2024); https://doi.org/10.1021/acs.chemrev.4c00094
15. Z.Dong, Z.Ren, S.J.Thompson, Y.Xu, G.Dong. *Chem. Rev.*, **117**, 9333 (2017); https://doi.org/10.1021/acs.chemrev.6b00574
16. D.Mandal, S.Roychowdhury, J.P.Biswas, S.Maiti, D.Maiti. *Chem. Soc. Rev.*, **51**, 7358 (2022); https://doi.org/10.1039/D1CS00923K
17. M.Röper. *Chem. Unser. Zeit*, **40**, 126 (2006); https://doi.org/10.1002/ciuz.200600373
18. M.A.Stoffels, F.J.R.Klauck, T.Hamadi, F.Glorius, J.Leker. *Adv. Synth. Catal.*, **362**, 1258 (2020); https://doi.org/10.1002/adsc.201901292
19. Z.Chen, J.Chen, Y.Li. *Chin. J. Catal.*, **38**, 1108 (2017); https://doi.org/10.1016/S1872-2067(17)62852-3
20. S.-C.Qi, X.-Y.Wei, Z.-M.Zong, Y.-K.Wang. *RSC Adv.*, **3**, 14219 (2013); https://doi.org/10.1039/C3RA40848E
21. F.Cárdenas-Lizana, M.A.Keane. *J. Mater. Sci.*, **48**, 543 (2013); https://doi.org/10.1007/s10853-012-6766-7
22. M.Pan, A.J.Brush, Z.D.Pozun, H.C.Ham, W.-Y.Yu, G.Henkelman, G.S.Hwang, C.B.Mullins. *Chem. Soc. Rev.*, **42**, 5002 (2013); https://doi.org/10.1039/C3CS35523C
23. K.Razmgar, M.Altarawneh, I.Oluwoye, G.Senanayake. *Catal. Surv. Asia*, **25**, 27 (2021); https://doi.org/10.1007/s10563-020-09319-z
24. Z.S.Guo Na. *Chin. J. Org. Chem.*, **35**, 1383 (2015); https://doi.org/10.6023/cjoc201502032
25. Y.Gu, J.R.Norton, F.Salahi, V.G.Lisnyak, Z.Zhou, S.A.Snyder. *J. Am. Chem. Soc.*, **143**, 9657 (2021); https://doi.org/10.1021/jacs.1c04683
26. S.Kuhaudomlap, O.Mekasuwandumrong, P.Praserthdam, S.-I.Fujita, M.Arai, J.Panpranot. *Catalysts*, **8**, 87 (2018); https://doi.org/10.3390/catal8020087
27. J.Julis, M.Hölscher, W.Leitner. *Green Chem.*, **12**, 1634 (2010); https://doi.org/10.1039/C004751A
28. F.-L.Zeng, Q.-Y.Lv, X.-L.Chen, B.Yu. *Curr. Chin. Chem.*, **1**, 3 (2021); https://doi.org/10.2174/2666001601999200817111836
29. Y.V.Gyrdymova, A.N.Potorochenko. *Russ. Chem. Bull.*, **74**, 1576 (2025); https://doi.org/10.1007/s11172-024-4649-0
30. A.B.Budaev, A.V.Ivanov, O.V.Petrova, V.A.Samsonov, I.A.Ushakov, A.Y.Tikhonov, L.N.Sobenina, B.A.Trofimov. *Mendeleev Commun.*, **29**, 53 (2019); https://doi.org/10.1016/j.mencom.2019.01.016
31. A.I.Mikhaleva, E.Y.Shmidt, A.V.Ivanov, A.M.Vasil'tsov, E.Y.Senotrusova, N.I.Protsuk. *Russ. J. Org. Chem.*, **43**, 228 (2007); https://doi.org/10.1134/S1070428007020133
32. K.K.Afanaseva, M.M.Efremova, S.V.Kuznetsova, A.V.Ivanov, G.L.Starova, A.P.Molchanov. *Tetrahedron*, **74**, 5665 (2018); https://doi.org/10.1016/j.tet.2018.07.040
33. A.P.Molchanov, R.S.Savinkov, A.V.Stepakov, G.L.Starova, R.R.Kostikov, V.S.Barnakova, A.V.Ivanov. *Synthesis*, **46**, 771 (2014); https://doi.org/10.1055/s-0033-1340479
34. *Mirovye moshchnosty po proizvodstvu polietilena znachitel'no vyrastut k 2028 godu.* Sait Kompanii MRS (Market Report) [*Global Polyethylene Production Capacity to Grow Significantly by 2028. MRS (Market Report)*]; website; https://www.mrc.ru/news/413825-mirovie-moschnosti-po-proizvodstvu-polietilena-znachitelno-virastut-k-2028-godu (Last access 19.07.2025)
35. Y.A.Treger, V.N.Rozanov. *Rev. J. Chem.*, **6**, 83 (2016); https://doi.org/10.1134/S2079978016010039
36. S.M.Sadrameli. *Fuel*, **140**, 102 (2015); https://doi.org/10.1016/j.fuel.2014.09.034
37. A.Akah, J.Williams, M.Ghrami. *Catal. Surv. Asia*, **23**, 265 (2019); https://doi.org/10.1007/s10563-019-09280-6
38. A.Borodziński, G.C.Bond. *Catal. Rev.*, **48**, 91 (2006); https://doi.org/10.1080/01614940500364909
39. Y.V.Gyrdymova, A.N.Lebedev, Y.-J.Du, K.S.Rodygin. *ChemPlusChem*, **84**, e202400247 (2024); https://doi.org/10.1002/cplu.202400247
40. M.Armbrüster, M.Behrens, F.Cinquini, K.Föttinger, Y.Grin, A.Haghofer, B.Klötzer, A.Knop-Gericke, H.Lorenz, A.Ota, S.Penner, J.Prinz, C.Rameshan, Z.Révay, D.Rosenthal, G.Rupprechter, P.Sautet, R.Schlögl, L.Shao, L.Szentmiklósi, D.Teschner, D.Torres, R.Wagner, R.Widmer, G.Wowsnick. *ChemCatChem*, **4**, 1048 (2012); https://doi.org/10.1002/cctc.201200100
41. W.Xie, L.Yang, J.Zhang, X.Zhao. *Chem. – Eur. J.*, **29**, e202300158 (2023); https://doi.org/10.1002/chem.202300158
42. G.Verma, J.Ren, S.Kumar, S.Ma. *Eur. J. Inorg. Chem.*, 4498 (2021); https://doi.org/10.1002/ejic.202100635
43. J.Palgunadi, H.S.Kim, J.M.Lee, S.Jung. *Chem. Eng. Proc.*, **49**, 192 (2010); https://doi.org/10.1016/j.cep.2009.12.009
44. L.Li, R.-B.Lin, R.Krishna, X.Wang, B.Li, H.Wu, J.Li, W.Zhou, B.Chen. *J. Mater. Chem.*, **5**, 18984 (2017); https://doi.org/10.1039/C7TA05598F
45. M.Takht Ravanchi, S.Sahebdelfar, S.Komeili. *Rev. Chem. Eng.*, **34**, 215 (2018); https://doi.org/10.1515/revce-2016-0036
46. J.Zhang, Z.Sui, Y.-A.Zhu, D.Chen, X.Zhou, W.Yuan. *Chem. Eng. Technol.*, **39**, 865 (2016); https://doi.org/10.1002/ceat.201600020
47. A.S.Al-Ammar, G.Webb. *J. Chem. Soc., Faraday Trans. 1*, **74**, 195 (1978); https://doi.org/10.1039/F19787400195
48. A.S.Al-Ammar, G.Webb. *J. Chem. Soc., Faraday Trans. 1*, **74**, 657 (1978); https://doi.org/10.1039/F19787400657
49. A.Sárkány, A.H.Weiss, T.Szilágyi, P.Sándor, L.Guczi. *Appl. Catal.*, **12**, 373 (1984); https://doi.org/10.1016/S0166-9834(00)81674-7
50. M.Szukiewicz, R.Petrus. *Chem. Eng. Technol.*, **22**, 1059 (1999); https://doi.org/10.1002/(SICI)1521-4125(199912)22:12<1059::AID-CEAT1059>3.0.CO;2-1
51. M.Takht Ravanchi, S.Sahebdelfar. *Appl. Catal. A: Gen.*, **525**, 197 (2016); https://doi.org/10.1016/j.apcata.2016.07.014

52. M.R.Rahimpour, O.Dehghani, M.R.Gholipour, M.S.S.Yancheshmeh, S.S.Haghighi, A.Shariati. *J. Chem. Eng.*, **198**–**199**, 491 (2012); https://doi.org/10.1016/j.cej.2012.06.005
53. Z.Sun, S.Wang, W.Chen. *J. Mater. Chem.*, **9**, 5296 (2021); https://doi.org/10.1039/D1TA00022E
54. H.Hu, J.Xi. *Chin. Chem. Lett.*, **34**, 107959 (2023); https://doi.org/10.1016/j.cclet.2022.107959
55. R.Huang, M.Xia, Y.Zhang, C.Guan, Y.Wei, Z.Jiang, M.Li, B.Zhao, X.Hou, Y.Wei, Q.Chen, J.Hu, X.Cui, L.Yu, D.Deng. *Nat. Catal.*, **6**, 1005 (2023); https://doi.org/10.1038/s41929-023-01026-y
56. Z.Wu, F.Wang, G.Sun, F.Xiong, B.Teng, W.Huang. *J. Phys. Chem. Lett.*, **13**, 7667 (2022); https://doi.org/10.1021/acs.jpclett.2c01810
57. Z.Wang, A.Garg, L.Wang, H.He, A.Dasgupta, D.Zanchet, M.J.Janik, R.M.Rioux, Y.Román-Leshkov. *ACS Catal.*, **10**, 6763 (2020); https://doi.org/10.1021/acscatal.9b04070
58. Y.Li, Y.Cao, X.Ge, H.Zhang, K.Yan, J.Zhang, G.Qian, Z.Jiang, X.Gong, A.Li, X.Zhou, W.Yuan, X.Duan. *J. Catal.*, **407**, 290 (2022); https://doi.org/10.1016/j.jcat.2022.02.005
59. O.B.Ayodele. *J. Energy Chem.*, **72**, 495 (2022); https://doi.org/10.1016/j.jechem.2022.05.035
60. J.Vito, M.Shetty. *ACS Appl. Mater. Interfaces,* **16**, 67010 (2024); https://doi.org/10.1021/acsami.3c11935
61. K.Xie, K.Xu, M.Liu, X.Song, S.Xu, H.Si. *Mater. Today Catal.*, **3**, 100029 (2023); https://doi.org/10.1016/j.mtcata.2023.100029
62. X.Cao, B.W.L.Jang, J.Hu, L.Wang, S.Zhang. *Molecules*, **28**, 2572 (2023) https://doi.org/10.3390/molecules28062572
63. G.Tiwari, S.Sarkar, B.R.Jagirdar. *ChemCatChem*, **16**, e202400586 (2024); https://doi.org/10.1002/cctc.202400586
64. I.S.Mashkovsky, P.V.Markov, A.V.Rassolov, E.D.Patil, A.Y.Stakheev. *Russ. Chem. Rev.*, **92** (8), RCR5087 (2023); https://doi.org/10.59761/RCR5087
65. D.A.Shlyapin, D.V.Glyzdova, T.N.Afonasenko, V.L.Temerev, A.V.Lavrenov. *Katal. Prom-ti*, **22**, 51 (2022); https://doi.org/10.18412/1816-0387-2022-6-51-67
66. D.A.Shlyapin, D.V.Yurpalova, T.N.Afonasenko, V.L.Temerev, A.V.Lavrenov. *Katal. Prom-ti*, **23**, 17 (2023); https://doi.org/10.18412/1816-0387-2023-6-17-51
67. D.Astruc, F.Lu, J.R.Aranzaes. *Angew. Chem., Int. Ed.*, **44**, 7852 (2005); https://doi.org/10.1002/anie.200500766
68. T.W.Lyons, M.S.Sanford. *Chem. Rev.*, **110**, 1147 (2010); https://doi.org/10.1021/cr900184e
69. F.Studt, F.Abild-Pedersen, T.Bligaard, R.Z.Sørensen, C.H.Christensen, J.K.Nørskov. *Science*, **320**, 1320 (2008); https://doi.org/10.1126/science.1156660
70. V.V.Rostovtsev, L.G.Green, V.V.Fokin, K.B.Sharpless. *Angew. Chem., Int. Ed.*, **41**, 2596 (2002); https://doi.org/10.1002/1521-3773(20020715)41:14<2596::AID-ANIE2596>3.0.CO;2-4
71. C.K.Prier, D.A.Rankic, D.W.C.MacMillan. *Chem. Rev.*, **113**, 5322 (2013); https://doi.org/10.1021/cr300503r
72. I.P.Beletskaya, A.V.Cheprakov. *Chem. Rev.*, **100**, 3009 (2000); 10.1021/cr9903048
73. X.Chen, K.M.Engle, D.-H.Wang, J.-Q.Yu. *Angew. Chem., Int. Ed.*, **48**, 5094 (2009); https://doi.org/10.1002/anie.200806273
74. A.S.K.Hashmi. *Chem. Rev.*, **107**, 3180 (2007); https://doi.org/10.1021/cr000436x
75. K.C.Nicolaou, P.G.Bulger, D.Sarlah. *Angew. Chem., Int. Ed.*, **44**, 4442 (2005); https://doi.org/10.1002/anie.200500368
76. S.S.Zalesskiy, V.P.Ananikov. *Organometallics*, **31**, 2302 (2012); https://doi.org/10.1021/om201217r
77. C.Drahl. *Chem. Eng. News*, **90** (27), 9 (2012); https://doi.org/10.1021/cen-09027-notw4
78. V.P.Ananikov, I.P.Beletskaya. *Organometallics*, **31**, 1595 (2012); https://doi.org/10.1021/om201120n
79. M.Haruta. *Catal. Today*, **36**, 153 (1997); https://doi.org/10.1016/S0920-5861(96)00208-8
80. L.Liu, A.Corma. *Chem. Rev.*, **118**, 4981 (2018); https://doi.org/10.1021/acs.chemrev.7b00776
81. M.-C.Daniel, D.Astruc. *Chem. Rev.*, **104**, 293 (2004); https://doi.org/10.1021/cr030698+
82. M.B.Gawande, A.Goswami, F.-X.Felpin, T.Asefa, X.Huang, R.Silva, X.Zou, R.Zboril, R.S.Varma. *Chem. Rev.*, **116**, 3722 (2016); https://doi.org/10.1021/acs.chemrev.5b00482
83. G.Kyriakou, M.B.Boucher, A.D.Jewell, E.A.Lewis, T.J.Lawton, A.E.Baber, H.L.Tierney, M.Flytzani-Stephanopoulos, E.C.H.Sykes. *Science*, **335**, 1209 (2012); https://doi.org/10.1126/science.1215864
84. X.-F.Yang, A.Wang, B.Qiao, J.Li, J.Liu, T.Zhang. *Acc. Chem. Res.*, **46**, 1740 (2013); https://doi.org/10.1021/ar300361m
85. G.Vilé, D.Albani, M.Nachtegaal, Z.Chen, D.Dontsova, M.Antonietti, N.López, J.Pérez-Ramírez. *Angew. Chem., Int. Ed.*, **54**, 11265 (2015); https://doi.org/10.1002/anie.201505073
86. A.Wang, J.Li, T.Zhang. *Nat. Rev. Chem.*, **2**, 65 (2018); https://doi.org/10.1038/s41570-018-0010-1
87. C.Gnad, A.Abram, A.Urstöger, F.Weigl, M.Schuster, K.Köhler. *ACS Catal.*, **10**, 6030 (2020); https://doi.org/10.1021/acscatal.0c01166
88. K.Köhler, R.G.Heidenreich, J.G.E.Krauter, J.Pietsch. *Chem. – Eur. J.*, **8**, 622 (2002); https://doi.org/10.1002/1521-3765(20020201)8:3<622::AID-CHEM622>3.0.CO;2-0
89. Y.Nian, X.Huang, M.Liu, J.Zhang, Y.Han. *ACS Catal.*, **13**, 11164 (2023); https://doi.org/10.1021/acscatal.3c02370
90. D.B.Eremin, V.P.Ananikov. *Coord. Chem. Rev.*, **346**, 2 (2017); https://doi.org/10.1016/j.ccr.2016.12.021
91. D.O.Prima, N.S.Kulikovskaya, A.S.Galushko, R.M.Mironenko, V.P.Ananikov. *Curr. Opin. Green Sustain. Chem.*, **31**, 100502 (2021); https://doi.org/10.1016/j.cogsc.2021.100502
92. A.S.Kashin, V.P.Ananikov. *J. Org. Chem.*, **78**, 11117 (2013); https://doi.org/10.1021/jo402038p
93. D.O.Prima, M.Madiyeva, J.V.Burykina, M.E.Minyaev, D.A.Boiko, V.P.Ananikov. *Catal. Sci. Technol.*, **11**, 7171 (2021); https://doi.org/10.1039/D1CY01601F
94. M.V.Polynski, V.P.Ananikov. *ACS Catal.*, **9**, 3991 (2019); https://doi.org/10.1021/acscatal.9b00207
95. V.M.Chernyshev, A.V.Astakhov, I.E.Chikunov, R.V.Tyurin, D.B.Eremin, G.S.Ranny, V.N.Khrustalev, V.P.Ananikov. *ACS Catal.*, **9**, 2984 (2019); https://doi.org/10.1021/acscatal.8b03683
96. D.O.Prima, N.S.Kulikovskaya, R.A.Novikov, A.Y.Kostyukovich, J.V.Burykina, V.M.Chernyshev, V.P.Ananikov. *Angew. Chem., Int. Ed.*, **63**, e202317468 (2024); https://doi.org/10.1002/anie.202317468
97. A.S.Galushko, V.P.Ananikov. *ACS Catal.*, **14**, 161 (2024); https://doi.org/10.1021/acscatal.3c03889
98. V.M.Chernyshev, V.P.Ananikov. *ACS Catal.*, **12**, 1180 (2022); https://doi.org/10.1021/acscatal.1c04705
99. L.Zhang, M.Zhou, A.Wang, T.Zhang. *Chem. Rev.*, **120**, 683 (2020); https://doi.org/10.1021/acs.chemrev.9b00230
100. X.Deng, J.Wang, N.Guan, L.Li. *Cell Rep. Phys. Sci.*, **3** (2022); https://doi.org/10.1016/j.xcrp.2022.101017
101. A.Mirich, M.Enmeier, K.Cunningham, K.Grossman, G.Recker, S.Jarman, T.Weinmaster, R.Mehaffey, G.Huldin, G.Bacchin, S.Kallepalli, L.Cogua, L.Johnson, B.Mattson. *J. Chem. Ed.*, **97**, 1579 (2020); https://doi.org/10.1021/acs.jchemed.9b01152
102. V.D.Stytsenko, D.P.Melnikov, A.P.Glotov, V.A.Vinokurov. *Mol. Catal.*, **533**, 112750 (2022); https://doi.org/10.1016/j.mcat.2022.112750
103. C.Che, G.Galian, W.He, L.Yulong, H.Wei, Z.Feng, X.Cai. *Inorg. Nano-Met. Chem.*, **51**, 70 (2021); https://doi.org/10.1080/24701556.2020.1762217
104. O.Dehghani, M.R.Rahimpour, A.Shariati. *Processes*, **7**, 136 (2019); https://doi.org/10.3390/pr7030136
105. E.A.Denisova, A.Y.Kostyukovich, A.N.Fakhrutdinov, V.A.Korabelnikova, A.S.Galushko, V.P.Ananikov. *ACS Catal.*, **12**, 6980 (2022); https://doi.org/10.1021/acscatal.2c01749
106. E.R.Saybulina, R.M.Mironenko, A.S.Galushko, V.V.Ilyushenkova, R.R.Izmailov, V.P.Ananikov. *J. Catal.*, **430**, 115293 (2024); https://doi.org/10.1016/j.jcat.2024.115293

107. X.Zhao, Y.Chang, W.-J.Chen, Q.Wu, X.Pan, K.Chen, B.Weng. *ACS Omega*, **7**, 17 (2022); https://doi.org/10.1021/acsomega.1c06244
108. J.Guo, Y.Lei, H.Liu, Y.Li, D.Li, D.He. *Catal. Sci. Technol.*, **13**, 4045 (2023); https://doi.org/10.1039/D3CY00615H
109. C.Deng, T.Wang, P.Wu, W.Zhu, S.Dai. *Nano Energy*, **120**, 109153 (2024); https://doi.org/10.1016/j.nanoen.2023.109153
110. M.Armbrüster, R.Schlögl, Y.Grin. *Sci. Technol. Adv. Mater.*, **15**, 034803 (2014); https://doi.org/10.1088/1468-6996/15/3/034803
111. W.-J.Kim, S.H.Moon. *Catal. Today*, **185**, 2 (2012); https://doi.org/10.1016/j.cattod.2011.09.037
112. T.P.Araújo, J.Morales-Vidal, G.Giannakakis, C.Mondelli, H.Eliasson, R.Erni, J.A.Stewart, S.Mitchell, N.López, J.Pérez-Ramírez. *Angew. Chem., Int. Ed.*, **62**, e202306563 (2023); https://doi.org/10.1002/anie.202306563
113. Y.V.Gyrdymova, E.R.Saybulina, R.M.Mironenko, K.S.Rodygin. *Asian J. Org. Chem.*, **13**, e202400147 (2024); https://doi.org/10.1002/ajoc.202400147
114. Y.V.Gyrdymova. *Russ. J. Gen. Chem.*, **94**, 743 (2024); https://doi.org/10.1134/S1070363224040017
115. A.N.Lebedev, K.S.Rodygin, R.M.Mironenko, E.R.Saybulina, V.P.Ananikov. *J. Catal.*, **407**, 281 (2022); https://doi.org/10.1016/j.jcat.2022.01.034
116. K.Wu, F.Zhan, R.Tu, W.-C.Cheong, Y.Cheng, L.Zheng, W.Yan, Q.Zhang, Z.Chen, C.Chen. *Chem. Commun.*, **56**, 8916 (2020); https://doi.org/10.1039/D0CC03620J
117. Z.Li, S.Ji, Y.Liu, X.Cao, S.Tian, Y.Chen, Z.Niu, Y.Li. *Chem. Rev.*, **120**, 623 (2020); https://doi.org/10.1021/acs.chemrev.9b00311
118. Y.Liu, Z.Li, Q.Yu, Y.Chen, Z.Chai, G.Zhao, S.Liu, W.-C.Cheong, Y.Pan, Q.Zhang, L.Gu, L.Zheng, Y.Wang, Y.Lu, D.Wang, C.Chen, Q.Peng, Y.Liu, L.Liu, J.Chen, Y.Li. *J. Am. Chem. Soc.*, **141**, 9305 (2019); https://doi.org/10.1021/jacs.9b02936
119. S.F.Yuk, G.Collinge, M.-T.Nguyen, M.-S.Lee, V.-A.Glezakou, R.Rousseau. *J. Chem. Phys.*, **152**, 154703 (2020); https://doi.org/10.1063/1.5142748
120. X.Liang, N.Fu, S.Yao, Z.Li, Y.Li. *J. Am. Chem. Soc.*, **144**, 18155 (2022); 10.1021/jacs.1c12642
121. M.Sun, F.Wang, G.Lv, X.Zhang. *Appl. Surf. Sci.*, **589**, 153021 (2022); https://doi.org/10.1016/j.apsusc.2022.153021
122. X.-T.Li, L.Chen, G.-F.Wei, C.Shang, Z.-P.Liu. *ACS Catal.*, **10**, 9694 (2020); https://doi.org/10.1021/acscatal.0c02158
123. D.Teschner, J.Borsodi, A.Wootsch, Z.Révay, M.Hävecker, A.Knop-Gericke, S.D.Jackson, R.Schlögl. *Science*, **320**, 86 (2008); https://doi.org/10.1126/science.1155200
124. W.Xie, J.Xu, Y.Ding, P.Hu. *ACS Catal.*, **11**, 4094 (2021); https://doi.org/10.1021/acscatal.0c05345
125. W.Xie, P.Hu. *Catal. Sci. Technol.*, **11**, 5212 (2021); https://doi.org/10.1039/D1CY00665G
126. S.Wei, A.Li, J.-C.Liu, Z.Li, W.Chen, Y.Gong, Q.Zhang, W.-C.Cheong, Y.Wang, L.Zheng, H.Xiao, C.Chen, D.Wang, Q.Peng, L.Gu, X.Han, J.Li, Y.Li. *Nat. Nanotechnol.*, **13**, 856 (2018); https://doi.org/10.1038/s41565-018-0197-9
127. Q.Feng, S.Zhao, Q.Xu, W.Chen, S.Tian, Y.Wang, W.Yan, J.Luo, D.Wang, Y.Li. *Adv. Mater.*, **31**, 1901024 (2019); https://doi.org/10.1002/adma.201901024
128. X.Huang, Y.Xia, Y.Cao, X.Zheng, H.Pan, J.Zhu, C.Ma, H.Wang, J.Li, R.You, S.Wei, W.Huang, J.Lu. *Nano Res.*, **10**, 1302 (2017); https://doi.org/10.1007/s12274-016-1416-z
129. S.Wei, Xingw.Liu, C.Wang, Xingc.Liu, Q.Zhang, Z.Li. *ACS Nano*, **17**, 14831 (2023); https://doi.org/10.1021/acsnano.3c03078
130. J.Zhang, G.Zhang, L.He, Y.Shi, R.Miao, Y.Zhu, Q.Guan. *Appl. Surf. Sci.*, **570**, 150881 (2021); https://doi.org/10.1016/j.apsusc.2021.150881
131. X.Tao, B.Nan, Y.Li, M.Du, L.-l.Guo, C.Tian, L.Jiang, L.Shen, N.Sun, L.-N.Li. *ACS Appl. Energy Mater.*, **5**, 10385 (2022); https://doi.org/10.1021/acsaem.2c02076
132. C.Qin, Q.Guo, J.Guo, P.Chen. *Chem. – Asian J.*, **16**, 1225 (2021); https://doi.org/10.1002/asia.202100218
133. Y.Guo, H.Qi, Y.Su, Q.Jiang, Y.-T.Cui, L.Li, B.Qiao. *ChemNanoMat*, **7**, 526 (2021); https://doi.org/10.1002/cnma.202100037
134. Y.Guo, Y.Li, X.Du, L.Li, Q.Jiang, B.Qiao. *Nano Res.*, **15**, 10037 (2022); https://doi.org/10.1007/s12274-022-4376-5
135. K.Li, T.Lyu, J.He, B.W.L.Jang. *Front. Chem. Sci. Eng.*, **14**, 929 (2020); https://doi.org/10.1007/s11705-019-1912-2
136. E.Wasim, N.U.Din, D.Le, X.Zhou, G.E.Sterbinsky, M.S.Pape, T.S.Rahman, S.L.Tait. *J. Catal.*, **413**, 81 (2022); https://doi.org/10.1016/j.jcat.2022.06.010
137. G.-C.Wang. *Appl. Surf. Sci.*, **646**, 158928 (2024); https://doi.org/10.1016/j.apsusc.2023.158928
138. Xin.Li, Xia.Li. *Mol. Catal.*, **564**, 114324 (2024); https://doi.org/10.1016/j.mcat.2024.114324
139. Y.Zeng, M.Xia, F.Gao, C.Zhou, X.Cheng, L.Liu, L.Jiao, Q.Wu, X.Wang, L.Yang, Y.Fan, Z.Hu. *Nano Res.*, **17**, 8243 (2024); https://doi.org/10.1007/s12274-024-6843-7
140. Y.Guo, Y.Huang, B.Zeng, B.Han, M.Akri, M.Shi, Y.Zhao, Q.Li, Y.Su, L.Li, Q.Jiang, Y.-T.Cui, L.Li, R.Li, B.Qiao, T.Zhang. *Nat. Commun.*, **13**, 2648 (2022); https://doi.org/10.1038/s41467-022-30291-x
141. Y.Yang, J.Yang, S.Shi, Y.Luo, X.Xu, Y.Liu, D.Li, J.Feng. *AIChE J.*, **69**, e18078 (2023); https://doi.org/10.1002/aic.18078
142. Z.Li, J.Zhang, J.Tian, K.Feng, Y.Chen, X.Li, Z.Zhang, S.Qian, B.Yang, D.Su, K.H.Luo, B.Yan. *ACS Catal.*, **14**, 1514 (2024); https://doi.org/10.1021/acscatal.3c05508
143. L.P.L.Gonçalves, J.Wang, S.Vinati, E.Barborini, X.-K.Wei, M.Heggen, M.Franco, J.P.S.Sousa, D.Y.Petrovykh, O.S.G.P.Soares, K.Kovnir, J.Akola, Y.V.Kolen'ko. *Int. J. Hydrogen Energy*, **45**, 1283 (2020); https://doi.org/10.1016/j.ijhydene.2019.04.086
144. L.Xu, S.Hua, J.Zhou, Y.Xu, C.Lu, F.Feng, J.Zhao, X.Xu, Q.Wang, Q.Zhang, X.Li. *Appl. Catal. A: Gen.*, **642**, 118690 (2022); https://doi.org/10.1016/j.apcata.2022.118690
145. T.Yang, M.Zhao, X.Wang, R.Ma, Y.Liu, Y.He, D.Li. *Catal. Lett.*, **152**, 227 (2022); https://doi.org/10.1007/s10562-021-03620-w
146. M.Sun, F.Wang, J.Hu, G.Lv, X.Zhang. *Chem. Eng. Sci.*, **247**, 116939 (2022); https://doi.org/10.1016/j.ces.2021.116939
147. Z.Li, G.Lin, Y.Chen, Q.Xue, K.Feng, B.Yan. *Catal. Today*, **423**, 114253 (2023); https://doi.org/10.1016/j.cattod.2023.114253
148. Y.Cao, X.Ge, Y.Li, R.Si, Z.Sui, J.Zhou, X.Duan, X.Zhou. *Engineering*, **7**, 103 (2021); https://doi.org/10.1016/j.eng.2020.06.023
149. H.Shariff, M.H.Al-Dahhan. *Ind. Eng. Chem. Res.*, **63**, 8899 (2024); https://doi.org/10.1021/acs.iecr.3c04115
150. Y.Guo, J.Xie, L.Jia, Y.Shi, J.Zhang, Q.Chen, Q.Guan. *J. Mater. Sci.*, **56**, 2129 (2021); https://doi.org/10.1007/s10853-020-05349-0
151. M.Sun, F.Wang, G.Lv, X.Zhang. *Ind. Eng. Chem. Res.*, **61**, 13341 (2022); https://doi.org/10.1021/acs.iecr.2c01477
152. D.Melnikov, M.Reshetina, A.Novikov, K.Cherednichenko, A.Stavitskaya, V.Stytsenko, V.Vinokurov, W.Huang, A.Glotov. *Appl. Clay Sci.*, **232**, 106763 (2023); https://doi.org/10.1016/j.clay.2022.106763
153. H.Dai, X.Xiao, L.Huang, C.Zhou, J.Deng. *Appl. Clay Sci.*, **211**, 106173 (2021); https://doi.org/10.1016/j.clay.2021.106173
154. X.Chen, Q.Xu, B.Zhao, S.Ren, Z.Wu, J.Wu, Y.Yue, D.Han, R.Li. *Catal. Lett.*, **151**, 3372 (2021); https://doi.org/10.1007/s10562-020-03485-5
155. M.Hu, Z.Wu, Z.Yao, J.Young, L.Luo, Y.Du, C.Wang, Z.Iqbal, X.Wang. *J. Catal.*, **395**, 46 (2021); https://doi.org/10.1016/j.jcat.2020.12.009
156. Q.Wu, C.Shen, C.-j.Liu. *Appl. Surf. Sci.*, **607**, 154976 (2023); https://doi.org/10.1016/j.apsusc.2022.154976

157. Q.Wang, Z.Li, Y.Zhou, Y.Wen, J.Zhai, L.Xu, Q.Zhang, Y.Qin, C.Lu, Q.Zhang, X.Li. *Ind. Eng. Chem. Res.*, **63**, 15778 (2024); https://doi.org/10.1021/acs.iecr.4c01677
158. Q.Wang, Y.Xu, J.Zhou, L.Xu, L.Yu, D.Jiang, C.Lu, Z.Pan, Q.Zhang, X.Li. *J. Ind. Eng. Chem.*, **93**, 448 (2021); https://doi.org/10.1016/j.jiec.2020.10.024
159. Y.Kim, T.Kim, K.H.Kang, I.Ro. *ChemCatChem*, **15**, e202201428 (2023); https://doi.org/10.1002/cctc.202201428
160. Y.Liu, B.Wang, Q.Fu, W.Liu, Y.Wang, L.Gu, D.Wang, Y.Li. *Angew. Chem., Int. Ed.*, **60**, 22522 (2021); https://doi.org/10.1002/anie.202109538
161. A.Viale, S.Aime. *Curr. Opin. Chem. Biol.*, **14**, 90 (2010); https://doi.org/10.1016/j.cbpa.2009.10.021
162. D.B.Burueva, K.V.Kovtunov, A.V.Bukhtiyarov, D.A.Barskiy, I.P.Prosvirin, I.S.Mashkovsky, G.N.Baeva, V.I.Bukhtiyarov, A.Y.Stakheev, I.V.Koptyug. *Chem. – Eur. J.*, **24**, 2547 (2018); https://doi.org/10.1002/chem.201705644
163. K.V.Kovtunov, I.E.Beck, V.V.Zhivonitko, D.A.Barskiy, V.I.Bukhtiyarov, I.V.Koptyug. *Phys. Chem. Chem. Phys.*, **14**, 11008 (2012); https://doi.org/10.1039/C2CP40690J
164. O.G.Salnikov, D.A.Barskiy, D.B.Burueva, Y.K.Gulyaeva, B.S.Balzhinimaev, K.V.Kovtunov, I.V.Koptyug. *Appl. Magn. Res.*, **45**, 1051 (2014); https://doi.org/10.1007/s00723-014-0586-7
165. K.V.Kovtunov, V.V.Zhivonitko, L.Kiwi-Minsker, I.V.Koptyug. *Chem. Commun.*, **46**, 5764 (2010); https://doi.org/10.1039/C0CC01411G
166. D.B.Burueva, S.V.Sviyazov, F.Huang, I.P.Prosvirin, A.V.Bukhtiyarov, V.I.Bukhtiyarov, H.Liu, I.V.Koptyug. *J. Phys. Chem. C*, **125**, 27221 (2021); https://doi.org/10.1021/acs.jpcc.1c08424
167. L.Meng, E.V.Pokochueva, Z.Chen, A.Fedorov, F.Viñes, F.Illas, I.V.Koptyug. *ACS Catal.*, **14**, 12500 (2024); https://doi.org/10.1021/acscatal.4c02534
168. I.V.Skovpin, A.I.Trepakova, L.M.Kovtunova, I.V.Koptyug. *Appl. Magn. Res.*, **54**, 1271 (2023); https://doi.org/10.1007/s00723-023-01587-y
169. E.V.Pokochueva, D.B.Burueva, O.G.Salnikov, I.V.Koptyug. *ChemPhysChem*, **22**, 1421 (2021); https://doi.org/10.1002/cphc.202100153
170. V.V.Zhivonitko, I.V.Skovpin, M.Crespo-Quesada, L.Kiwi-Minsker, I.V.Koptyug. *J. Phys. Chem. C*, **120**, 4945 (2016); https://doi.org/10.1021/acs.jpcc.5b12391
171. V.V.Zhivonitko, K.V.Kovtunov, P.L.Chapovsky, I.V.Koptyug. *Angew. Chem., Int. Ed.*, **52**, 13251 (2013); https://doi.org/10.1002/anie.201307389
172. S.V.Sviyazov, S.V.Babenko, I.V.Skovpin, L.M.Kovtunova, N.V.Chukanov, A.Y.Stakheev, D.B.Burueva, I.V.Koptyug. *Phys. Chem. Chem. Phys.*, **26**, 7821 (2024); https://doi.org/10.1039/D3CP04983C
173. Y.V.Gyrdymova, D.E.Samoylenko, K.S.Rodygin. *Chem. – Asian J.*, **18**, e202201063 (2023); https://doi.org/10.1002/asia.202201063
174. K.S.Rodygin, A.S.Bogachenkov, Y.V.Gyrdymova, A.N.Potorochenko. *Chem. Methods*, **5**, e202400045 (2025); https://doi.org/10.1002/cmtd.202400045
175. I.V.Skovpin, S.V.Sviyazov, D.B.Burueva, L.M.Kovtunova, A.V.Nartova, R.I.Kvon, V.I.Bukhtiyarov, I.V.Koptyug. *Dokl. Phys. Chem.*, **512**, 149 (2023); https://doi.org/10.1134/S0012501623600237
176. X.Cao, B.W.L.Jang, J.Hu, L.Wang, S.Zhang. *Molecules*, **28** (2023); https://doi.org/10.3390/molecules28062572
177. T.D.Shittu, O.B.Ayodele. *Front. Chem. Sci. Eng.*, **16**, 1031 (2022); https://doi.org/10.1007/s11705-021-2113-3
178. D.V.Yurpalova, T.N.Afonasenko, M.V.Trenikhin, N.N.Leont'eva, A.B.Arbuzov, V.L.Temerev, D.A.Shlyapin. *Pet. Chem.*, **63**, 982 (2023); https://doi.org/10.1134/S0965544123060129
179. J.Wang, H.Xu, C.Che, J.Zhu, D.Cheng. *ACS Catal.*, **13**, 433 (2023); https://doi.org/10.1021/acscatal.2c05498
180. X.-T.Li, L.Chen, C.Shang, Z.-P.Liu. *J. Am. Chem. Soc.*, **143**, 6281 (2021); 10.1021/jacs.1c02471
181. K.S.Kley, J.De Bellis, F.Schüth. *Catal. Sci. Technol.*, **13**, 119 (2023); https://doi.org/10.1039/D2CY01424F
182. J.A.Delgado, O.Benkirane, S.de Lachaux, C.Claver, J.Ferré, D.Curulla-Ferré, C.Godard. *ChemNanoMat*, **8**, e202200058 (2022); https://doi.org/10.1002/cnma.202200058
183. P.Naumann, S.Scholz, T.Herzfeld. *Appl. Catal. A: Gen.*, **664**, 119346 (2023); https://doi.org/10.1016/j.apcata.2023.119346
184. A.V.Bukhtiyarov, M.A.Panafidin, I.P.Prosvirin, I.S.Mashkovsky, P.V.Markov, A.V.Rassolov, N.S.Smirnova, G.N.Baeva, C.Rameshan, R.Rameshan, Y.V.Zubavichus, V.I.Bukhtiyarov, A.Y.Stakheev. *Appl. Surf. Sci.*, **604**, 154497 (2022); https://doi.org/10.1016/j.apsusc.2022.154497
185. I.S.Mashkovsky, D.P.Melnikov, P.V.Markov, G.N.Baeva, N.S.Smirnova, G.O.Bragina, A.Y.Stakheev. *Dokl. Chem.*, **512**, 272 (2023); https://doi.org/10.1134/S0012500823600736
186. P.V.Markov, I.S.Mashkovsky, G.N.Baeva, D.P.Melnikov, A.Y.Stakheev. *Mendeleev Commun.*, **33**, 836 (2023); https://doi.org/10.1016/j.mencom.2023.10.032
187. K.Liu, B.Wang, M.Fan, L.Ling, R.Zhang. *Mol. Catal.*, **566**, 114416 (2024); https://doi.org/10.1016/j.mcat.2024.114416
188. F.Liu, Y.Xia, W.Xu, L.Cao, Q.Guan, Q.Gu, B.Yang, J.Lu. *Angew. Chem., Int. Ed.*, **60**, 19324 (2021); https://doi.org/10.1002/anie.202105931
189. C.Miao, L.Cai, Y.Wang, X.Xu, J.Yang, Y.He, D.Li, J.Feng. *Ind. Eng. Chem. Res.*, **60**, 8362 (2021); https://doi.org/10.1021/acs.iecr.1c00423
190. Z.Kang, Y.Wang, B.Liu, Z.Huang, X.Lan, T.Wang. *J. Chem. Eng.*, **491**, 151755 (2024); https://doi.org/10.1016/j.cej.2024.151755
191. M.Zhong, J.Zhao, Y.Fang, D.Wu, L.Zhang, C.Du, S.Liu, S.Yang, S.Wan, Y.Jiang, J.Huang, H.Xiong. *Appl. Catal. A: Gen.*, **662**, 119288 (2023); https://doi.org/10.1016/j.apcata.2023.119288
192. S.Liu, D.Wu, F.Yang, K.Chen, Z.Luo, J.Li, Z.Zhang, J.Zhao, L.Zhang, Y.Zhang, H.Zhang, S.Wan, Y.-k.Peng, K.H.L.Zhang, H.Xiong. *J. Chem. Eng.*, **481**, 148658 (2024); https://doi.org/10.1016/j.cej.2024.148658
193. R.Li, Y.Yue, Z.Chen, X.Chen, S.Wang, Z.Jiang, B.Wang, Q.Xu, D.Han, J.Zhao. *Appl. Catal. Environ.*, **279**, 119348 (2020); https://doi.org/10.1016/j.apcatb.2020.119348
194. D.Melnikov, V.Stytsenko, E.Saveleva, M.Kotelev, V.Lyubimenko, E.Ivanov, A.Glotov, V.Vinokurov. *Catalysts*, **10**, 624 (2020); https://doi.org/10.3390/catal10060624
195. Q.Wu, C.Shen, K.Sun, M.Liu, C.-j.Liu. *J. Chem. Eng.*, **486**, 150333 (2024); https://doi.org/10.1016/j.cej.2024.150333
196. G.Tiwari, G.Sharma, R.Verma, P.Gakhad, A.K.Singh, V.Polshettiwar, B.R.Jagirdar. *Chem. – Eur. J.*, **29**, e202301932 (2023); https://doi.org/10.1002/chem.202301932
197. D.V.Glyzdova, T.N.Afonasenko, E.V.Khramov, N.N.Leont'eva, M.V.Trenikhin, I.P.Prosvirin, A.V.Bukhtiyarov, D.A.Shlyapin. *Top. Catal.*, **63**, 139 (2020); https://doi.org/10.1007/s11244-019-01215-9
198. D.V.Glyzdova, T.N.Afonasenko, E.V.Khramov, M.V.Trenikhin, I.P.Prosvirin, D.A.Shlyapin. *ChemCatChem*, **14**, e202200893 (2022); https://doi.org/10.1002/cctc.202200893
199. Z.Yuan, L.Liu, W.Ru, D.Zhou, Y.Kuang, J.Feng, B.Liu, X.Sun. *Nano Res.*, **15**, 6010 (2022); https://doi.org/10.1007/s12274-022-4291-9
200. L.Xu, Y.Qin, Qi.Zhang, J.Zhou, J.Zhao, F.Feng, T.Sun, X.Xu, Y.Zhu, C.Lu, Qu.Zhang, Q.Wang, X.Li. *J. Chem. Eng.*, **495**, 153632 (2024); https://doi.org/10.1016/j.cej.2024.153632
201. X.Pei, D.Zhang, R.Tang, S.Wang, C.Zhang, W.Yuan, W.Sun. *Nanoscale*, **16**, 12411 (2024); https://doi.org/10.1039/D4NR01911C
202. J.Ballesteros-Soberanas, N.Martín, M.Bacic, E.Tiburcio, M.Mon, J.C.Hernández-Garrido, C.Marini, M.Boronat, J.Ferrando-Soria, D.Armentano, E.Pardo, A.Leyva-Pérez.

Nat. Catal., **7**, 452 (2024); https://doi.org/10.1038/s41929-024-01130-7
203. D.V.Yurpalova, T.N.Afonasenko, I.P.Prosvirin, A.V.Bukhtiyarov, L.M.Kovtunova, Z.S.Vinokurov, M.V.Trenikhin, E.Y.Gerasimov, E.V.Khramov, D.A.Shlyapin. *J. Catal.*, **432**, 115417 (2024); https://doi.org/10.1016/j.jcat.2024.115417
204. T.N.Afonasenko, V.L.Temerev, D.V.Glyzdova, N.N.Leont'eva, M.V.Trenikhin, I.P.Prosvirin, D.A.Shlyapin. *Mater. Lett.*, **305**, 130843 (2021); https://doi.org/10.1016/j.matlet.2021.130843
205. B.Lou, H.Kang, W.Yuan, L.Ma, W.Huang, Y.Wang, Z.Jiang, Y.Du, S.Zou, J.Fan. *ACS Catal.*, **11**, 6073 (2021); https://doi.org/10.1021/acscatal.1c00804
206. H.Kang, J.Wu, B.Lou, Y.Wang, Y.Zhao, J.Liu, S.Zou, J.Fan. *Molecules*, **28** (2023); https://doi.org/10.3390/molecules28052335
207. Y.Chen, P.Ning, R.Miao, Y.Shi, L.He, Q.Guan. *New J. Chem.*, **44**, 20812 (2020); 10.1039/D0NJ04401F
208. C.Sui, H.Ma, F.Huang, M.Wang, X.Cai, J.Diao, P.Ren, X.Wen, L.Jin, G.Wang, D.Ma, H.Liu. *ACS Catal.*, **14**, 14689 (2024); https://doi.org/10.1021/acscatal.4c04462
209. J.Zhao, L.He, J.Yu, Y.Shi, R.Miao, Q.Guan, P.Ning. *New J. Chem.*, **45**, 1054 (2021); https://doi.org/10.1039/D0NJ03632C
210. Z.Xu, S.Zhou, M.Zhu. *Catal. Commun.*, **149**, 106241 (2021); https://doi.org/10.1016/j.catcom.2020.106241
211. H.Liao, Z.Li. *Tetrahedron Lett.*, **120**, 154445 (2023); https://doi.org/10.1016/j.tetlet.2023.154445
212. E.Papaplioura, M.Mercier, S.Jerhaoui, M.Schnürch. *ChemCatChem*, **16**, e202400513 (2024); https://doi.org/10.1002/cctc.202400513
213. R.Fu, Y.Lu, G.Yue, D.Wu, L.Xu, H.Song, C.Cao, X.Yu, Y.Zong. *Org. Lett.*, **23**, 3141 (2021); https://doi.org/10.1021/acs.orglett.1c00821
214. Z.Zhang, F.Wen, H.Liu, Z.Li. *ChemistrySelect*, **7**, e202201463 (2022); https://doi.org/10.1002/slct.202201463
215. Y.Wang, F.Wen, Z.Li. *Chem. – Asian J.*, **17**, e202200698 (2022); https://doi.org/10.1002/asia.202200698
216. K.A.Lotsman, K.S.Rodygin, I.Skvortsova, A.M.Kutskaya, M.E.Minyaev, V.P.Ananikov. *Org. Chem. Front.*, **10**, 1022 (2023); 10.1039/D2QO01652D
217. K.S.Rodygin, K.A.Lotsman, D.E.Samoylenko, V.M.Kuznetsov, V.P.Ananikov. *Int. J. Mol. Sci.*, **23**, 11828 (2022); https://doi.org/10.3390/ijms231911828
218. K.A.Lotsman, K.S.Rodygin. *Green Chem.*, **25**, 3524 (2023); https://doi.org/10.1039/D2GC04932E
219. H.Zhou, B.Li, H.Fu, X.Zhao, M.Zhang, X.Wang, Y.Liu, Z.Yang, X.Lou. *ACS Sustain. Chem. Eng.*, **10**, 4849 (2022); https://doi.org/10.1021/acssuschemeng.1c07263
220. W.Ma, Z.Chen, J.Bu, Z.Liu, J.Li, C.Yan, L.Cheng, L.Zhang, H.Zhang, Jic.Zhang, T.Wang, Jia.Zhang. *J. Mater. Chem.*, **10**, 6122 (2022); https://doi.org/10.1039/D1TA08002D
221. D.Wang, R.Ye, C.Zhang, C.Jin, Z.-H.Lu, M.Shakouri, B.Han, T.Wang, Y.Zhang, R.Zhang, Y.Hu, J.Zhou, G.Feng. *Energ. Fuel*, **37**, 13305 (2023); https://doi.org/10.1021/acs.energyfuels.3c01891
222. H.Liu, M.Chai, G.Pei, X.Liu, L.Li, L.Kang, A.Wang, T.Zhang. *Chin. J. Catal.*, **41**, 1099 (2020); https://doi.org/10.1016/S1872-2067(20)63568-9
223. S.Zhou, Q.Wan, C.Lu, A.Zeng, A.Wang, Q.Li, C.Zhou, L.Tan, L.Dong. *Appl. Catal. A: Gen.*, **673**, 119590 (2024); https://doi.org/10.1016/j.apcata.2024.119590
224. X.Ge, M.Dou, Y.Cao, X.Liu, Q.Yuwen, J.Zhang, G.Qian, X.Gong, X.Zhou, L.Chen, W.Yuan, X.Duan. *Nat. Commun.*, **13**, 5534 (2022); https://doi.org/10.1038/s41467-022-33250-8
225. Y.Wang, B.Liu, X.Lan, T.Wang. *ACS Catal.*, **11**, 10257 (2021); https://doi.org/10.1021/acscatal.1c02099
226. H.Zhou, H.Fu, B.Li, X.Yan, Y.Su, X.Pan, Q.Tang, X.Wang, X.Zhao, Y.Liu, Z.Yang, Z.Lu, X.Lou, L.Li. *ACS Sustain. Chem. Eng.*, **11**, 11052 (2023); https://doi.org/10.1021/acssuschemeng.3c01036
227. Y.Song, S.Weng, F.Xue, A.J.McCue, L.Zheng, Y.He, J.Feng, Y.Liu, D.Li. *ACS Catal.*, **13**, 1952 (2023); https://doi.org/10.1021/acscatal.2c06091
228. Z.Almisbaa, H.A.Aljama, K.Almajnouni, L.Cavallo, P.Sautet. *ACS Catal.*, **13**, 7358 (2023); https://doi.org/10.1021/acscatal.3c01175
229. Y.Cao, H.Zhang, S.Ji, Z.Sui, Z.Jiang, D.Wang, F.Zaera, X.Zhou, X.Duan, Y.Li. *Angew. Chem., Int.Ed.*, **59**, 11647 (2020); https://doi.org/10.1002/anie.202004966
230. X.Ge, Z.Ren, Y.Cao, X.Liu, J.Zhang, G.Qian, X.Gong, L.Chen, X.Zhou, W.Yuan, X.Duan. *J. Mater. Chem.*, **10**, 19722 (2022); https://doi.org/10.1039/D2TA02216H
231. J.Ma, F.Xing, Y.Nakaya, K.-i.Shimizu, S.Furukawa. *Angew. Chem., Int. Ed.*, **61**, e202200889 (2022); https://doi.org/10.1002/anie.202200889
232. C.Zhang, L.Wu, R.Ye, G.Feng, R.Zhang. *Catal. Lett.*, **154**, 3619 (2024); https://doi.org/10.1007/s10562-023-04555-0
233. Z.Yuan, A.Kumar, D.Zhou, J.Feng, B.Liu, X.Sun. *J. Catal.*, **414**, 374 (2022); https://doi.org/10.1016/j.jcat.2022.09.005
234. X.Shi, Y.Lin, L.Huang, Z.Sun, Y.Yang, X.Zhou, E.Vovk, X.Liu, X.Huang, M.Sun, S.Wei, J.Lu. *ACS Catal.*, **10**, 3495 (2020); https://doi.org/10.1021/acscatal.9b05321
235. C.Lu, A.Zeng, Y.Wang, A.Wang. *Ind. Eng. Chem. Res.*, **61**, 18696 (2022); https://doi.org/10.1021/acs.iecr.2c03502
236. F.Fu, Y.Liu, Y.Li, B.Fu, L.Zheng, J.Feng, D.Li. *ACS Catal.*, **11**, 11117 (2021); https://doi.org/10.1021/acscatal.1c02162
237. F.Huang, M.Peng, Y.Chen, Z.Gao, X.Cai, J.Xie, D.Xiao, L.Jin, G.Wang, X.Wen, N.Wang, W.Zhou, H.Liu, D.Ma. *ACS Catal.*, **12**, 48 (2022); https://doi.org/10.1021/acscatal.1c04832
238. T.Liu, J.Xiong, Q.Luo, S.Mao, Y.Wang. *ACS Catal.*, **14**, 5838 (2024); https://doi.org/10.1021/acscatal.3c05466
239. C.Lu, A.Zeng, Y.Wang, A.Wang. *ACS Omega*, **6**, 3363 (2021); https://doi.org/10.1021/acsomega.0c05759
240. C.Lu, A.Zeng, Y.Wang, A.Wang. *Eur. J. Inorg. Chem.*, 997 (2021); https://doi.org/10.1002/ejic.202001073
241. X.Jiang, L.Tang, L.Dong, X.Sheng, W.Zhang, Z.Liu, J.Shen, H.Jiang, C.Li. *Angew. Chem., Int. Ed.*, **62**, e202307848 (2023); https://doi.org/10.1002/anie.202307848
242. J.Bu, Z.Liu, W.Ma, L.Zhang, T.Wang, H.Zhang, Q.Zhang, X.Feng, J.Zhang. *Nat. Catal.*, **4**, 557 (2021); https://doi.org/10.1038/s41929-021-00641-x
243. R.Shi, Z.Wang, Y.Zhao, G.I.N.Waterhouse, Z.Li, B.Zhang, Z.Sun, C.Xia, H.Wang, T.Zhang. *Nat. Catal.*, **4**, 565 (2021); https://doi.org/10.1038/s41929-021-00640-y
244. W.Xue, X.Liu, C.Liu, X.Zhang, J.Li, Z.Yang, P.Cui, H.-J.Peng, Q.Jiang, H.Li, P.Xu, T.Zheng, C.Xia, J.Zeng. *Nat. Commun.*, **14**, 2137 (2023); https://doi.org/10.1038/s41467-023-37821-1
245. S.Hu, C.Zhang, M.Wu, R.Ye, D.Shi, M.Li, P.Zhao, R.Zhang, G.Feng. *Catalysts*, **12** (2022); https://doi.org/10.3390/catal12091072
246. Z.Li, J.Zhang, J.Tian, K.Feng, Z.Jiang, B.Yan. *J. Chem. Eng.*, **450**, 138244 (2022); https://doi.org/10.1016/j.cej.2022.138244
247. C.D.Adegbesan, S.Daniel, C.K.F.Monguen, H.N.Otieno, Z.-Y.Tian. *Eng. Sci.*, **30**, 1148 (2024); https://doi.org/10.30919/es1148
248. Y.Zhang, X.Sun, Y.Zhao, H.Su, T.Murayama, C.Qi. *Top. Catal.*, **64**, 197 (2021); https://doi.org/10.1007/s11244-020-01378-w
249. T.Zheng, Y.Zhu, R.Ma, L.Bai, H.Yu, S.Zhao, Y.He, Y.Liu, D.Li. *Ind. Eng. Chem. Res.*, **63**, 2717 (2024); https://doi.org/10.1021/acs.iecr.3c04024
250. H.Zhou, B.Li, Y.Zhang, X.Yan, W.Lv, X.Wang, B.Yuan, Y.Liu, Z.Yang, X.Lou. *ACS Appl. Mater. Interfaces*, **13**, 40429 (2021); https://doi.org/10.1021/acsami.1c02723
251. J.Wang, H.Xu, C.Ao, X.Pan, X.Luo, S.Wei, Z.Li, L.Zhang, Z.-l.Xu, Y.Li. *iScience*, **23** (2020); https://doi.org/10.1016/j.isci.2020.101233
252. D.Zhou, G.Zhang, Y.Li, S.Liu, S.Han, Y.Zhou, W.Shen. *J. Chem. Eng.*, **472**, 144875 (2023); https://doi.org/10.1016/j.cej.2023.144875

253. O.B.Ayodele, T.D.Shittu, O.S.Togunwa, D.Yu, Z.-Y.Tian. *J. Chem. Eng.*, **479**, 147496 (2024); https://doi.org/10.1016/j.cej.2023.147496
254. O.B.Ayodele, G.Jacobs. *J. Chem. Eng.*, **498**, 155168 (2024); https://doi.org/10.1016/j.cej.2024.155168
255. S.Zhou, W.Zhou, C.Lu, Y.Chen, C.Zhou, A.Zeng, A.Wang, Y.-W.Zhang, L.Tan, L.Dong. *Ind. Eng. Chem. Res.*, **63**, 13169 (2024); https://doi.org/10.1021/acs.iecr.4c01880
256. Y.Zhao, Ö.D.Bozkurt, S.F.Kurtoğlu-Öztulum, M.S.Yordanli, A.S.Hoffman, J.Hong, J.E.Perez-Aguilar, A.Saltuk, D.Akgül, O.Demircan, T.A.Ateşin, V.Aviyente, B.C.Gates, S.R.Bare, A.Uzun. *J. Catal.*, **429**, 115196 (2024); https://doi.org/10.1016/j.jcat.2023.115196
257. L.Chen, X.-T.Li, S.Ma, Y.-F.Hu, C.Shang, Z.-P.Liu. *ACS Catal.*, **12**, 14872 (2022); https://doi.org/10.1021/acscatal.2c04379
258. C.Lin, B.C.S.Lee, U.Anjum, A.M.Prabhu, N.Chaudhary, R.Xu, T.S.Choksi. *Appl. Catal. B*, **371**, 125192 (2025); https://doi.org/10.1016/j.apcatb.2025.125192
259. M.Tamtaji, H.Gao, M.D.Hossain, P.R.Galligan, H.Wong, Z.Liu, H.Liu, Y.Cai, W.A.Goddard, Z.Luo. *J. Mater. Chem. A*, **10**, 15309 (2022); 10.1039/D2TA02039D
260. X.Cheng, C.Wu, J.Xu, Y.Han, W.Xie, P.Hu. *Prec. Chem.*, **2**, 570 (2024); 10.1021/prechem.4c00051
261. H.Li, Y.Jiao, K.Davey, S.-Z.Qiao. *Angew. Chem., Int. Ed.*, **62**, e202216383 (2023); https://doi.org/10.1002/anie.202216383
262. X.Xu, Q.Wang, L.Xie, Y.Liu, D.Li, J.Feng, X.Duan. *AIChE J.*, **69**, e18042 (2023); https://doi.org/10.1002/aic.18042
263. F.Huang, Y.Deng, Y.Chen, X.Cai, M.Peng, Z.Jia, P.Ren, D.Xiao, X.Wen, N.Wang, H.Liu, D.Ma. *J. Am. Chem. Soc.*, **140**, 13142 (2018); https://doi.org/10.1021/jacs.8b07476
264. Q.Gao, Z.Yan, W.Zhang, H.S.Pillai, B.Yao, W.Zang, Y.Liu, X.Han, B.Min, H.Zhou, L.Ma, B.Anaclet, S.Zhang, H.Xin, Q.He, H.Zhu. *J. Am. Chem. Soc.*, **145**, 19961 (2023); https://doi.org/10.1021/jacs.3c06514
265. S.Zou, B.Lou, K.Yang, W.Yuan, C.Zhu, Y.Zhu, Y.Du, L.Lu, J.Liu, W.Huang, B.Yang, Z.Gong, Y.Cui, Y.Wang, L.Ma, J.Ma, Z.Jiang, L.Xiao, J.Fan. *Nat. Commun.*, **12**, 5770 (2021); https://doi.org/10.1038/s41467-021-25984-8
266. F.Huang, Y.Deng, Y.Chen, X.Cai, M.Peng, Z.Jia, J.Xie, D.Xiao, X.Wen, N.Wang, Z.Jiang, H.Liu, D.Ma. *Nat. Commun.*, **10**, 4431 (2019); https://doi.org/10.1038/s41467-019-12460-7
267. J.Gu, M.Jian, L.Huang, Z.Sun, A.Li, Y.Pan, J.Yang, W.Wen, W.Zhou, Y.Lin, H.-J.Wang, X.Liu, L.Wang, X.Shi, X.Huang, L.Cao, S.Chen, X.Zheng, H.Pan, J.Zhu, S.Wei, W.-X.Li, J.Lu. *Nat. Nanotechnol.*, **16**, 1141 (2021); https://doi.org/10.1038/s41565-021-00951-y